Accepted Manuscript

Geological Society, London, Special Publications

Cretaceous Large Igneous Provinces: from volcanic formation to environmental catastrophes and biological crises

L. M. E. Percival, H. Matsumoto, S. Callegaro, E. Erba, A. C. Kerr, J. Mutterlose & K. Suzuki

DOI: https://doi.org/10.1144/SP544-2023-88

To access the most recent version of this article, please click the DOI URL in the line above. When citing this article please include the above DOI.

Received 17 May 2023
Revised 10 December 2023
Accepted 9 January 2024

Supplementary material at https://doi.org/10.6084/m9.figshare.c.7026011

Cretaceous Large Igneous Provinces: from volcanic formation to environmental catastrophes and biological crises

L. M. E. Percival[1,2*], H. Matsumoto[3], S. Callegaro[4], E. Erba[5], A. C. Kerr[6], J. Mutterlose[7], K. Suzuki[3]

[1]*Archaeology, Environmental Changes and Geo-Chemistry (AMGC) Group, Vrije Universiteit Brussel, Pleinlaan 2, 1050 Brussels, Belgium*

[2]*Department of Earth Sciences, Faculty of Science, Vrije Universiteit Amsterdam, De Boelelaan 1085, 1081 HV Amsterdam, Netherlands*

[3]*Japan Agency for Marine-Earth Sciences and Technology (JAMSTEC), Natsushima, Yokosuka, Kanagawa, 237-0061, Japan*

[4]*The Centre for Planetary Habitability (PHAB), University of Oslo, Sem Sælands vei 2, 0371 Oslo, Norway*

[5]*Dipartimento di Scienze della Terra, Università degli Studi di Milano, 20133 Milan, Italy*

[6]*School of Earth and Environmental Sciences, Cardiff University, Park Place, Cardiff, CF10 3AT, UK*

[7]*Institut für Geologie, Mineralogie und Geophysik, Ruhr-Universität Bochum, Universitätsstraße 150, 44801 Bochum, Germany*

*Corresponding author: l.m.e.percival@vu.nl

Abstract

The Cretaceous Period was marked by the formation of numerous Large Igneous Provinces (LIPs), several of which were associated with geologically rapid climate, environmental, and biosphere perturbations, including the early Aptian and latest Cenomanian Oceanic Anoxic Events (OAEs 1a and 2, respectively). In most cases, magmatic CO_2 emissions are thought to have been the major driver of climate and biosphere degradation. This work summarises the relationships between

Cretaceous LIPs and environmental perturbations, focussing on how volcanism caused climate warming during OAE 1a using osmium-isotope and mercury concentration data. The new results support magmatic CO_2 output from submarine LIP activity as the primary trigger of climate warming and biosphere stress before/during OAE 1a. This submarine volcanic trigger of OAE 1a (and OAE 2), two of the most climatically/biotically severe Cretaceous events, highlights the capacity of oceanic LIPs to impact Earth's environment as profoundly as many continental provinces. Cretaceous magmatism (and likely output of CO_2 and trace-metal micronutrients) was apparently most intense during those OAEs; further studies are needed to better constrain eruption histories of those oceanic plateaus. Another open question is why the Cretaceous Period overall featured a higher rate of magmatic activity and LIP formation compared to before and afterwards.

1. INTRODUCTION

Large igneous provinces (LIPs) represent the formation of huge volumes of igneous material emplaced into and/or on to the Earth's continental or oceanic crust over a geologically short time interval (Coffin and Eldholm, 1994). This emplacement occurs through a combination of both intrusive magmatism and extrusive volcanic activity: the latter are most famously in the form of continental flood basalts, some of which featured individual lava flows with an aerial extent on the order of 10^4 km^2 (e.g., Coffin and Eldholm, 1994; Bryan and Ernst, 2008; Bryan and Ferrari, 2013; Ernst, 2014). Several different formal definitions for large igneous provinces have been proposed, characterising them as magmatic provinces with high volumes of igneous material that can form in a range of intraplate tectonic settings, with the majority of magmas emplaced over a geologically short space of time (e.g., >0.1 Mkm^3 in ~1–5 Myr; Bryan and Ernst, 2008; or >0.1 Mkm^3, frequently >1 Mkm^3, in <5 Myr, often <2 Myr; Ernst *et al.*, 2021).

The history of LIP formation over the last 300 million years, since the formation of the Pangaean supercontinent, is well established. Several provinces are preserved as flood basalt units and/or large-scale intrusive sill and dyke swarms on the continents, or as oceanic plateaus in the Pacific and Indian ocean basins (see e.g., Coffin and Edholm, 1994; Ernst, 2014; Kerr, 2014; Ernst *et al.*, 2021). These LIPs are generally better preserved than those that formed prior to 300 Ma, and are typically estimated to have had original volumes of emplaced magma greater than 0.1 Mkm^3; frequently above 1 Mkm^3 (Bryan and Ernst, 2008; Ernst *et al.*, 2021). However, the Greater Ontong-Java Plateau in the western Pacific Ocean may have been an order of magnitude more voluminous still (Gladczenko *et al.*, 1997; Taylor, 2006; Hoernle *et al.*, 2010). The rapid emplacement of most provinces (within ~1 Myr; see Kasbohm *et al.*, 2021, and references therein) highlights that the rate of magma production during LIP formation was typically both higher and sustained for longer time periods than for any observed volcanic activity in human history. In this context, it is notable that the large majority of geologically rapid changes to Earth's global climate and environment, particularly in the last 300 million years, broadly coincided with an interval of LIP formation. These events include at least four of the so called

'Big Five' mass extinctions of the Phanerozoic Aeon (e.g., Wignall, 2001; Courtillot and Renne, 2003; Bond and Wignall, 2014; Ernst *et al.*, 2020; Kasbohm *et al.*, 2021).

The Cretaceous Period (143–66 Ma; Gale *et al.*, 2020) was marked by the highest rate of LIP formation in at least the last 300 Myr. Numerous provinces were emplaced into both the continental and oceanic crust, and estimates of the total number of Cretaceous LIPs vary (but see recent lists by e.g., Torsvik, 2019; Ernst *et al.*, 2021). However, there are seven major Cretaceous LIPs that comprise both high volumes of igneous material and have been widely linked with climate/environmental change and/or elevated biotic stress/extinction during that Period (Figure 1). Continental flood-basalt provinces include the Paraná-Etendeka LIP, the High Arctic LIP (HALIP), the Madagascan LIP, and the Deccan Traps (although the latter three also comprise offshore components). Additionally, the Greater Ontong-Java, Kerguelen, and Caribbean plateaus were emplaced into continental margins and ocean crust to form oceanic plateaus, which are considered to represent large areas of elevated and thickened basaltic ocean floor formed through mantle-plume activity rather than seafloor spreading-related magmatic processes (Kerr, 2014). Indeed, due to the subduction of most pre-Jurassic crust, many currently known oceanic LIPs are Cretaceous in age, including those that are best preserved and most extensively investigated (see Kerr, 2014). This work reviews the seven major Cretaceous LIPs that are thought to have impacted Earth's environment and/or biosphere, and relationship between these phenomena, utilising both new datasets for one such environmental episode, the Early Aptian Oceanic Anoxic Event (OAE 1a), and published datasets relating to this and other Cretaceous LIPs.

2. CRETACEOUS LIPs AND EPISODES OF ENVIRONMENTAL CHANGE

2.1. The Paraná-Etendeka LIP and Valanginian 'Weissert' Event

The Paraná-Etendeka LIP covers an area of ~4 Mkm^2 in western South America (principally Brazil, but also Paraquay, Uruguay, and Argentina) and western Africa (Namibia and Angola), and has long been associated with the opening of the South Atlantic Ocean (Peate, 1997). Extrusive magmas largely comprise tholeiitic basalt flows, with some silicic and alkaline units and intrusive sills and dyke swarms, particularly in the South American Paraná part of the province (e.g., Erlank *et al.*, 1984; Milner *et al.*, 1992, 1995; Peate, 1997; Marsh *et al.*, 2001; De Min *et al.*, 2018; see also Gomes and Vasconcelos, 2021, and references therein). The volatile budget of Paraná-Etendeka magmas may have been relatively low compared to other LIPs, as calculated from phenocrysts and measured from melt inclusions (maximum of 900–1100 ppm S, 125 ppm Cl, and 450 ppm F; Callegaro et al., 2014; Marks et al., 2014). Moreover, the magmas were emplaced within or erupted on to country rocks that largely consisted of aeolian sandstones, organic-lean shales, and crystalline basement (Jones *et al.*, 2016; Barreto *et al.*, 2016). These lithologies were all likely volatile-depleted and would not have been a major source of thermogenic carbon or sulphur following heating by the intruding magmas (c.f., Svensen *et al.*, 2004, 2009; Heimdal *et al.*, 2018).

Paraná-Etendeka volcanism is widely attributed to have caused an episode of prolonged environmental perturbation during the Valanginian Stage (137.7–132.6 Ma), known as the Weissert Event (Erba *et al.*, 2004). This episode of environmental change is characterised in the upper Valanginian stratigraphic record by a positive carbon-isotope ($\delta^{13}C$) excursion of ~1.5–2 ‰ in carbonate and up to 4 ‰ in bulk organic matter (e.g., Lini *et al.*, 1992; Weissert *et al.*, 1998; Erba *et al.*, 2004; Price and Mutterlose, 2004; Gröcke *et al.*, 2005; McArthur *et al.*, 2007; Bornemann and Mutterlose, 2008; Littler *et al.*,2011; Price *et al.*, 2018; Jelby *et al.*, 2020). The end of the Weissert Event is marked by the maximum value of the positive carbon-isotope excursion in upper Valanginian strata (Erba *et al.*, 2004), although $\delta^{13}C$ values decrease gradually through lower Hauterivian strata. This $\delta^{13}C$ shift was initially hypothesised to result from enhanced burial of organic carbon (which is isotopically light) in sediments as they are deposited, leaving the residual seawater carbon inventory, and any carbonates or organic material subsequently formed from it, isotopically heavier (Weissert *et al.*, 1998; Erba *et al.*, 2004). However, whilst some Valanginian strata do preserve organic-rich facies consistent with this hypothesis, the majority do not. Thus, enhanced primary productivity and burial of organic carbon in terrestrial sediments have been proposed as alternative contributors towards the carbon-cycle change (Westermann *et al.*, 2010).

The nature of climate change during the Weissert Event is debated. The Early Valanginian interval prior to and during the onset of the Weissert Event was marked by a warm global climate (Littler *et al.*, 2011), and evidence for surface warming at that time has been documented from bulk-rock oxygen-isotope ($\delta^{18}O$) records in some NW Tethyan and proto-Atlantic archives (Duchamp-Alphonse *et al.*, 2007; Charbonnier *et al.*, 2020c). Clay mineralogy and calcareous nannofossil and spore-pollen assemblages also indicate enhanced humidity in and around the former region (Kujau *et al.*, 2013; Charbonnier *et al.*, 2020c; Möller *et al.*, 2020). Thus far, this warming has not been as clearly recorded by other palaeotemperature proxies or robustly documented in other areas around the world, with only modest temperature increases of at most 1 °C that do not significantly exceed pre-event variations reported from some sites (e.g., Littler *et al.*, 2011 Price *et al.*, 2018; Charbonnier *et al.*, 2020c; Cavalheiro *et al.*, 2021). By contrast, in several Valanginian records, particularly those from the Boreal Realm but also in the NW Tethys and southern high latitudes, the turning point in $\delta^{13}C$ values at the peak of the positive excursion stratigraphically correlates with evidence for the onset of a transient fall in surface temperatures, (e.g., Erba *et al.*, 2004; McArthur *et al.*, 2007; Meissner *et al.*, 2015; Price *et al.*, 2018; Cavalheiro *et al.*, 2021). This correlation between the $\delta^{13}C$ peak and onset of temperature decrease is consistent with enhanced atmospheric CO_2 sequestration through the hypothesised increase in organic-carbon burial. However, proto-Atlantic sea-surface temperature reconstructions based on the biomarker-based TEX_{86} palaeothermometer suggest that stable warm conditions persisted throughout the Valanginian in that low-latitude environment (Littler *et al.*, 2011), potentially highlighting a steepening of global temperature gradients during the Weissert Event (Charbonnier *et al.*, 2020c; Cavalheiro *et al.*, 2021).

Age constraints for Paraná-Etendeka volcanism are based on magnetostratigraphy and both argon-argon ($^{40}Ar/^{39}Ar$) and uranium-lead (U-Pb) geochronology. Collectively, these data suggest a duration of at least 2–3 million years of effusive volcanic activity for the LIP as a whole, with Etendeka magnetostratigraphy suggesting even more protracted eruptions in that part of the province (see compilations by Mena *et al.*, 2011; Dodd *et al.*, 2015; Gomes and Vasconcelos, 2021; Bacha *et al.*, 2022; Jiang *et al.*, 2023). U-Pb and $^{40}Ar/^{39}Ar$ dating of Paraná and Etendeka units by several studies have outlined a pronounced pulse of volcanic activity that likely reached its maximum between 134–135 Ma (Renne *et al.*, 1992, 1996; following recalculation by Thiede and Vasconcelos, 2010; also Ernesto *et al.*, 1999; Pinto *et al.*, 2011; Janasi *et al.*, 2011; Florisbal *et al.*, 2014; Almeida *et al.*, 2018; Gomes and Vasconcelos, 2021; Bacha *et al.*, 2022). These magmatic ages broadly overlap with the onset date of the Weissert Event based on both magnetostratigraphic (133.9 Ma; Cavalheiro *et al.*, 2021) and cyclostratigraphic (134.56 Ma; Martinez *et al.*, 2023) age modelling. However, recent high-precision U-Pb dating of Paraná rocks has shown that at least part of the intense volcanic activity postdated the start of the Weissert Event (Rocha *et al.*, 2020). To what extent the older *vs* younger dates of Paraná-Etendeka magmas are representative of rates of extrusive volcanic activity across the province as a whole is unclear. Because the majority of dated rocks are coeval with the onset of the Weissert Event, it is widely assumed that there was a causal relationship between the two phenomena (e.g., Erba *et al.*, 2004; Gomes and Vasconcelos, 2021; Bacha *et al.*, 2022; Martinez *et al.*, 2015, 2023), although it cannot be excluded that significant Paraná-Etendeka volcanism occurred later, potentially questioning the nature of any link (Rocha *et al.*, 2020).

2.2. The Greater Ontong-Java Plateau and Early Aptian OAE (OAE 1a)

The total magmatic volume comprised by the Greater Ontong-Java Plateau (G-OJP) is debated, but is often defined as the Ontong-Java Plateau together with subsidiary nearby flood-basalt provinces such as the Nauru, East Mariana, Manihiki and Hikurangi (after Ingle and Coffin, 2004; Charbonnier and Föllmi, 2017; see also Svensen *et al.*, 2019, and references therein). These provinces were collectively emplaced on to the western Pacific oceanic crust during the Early Cretaceous, covering an area over 2 Mkm^2, and comprising a combined total volume of several 10s Mkm^3, significantly greater than any other preserved LIP (Taylor, 2006; Hoernle *et al.*, 2010). Moreover, at least the south-western part of the original plateau has been subducted since its emplacement (see Schlanger *et al.*, 1981; Larson, 1991). Accreted and exposed Ontong-Java magmas in Malaita

(Solomon Islands) consist of massive sheeted and pillowed basalt flows, with basaltic rocks also recovered from ODP drill sites on the plateau (e.g., Saunders *et al*., 1996; Tejada *et al*., 1996; Neal *et al*., 1997; Fitton and Godard, 2004). It is likely that much of the G-OJP was emplaced via submarine volcanic activity (Saunders *et al*., 1996). However, preservation of phreatomagmatic deposits at ODP Site 1184 in the Eastern Salient of the Ontong-Java Plateau shows that at least some eruptions occurred near or above the sea surface (Thordarson, 2004; Chambers *et al*., 2004).

Geochronological $^{40}Ar/^{39}Ar$ studies on Ontong-Java basalts and volcaniclastic sediments from southern Malaitia, Ramos Island, and ODP sites 289, 807, and 1184 indicate a pulse of volcanic activity that covered a huge area around 122 Ma (Mahoney *et al*., 1993; Tejada *et al*., 1996, 2002; Chambers *et al*., 2004). Submarine eruptions of a broadly similar age have also been reported from studies of whole rock basalts recovered from the Manihiki and Hikurangi plateaus (Ingle *et al*., 2007; Hoernle *et al*., 2010; Timm *et al*., 2011). Recently, this geochronology has been challenged by Davidson *et al*. (2023), on the basis that older ages might be affected by recoil, whilst plagioclase $^{40}Ar/^{39}Ar$ dates from Ontong-Java and Manihiki plateau rocks have ages closer to 110 Ma than 120 Ma. However, those authors do not discount the possibility that the G-OJP had a protracted emplacement over several million years across the late Barremian to early Albian interval, in which their dates are from volcanic rocks that were erupted towards the end of the plateau's formation. Mahoney *et al*. (1993) and Tejada *et al*. (1996) also report eruption ages of ~90 Ma at Sigana Island and ODP Site 803, potentially highlighting a second major pulse of volcanism on the G-OJP. Plateau formation through two distinct spells of volcanism 30 Myr apart is at odds with the mantle plume model of LIP emplacement, and it has been suggested that the younger dates are also affected by argon recoil, and may represent minimum ages (Chambers *et al*., 2002).

The 122 Ma pulse of volcanism has long been associated with the Early Aptian Oceanic Anoxic Event (OAE 1a; 121 Ma), based on the broad temporal correlation between the two phenomena (e.g., Larson and Erba, 1999; Courtillot and Renne, 2003; Erba *et al*., 2015). OAE 1a was marked by the development of marine anoxia/euxinia across the global ocean for approximately 1–1.4 Myr (Li *et al*., 2008; Malinverno *et al*., 2010; Leandro *et al*., 2022). Widespread oxygen-depleted conditions were initially interpreted from the preservation of laminated, organic-rich, mudstones, dubbed the Selli Level in the Umbria-Marche Basin of central Italy (e.g., Schlanger and Jenkyns, 1976; Weissert, 1989; Jenkyns, 1995; Pancost *et al.*, 2004; Föllmi *et al.*, 2006; van Breugel *et al.*, 2007; see also reviews by Jenkyns, 2010, and Robinson *et al.*, 2017). Global stratigraphic records of OAE 1a are further characterised by a series of $\delta^{13}C$ excursions, reflecting sequential carbon-cycle perturbations during the Early Aptian (Weissert, 1989; Jenkyns, 1995; Menegatti *et al.*, 1998; Gröcke *et al.*, 1999; Ando *et al.*, 2008; Robinson *et al.*, 2008; Vickers *et al.*, 2016). These $\delta^{13}C$ excursions have been subdivided into segments (C3–C7) based on Tethyan archives (Menegatti *et al.*, 1998). Following a relatively stable $\delta^{13}C$ signature through uppermost Barremian–lowermost Aptian strata (C1–C2), a sharp negative shift is documented at the base of the OAE 1a level (C3), highlighting a large influx of isotopically light carbon to the Earth's surface from one or more of volcanic activity, thermogenic emissions, and methane clathrate destabilisation (e.g., Jahren *et al.*, 2001; Méhay *et al.*, 2009; Kuhnt *et al.*, 2011; Naafs *et al.*, 2016; Bauer *et al.*, 2017; Adloff *et al.*, 2020). The negative isotopic signature is followed by a positive rebound (C4), another stable spell (C5), a second positive excursion at the top of the OAE level (C6), and a continuation of elevated $\delta^{13}C$ values that remain high above it (C7), with these later shifts likely reflecting the widespread deposition of organic carbon (Jenkyns, 2010). The various carbon-cycle perturbations impacted Earth's surface climate during OAE 1a, with overarching climate warming and transient interludes of cooling during the event interpreted from palaeontological and geochemical evidence (e.g., Menegatti *et al.*, 1998; Jenkyns, 2003, 2018; Dumitrescu *et al.*, 2006; Ando *et al.*, 2008; Kuhnt *et al.*, 2011; Bottini *et al.*, 2015; Naafs and Pancost, 2016). As well as oceanic anoxia and global temperature changes, OAE 1a is thought to have been marked by seawater acidification, biospheric stress, accelerated hydrological cycling, and enhanced continental weathering (e.g., Erba, 2004; Erba *et al.*, 2010, 2015; Bottini *et al.*, 2012; Mutterlose *et al.*, 2014; Lechler *et al.*, 2015; Naafs and Pancost, 2016).

2.3. The Kerguelen Plateau and Aptian–Albian OAE (OAE 1b)

The Kerguelen Plateau began to form during the break-up of India from Australia and Antarctica during the Early Cretaceous, and today encompasses an area of elevated oceanic crust comprising >2 Mkm^3 of mainly basaltic rock, with some dacites and rhyolites (Kerr, 2014). Additional fragments of the plateau such as Broken Ridge and Ninetyeast Ridge are preserved in the Indian Ocean (see Wallace *et al*., 2002, and references therein). Some older magmas that formed during the initial break-up of southern Gondwana are also preserved in NE India and western Australia (Frey *et al*., 1996; Coffin *et al*., 2002; Kent *et al*., 2002). Unlike many LIPs, the Kerguelen Plateau has a long volcanic history, commencing in the Early Cretaceous and continuing (less voluminously) to the present day (see Coffin *et al*., 2002; Jiang *et al*., 2021). The onshore volcanics all date to 114 Ma or older; Baksi, 1995; Frey *et al*., 1996; Coffin *et al*., 2002; Kent *et al*., 2002). The oldest part of the main oceanic province is the Southern Kerguelen Plateau, for which $^{40}Ar/^{39}Ar$ dates suggest that volcanic activity commenced by 125 Ma at least, and possibly earlier (Jiang *et al*., 2022). Volcanic activity on the Southern Kerguelen Plateau continued until 110 Ma (Whitechurch *et al*., 1992; Coffin *et al*., 2002; Duncan, 2002; Jiang *et al*., 2022), with later eruptions occurring on the Central Kerguelen Plateau and Elan Bank (100.4±0.7 Ma and 107.7 Ma, respectively; Duncan, 2002). Further north, Broken Ridge samples have been dated to ~95 Ma (Duncan, 2002), whilst ages for rocks from Ninetyeast Ridge and Skiff Bank are younger still (~85–35 Ma; Duncan, 1978, 1991; 2002).

Jiang *et al*. (2022, 2023) have recently proposed a revision of the temporal magmatic history of Kerguelen, and argue that the volcanism commenced at 125 Ma or earlier. As such, these authors suggest that early volcanic activity on the plateau may have contributed towards the environmental change associated with OAE 1a, whilst acknowledging the Kerguelen carbon emissions were unlikely to have caused the OAE alone. More frequently, a link has been postulated between the Kerguelen Plateau and more moderate environmental change during the Aptian–Albian transition (~113 Ma), often referred to as OAE 1b, based on a better age correlation between the two phenomena (e.g., Trabucho Alexandre *et al*., 2011; Erba *et al*., 2015; Sabatino *et al*., 2018; Matsumoto *et al*., 2020).

This interval of marine anoxia is documented in the Vocontian Basin (SE France) and NW Tethys by the preservation of four main discrete organic-rich shale intervals (the Jacob, Kilian, Paquier or Urbino level, and Leenhardt levels; Bréhéret, 1988; Coccioni *et al.*, 2014). Some of these shale horizons have also been identified in Atlantic sites (e.g., Herrle *et al.*, 2004; Erbacher *et al.*, 2001; Trabucho Alexandre *et al.*, 2011). Of those four shale levels, the Kilian and Paquier horizons are the two that have been the most widely identified around the world (see compilation in Bodin *et al.*, 2023), with OAE 1b sometimes referred to as the Paquier Event (Jenkyns, 2010). Upper Aptian–lower Albian strata also document a series of $\delta^{13}C$ excursions, with the Kilian and Paquier levels both marked by sharp negative carbon-isotope shifts of 2–3 ‰ that have been used to identify OAE 1b strata at sites around the world not marked by deposition of organic-rich sediments (e.g., Gröcke *et al.*, 1999; Tsikos *et al.*, 2004b; Millán *et al.*, 2014; Herrle *et al.*, 2015; Phelps *et al.*, 2015; Navarro-Ramirez *et al.*, 2015; Li *et al.*, 2016; Zhao *et al.*, 2022). Upper Aptian palaeotemperature records from the North Atlantic indicate a prolonged cooling pulse prior to/during the onset of OAE 1b (McAnena *et al.*, 2013), and a cold pulse has also been postulated from study of Vocontian Basin and northwest Tethys Ocean sites (Herrle and Mutterlose, 2003; Bottini and Erba, 2018). However, there is no clear evidence for a similar fall in temperatures in the South Atlantic (Jenkyns *et al.*, 2012). By contrast, the Paquier level (or its stratigraphic equivalent) is marked by evidence for climate warming in the Vocontian Basin, North Atlantic, and northwest Tethys (Erbacher *et al.*, 2001; Herrle *et al.*, 2003; Huber *et al.*, 2011; Bottini and Erba, 2018).

2.4. The Caribbean LIP and the latest Cenomanian OAE (OAE 2)

The Caribbean (or Caribbean–Colombian) LIP was an oceanic plateau that is preserved today as obducted fragments outcropping in Ecuador, Colombia (including Isla Gorgona) Costa Rica, and several Caribbean islands, most prominently Haiti, Jamaica, Curaçao, and Aruba (Kerr *et al.*, 1997). The plateau also comprises a substantial proportion of the thickened oceanic crust of the Caribbean

(Mauffret and Leroy, 1997). The fragmentary nature of the remnants of this LIP hinders determination of its original volume, although 4–4.5 Mkm^3 has been estimated (see Kerr *et al*., 2003; Courtillot and Renne, 2003; Kuroda *et al*., 2007). It is widely accepted that the plateau formed on the Farallon (proto-Pacific) plate and possibly represents the 'head' phase of the Galápagos plume (Kerr et al., 2003; Nerlich et al. 2014; Boschman et al. 2014). After its formation, the southern part of the plateau collided with and accreted onto the NW margin of South America, while the northern portion moved into the inter-American gap that had been opening between north and south America since the Jurassic (see reviews in Kerr et al., 2003; Boschman et al. 2014). Studies of the exposed outcrop and recovered rocks from ODP sites indicate that the emplaced magmas largely consist of tholeiitic pillow basalts, with some basaltic and dolerite sills in addition to picritic and komatiitic lavas also preserved (Kerr *et al*., 2003). Whilst it is evident that the plateau predominantly formed through submarine volcanism, Buchs et al. (2018) reported layered tuffs with accretionary lapilli and interbedded lahar deposits with rounded clasts of basalt in accreted oceanic plateau sequences from western Colombia. These tuffs indicate that, like other Cretaceous Pacific plateaus, the Caribbean LIP became subaerial. The preservation of corals and carbonized tree-trunk fragments in sediments interbedded with LIP basalts in the Western Cordillera of Colombia support the occurrence of eruptions in either shallow water depths or a subaerial context (Hall *et al*., 1972; Moreno-Sanchez and Pardo-Trujillo, 2003). Dating of Caribbean LIP samples through $^{40}Ar/^{39}Ar$ and Re-Os geochronology has highlighted a wide range of ages spanning the Cretaceous to the Early Palaeogene (see Kerr *et al*., 2003). However, $^{40}Ar/^{39}Ar$ ages from DSDP Leg 15, Haiti, Gorgona Island, Costa Rica, Hispaniola, Western Colombia, and Curaçao suggest a major pulse of volcanism between 93–88 Ma (Walker *et al*., 1991, 1999; Sinton *et al*., 1998; Kerr *et al*., 2004; Snow *et al*., 2005; see also Kasbohm *et al*., 2021).

The Cenomanian–Turonian boundary has been dated to 93.9 Ma (Meyers *et al*., 2012), and records another interval of widespread oceanic anoxia (OAE 2), which has been widely linked to the coeval Caribbean volcanism (e.g., Sinton and Duncan, 1997; Kerr, 1998; Snow *et al*., 2005; Turgeon and Creaser, 2008; Du Vivier *et al*., 2014, 2015; Scaife *et al*., 2017; Percival *et al*., 2018). Stratigraphic archives of this episode of global environmental perturbation are characterised by a positive $\delta^{13}C$

excursion of up to 6 ‰ in all of carbonates, bulk-, and compound-specific organic matter (e.g., Scholle and Arthur, 1980; Hasegawa, 1997; Tsikos *et al*., 2004a; Erbacher *et al*, 2005; Sageman *et al*., 2006; Jarvis *et al*., 2011). Well-preserved laminated organic-rich shales have been reported from uppermost Cenomanian–lowermost Turonian strata in numerous sites, particularly in the Atlantic, NW Tethys, and Boreal Realm (Schlanger and Jenkyns, 1976; Arthur *et al*., 1987; Linnert *et al*., 2010; see also reviews by Jenkyns, 2010; Robinson *et al*., 2017). Thus, this isotopic shift is typically interpreted as reflecting enhanced organic-carbon burial in the global ocean. Palaeotemperature reconstructions based on carbonate oxygen-isotope (and in some locations, TEX_{86}) trends indicate a rise in temperatures at the onset of OAE 2, with both proxies highlighting that the warm conditions continued after the end of the event (Paul *et al*., 1999; Forster *et al*., 2007; Jarvis *et al*., 2011; van Helmond *et al*., 2014, 2015; O'Connor *et al*., 2020).

However, the elevated temperatures were punctuated by a transient interval of climate cooling (and seawater re-oxygenation) across large parts of the marine realm, dubbed the Plenus Cold Event due to its initial recognition by the southward migration of the boreal belemnite species *Praeactinocamax plenus* (Gale and Christensen, 1996). This cooling/reoxygenation pulse is further documented by multiple geochemical palaeothermometers, a shift in the abundance of specific nannofossils (notably cold-water species), and often a return to pre-OAE lithologies and disappearance of organic-rich shales (e.g., Tsikos *et al*., 2004a; Forster *et al*., 2007; Sinninghe-Damsté *et al*., 2008; Linnert *et al*., 2010; van Helmond *et al*., 2014, 2015, 2016; Desmares *et al*., 2016; O'Connor *et al*., 2020). The transient temperature decrease likely resulted from sequestration of organic carbon caused by one or both of the documented organic-carbon burial and enhanced silicate weathering (Pogge von Strandmann *et al*., 2013; Robinson *et al*., 2019; Percival *et al*., 2020; Papadomanolaki *et al*., 2022). However, this fall in temperatures did not occur synchronously across the world, suggesting that local oceanographic and climatic conditions significantly influenced the regional manifestation of any cooling (O'Connor *et al*., 2020; Percival *et al*., 2020).

2.5. The High Arctic LIP (HALIP) and its relation to the Cretaceous OAEs

Numerous studies have documented the preservation of Cretaceous magmatic units across much of the High Arctic, spanning Svalbard, Franz Josef Land, Novaya Zemlya, the Barents Sea, Northern Greenland, the Canadian Arctic islands, and New Siberian Islands, together with the offshore Alpha-Mendeleev Ridge and Chukchi Plateau (see e.g., Tarduno *et al.*, 1998; Maher, 2001; Buchan and Ernst, 2006; Tegner *et al.*,2011; Corfu *et al.*, 2013; Senger et al., 2014; Naber *et al.*, 2021; Bédard et al., 2021a, 2021b; Senger and Galland, 2022). Comprising both extrusive volcanic units and intrusive dyke swarms in particular, these magmatic formations have been postulated to collectively represent the High Arctic LIP (HALIP; Tarduno *et al.*, 1998). Thus far, geochronology studies of the HALIP have primarily focussed on areas in Arctic Canada (particularly the islands of Axel Heiberg and Ellesmere), with U-Pb and $^{40}Ar/^{39}Ar$ dates indicating that the LIP formed through numerous spells of emplacement over a 40 Myr interval of the Cretaceous (Tegner *et al.*, 2011; Dockman *et al.*, 2018). In particular, two major magmatic pulses at 135–120 Ma and 105–90 Ma have been identified (e.g., Corfu *et al.*, 2013; Evenchick *et al.*, 2015; Estrata *et al.*, 2016; Polteau *et al.*, 2016; Dockman *et al.*, 2018; Kingsbury *et al.*, 2018; Naber *et al.*, 2021; Deegan *et al.*, 2022). Dating of alkaline HALIP rocks in Northern Greenland potentially indicates a later episode of HALIP-related alkaline volcanism between 85–70 Ma (Tegner *et al.*, 2011; Thórarinsson *et al.*, 2015). Recognised magmatic pulses of HALIP overlap in age with both OAEs 1a and 2; consequently, the province has been linked with both episodes of environmental change (e.g., Tegner *et al.*, 2011; Zheng *et al.*, 2013; Polteau *et al.*, 2016; Adloff *et al.*, 2020). In the case of OAE 1a, this link may be related to emission of thermogenic carbon following intrusion of organic-rich sedimentary rocks by basaltic sills, providing a source of isotopically light carbon to the Earth's surface that could have caused the C3 negative excursion in $\delta^{13}C$ (Polteau *et al.*, 2016; Adloff *et al.*, 2020; Deegan et al., 2022).

2.6. The Madagascan LIP

The Madagascan LIP largely comprises tholeiitic flood basalt sequences, with minor alkaline and silicic occurrences, and associated sill and dyke swarms, and intrusive complexes, and has been attributed to the Marion plume prior to the separation of Madagascar from Greater India (e.g., Storey *et al*., 1995; Torsvik *et al*., 1998, 2000; Kumar *et al*., 2001). Remnants of the province are well-exposed and preserved along Mahajanga and the eastern coastal area, and in the Morondava sedimentary basins in western Madagascar (Mahoney *et al*., 1991; Storey *et al*., 1995; Melluso *et al*., 2001; Cucciniello *et al*., 2022). Further volcanism is also recorded through intrusions in to and extrusions on to Precambrian basement. The original volume of the province is poorly constrained, but likely exceeded 1 Mkm^3, including the Madagascar Plateau flanking the south coast of the island, as well as the Conrad Rise (Storey *et al*., 1995). Age estimates for Madagascar LIP volcanism largely range between ~93–86 Ma, based largely on $^{40}Ar/^{39}Ar$ and some U-Pb dating, together with biostratigraphic constraints based on interbedded sedimentary rocks (Storey *et al*., 1995; Torsvik *et al*., 2000; Melluso *et al*., 2001, 2005; Pande *et al*., 2001; Mahoney *et al*., 2008; Cucciniello *et al*., 2011, 2013, 2021, 2022; see also Jiang *et al*., 2023). Because these ages are close to that of the Cenomanian–Turonian boundary, it has been postulated that the Madagascan LIP might have contributed to environmental change associated with OAE 2. However, statistical appraisals of the available ages shows that volcanic activity initially peaked in northern Madagascar and spanned 3 Myr between 93–90 Ma (Cucciniello *et al*., 2022), slightly postdating OAE 2. Thus, it is unlikely that the Madagascan LIP played a major role in triggering environmental change associated with that OAE.

2.7. The Deccan–Traps and the Cretaceous–Palaeogene interval

Major eruptions associated with the Deccan Traps (western India) commenced during the latest Maastrichtian, 300–400 kyr prior to the end of the Cretaceous Period (66.04 Ma; Gale *et al*., 2020), and continued into the earliest Palaeogene (Schoene et al., 2019; Sprain et al., 2019 and references therein). It has been suggested that a smaller-scale phase of Deccan eruptions occurred earlier in the Cretaceous (68–67 Ma; see Chenet *et al.*, 2007; Parisio *et al.*, 2016). However, subsequent data have cast doubt on the occurrence of major eruptions significantly prior to the main-phase of Deccan volcanism (Schoene *et al.*, 2015). By far the most intensely studied part of the Deccan Traps is the Western Ghats region, which comprises a cumulative thickness of ~3000 m of tholeiitic basalts in multiple flood basalt units stratigraphically separated by oxidised 'red-bole' palaeosols (Widdowson *et al.*, 1997, and references therein). Magnetostratigraphic studies of the Western Ghats basalts show that the main phase of Deccan volcanism began just prior to the start of the C30n–C29r chron reversal (66.38 Ma), and concluded just after the C29r–C29n reversal at 65.7 Ma (Courtillot *et al.*, 1986, 2000; Chenet *et al.*, 2009). This <1 Myr duration is supported by numerous recent geochronological investigations utilising both $^{40}Ar/^{39}Ar$ ages of Deccan basalts (66.31–65.72 Ma; e.g., Renne *et al.*, 2015; Sprain *et al.*, 2019) and U-Pb dating of zircons preserved in the red-boles interbedded between with them (66.26–65.63 Ma; e.g., Schoene *et al.*, 2015, 2019; Eddy *et al.*, 2020). Recent modelling of eruption rates in the Western Ghats, based on $^{40}Ar/^{39}Ar$ geochronology, highlighted a pronounced rise in eruption volume between the Bushe and Poladpur formations, around the time of the Cretaceous–Palaeogene (KPg) transition and Chicxulub impact (Renne *et al.*, 2015; Sprain *et al.*, 2019). An acceleration in volcanism beginning with Poladpur eruptions is also shown by U-Pb based modelling, but manifesting as a series of discrete pulses that began 50–100 kyr prior to the KPg event and bolide impact (Schoene *et al.*, 2019). However, U-Pb geochronology of red-bole zircons from the Malwa plateau indicate that there were highly voluminous Deccan eruptions occurring between in the northern part of the province up to 350 kyr prior to the KPg event (Eddy *et al.*, 2020). Additionally, part of the Deccan magmas are preserved offshore from the Indian coast and may comprise a volume significantly greater than the well-studied onshore volcanics, with little known regarding their eruptive history (Mittal *et al.*, 2022).

The last 300–400 kyr of the Cretaceous were marked by up to 2–3 °C of climate warming (the Late Maastrichtian Warming Event), which has been documented in shallow and deep marine settings around the world by both oxygen-isotope and TEX_{86} data (e.g., Li and Keller, 1998a; Westerhold *et* *al*., 2011; Esmeray-Senlet *et al*., 2015; Vellekoop *et al*., 2016; Barnet *et al*., 2017; Woelders *et al*., 2017, 2018; Hull *et al*., 2020). Cyclostratigraphic and magnetostratigraphic age models across a number of these sites demonstrate that the warming commenced coevally with the onset of Deccan volcanism, supporting a causal link between the two phenomena (Barnet *et al*., 2017; Woelders *et al*., 2017; Hull *et al*., 2020; Gilabert *et al*., 2022). Intriguingly, temperatures then declined around 100–200 kyr before the end of the Cretaceous, despite continuing Deccan activity (Vellekoop *et al*., 2016; Barnet *et al*., 2017; Woelders *et al*., 2017, 2018; Hull *et al*., 2020). A rise in SO_2 contents of Deccan basalts from 750 ppm to 1800 ppm, and thus of assumed volatile emissions, just prior to the end of the Cretaceous may have aided this cooling pulse (Callegaro *et al*., 2023). A second (geologically brief) warming pulse in the final 10s kyr of the period has been postulated, although evidence for this second temperature increase has been reported from only a few locations (Stüben *et al*., 2003; Keller *et al*., 2020; O'Connor *et al*., 2023; c.f., Vellekoop *et al*., 2016; Woelders *et al*., 2017; Barnet *et al*., 2018; Hull *et al*., 2020). It is assumed that these temperature changes occurred in response to carbon cycle disturbances following Deccan CO_2 emissions (e.g., Li and Keller, 1998a; Robinson *et al*., 2009; Esmeray-Senlet *et al*., 2015; Vellekoop *et al*., 2016; Hull *et al*., 2020). However, there is no clear $\delta^{13}C$ excursion in upper Maastrichtian strata comparable in magnitude to those of the Cretaceous OAEs (Woelders *et al*., 2017; Barnet *et al*., 2018), although the lack of a negative isotopic shift may result from Deccan carbon output being primarily magmatic in origin, rather than thermogenic (Self *et al*., 2006; see also Ganino and Arndt, 2009).

The KPg boundary, which marks the most recent of the 'Big Five' Phanerozoic mass extinctions (Raup and Sepkowski, 1982), also overlapped in time with Deccan volcanism. This extinction has been compellingly linked to the coeval Chicxulub impact by global enrichment of iridium and other platinum group elements in the extinction horizon, together with documented microspherules, shocked-quartz grains, and tsunami sediments (e.g., Alvarez *et al*., 1980; Schulte *et al*., 2010; Goderis *et al*., 2021). Nonetheless, it has been hypothesised that Deccan eruptions contributed towards causing this biospheric crisis, either in combination with the Chicxulub impact or independently (e.g., Courtillot and Renne, 2003; Keller, 2012; Font *et al*., 2016; Petersen *et al*., 2016; Callegaro *et al*., 2023; Cox and Keller, 2023). The different hypotheses proposed regarding the links between the Chicxulub impact, Deccan Traps, and extinction event are outlined in more detail elsewhere (see e.g., Schulte *et al.*, 2010; Richards *et al.*, 2015; Punekar *et al.*, 2016; Schoene *et al.*, 2019; Hull *et al.*, 2020; Callegaro *et al.*, 2023; Cox and Keller, 2023; Senel *et al.*, 2023), and are not further discussed here.

2.8. The link between LIP volcanism and environmental change

Many major environmental perturbations during the Cretaceous were marked by pronounced climate warming on a global scale (with the Weissert Event and parts of OAE 1b the likely exceptions), and LIP related emissions of carbon dioxide are widely accepted to have been a key trigger of this temperature rise (e.g., Jenkyns, 2010; Weissert and Erba, 2004; Bond and Wignall, 2014; Bodin *et al.*, 2015). Carbon outgassing of LIP basalts remains poorly constrained, however, and it is uncertain whether magmatic emissions would have been sufficient to greatly impact atmospheric CO_2 levels (see Self *et al.*, 2006, 2014; Black *et al.*, 2021). As noted above, thermogenic carbon emissions associated with heating of organic-rich sediments by intruding magmas have been proposed as an additional/alternative trigger of climate warming during OAE 1a (Polteau *et al.*, 2016; Deegan *et al.*, 2022). This mechanism has also been suggested for the Late Maastrichtian Warming Event (Eddy *et al.*, 2020; Hernandez Nava *et al.*, 2021), although the limited evidence for organic-rich sediments that were intruded by Deccan magmas and the lack of a $\delta^{13}C$ negative excursion in uppermost Cretaceous strata do not support this hypothesis. Regardless of the specific carbon source, any episode of Cretaceous climate warming likely resulted in acceleration of the global hydrological cycle, enhancing continental weathering and nutrient runoff to the oceans, and consequently stimulating eutrophication and seawater oxygen depletion, aided by ocean stratification and stagnation directly caused by oceanic temperature increase (see Jenkyns, 2010; Bond and Sun, 2021, and references therein). The carbon emissions themselves could also have directly resulted in ocean acidification and associated environmental stress (Erba *et al.*, 2010).

Establishing better constraints on the timing of volcanic activity from sedimentary records that document surface temperature fluctuations and/or environmental conditions and biospheric changes is key to resolving the complex relationships between LIP emplacement and their impact on Earth's climate and environment. In recent years, the development of several geochemical proxies of volcanism has enabled reconstruction of the timing of LIP activity in the stratigraphic archives that record episodes of environmental and/or biota perturbation. Osmium-isotope compositions (specifically $^{187}Os/^{188}Os$) and mercury (Hg) concentrations represent two such proxies (see reviews by Grasby *et al.*, 2019; Dickson *et al.*, 2021; Percival *et al.*, 2021a). Differences in the compatibility of osmium and rhenium (Re) within silicates result in mantle rocks and LIP basalts derived from mantle-plume volcanism typically being enriched in primitive osmium compared to rhenium, giving them an unradiogenic Os-isotope composition ($^{187}Os/^{188}Os \sim 0.13$; Allègre *et al.*, 1999). Thus, intense LIP volcanism and/or the weathering (or submarine alteration) of juvenile basalts should cause a geologically rapid increase in the flux of unradiogenic Os to the global ocean relative to the comparatively constant background input from mid-ocean ridges and extraterrestrial material, lowering seawater $^{187}Os/^{188}Os$ ratios (e.g., Peucker-Ehrenbrink and Ravizza, 2000). Conversely, the felsic crust is marked by higher Re/Os ratios, with decay of ^{187}Re to ^{187}Os over long geological timescales eventually resulting in a more radiogenic osmium-isotope composition of continental material and the riverine runoff derived from its erosion (average $^{187}Os/^{188}Os \sim 1.4$ today; Peucker-Ehrenbrink and Jahn, 2001). Thus, seawater $^{187}Os/^{188}Os$ ratios can also increase if continental weathering rates increase. Because osmium has a seawater residence time of 10s kyr, any significant change in the oceanic $^{187}Os/^{188}Os$ composition should be recorded in the hydrogenous phase of sedimentary rocks deposited throughout the global ocean, apart from hydrographically restricted basins where local sources may dominate (e.g., Paquay and Ravizza, 2012; Dickson *et al.*, 2015).

Mercury is emitted to the atmosphere as a volcanic volatile, with this source acting as a major natural source of the element to the Earth's surface today (Pyle and Mather, 2003). In the stratosphere, mercury has a residence time of 0.5–2 years, enabling it to be distributed over a hemispherical–global scale before being deposited in sediments (Schroeder and Munthe, 1998; Selin, 2009). Hence, numerous studies have utilised Hg contents as a proxy for volcanic activity in Earth's past, normalising against total organic carbon (TOC) to account for the element typically being bound to organic compounds during deposition (see reviews by Grasby *et al*., 2019; Shen *et al*., 2020; Percival *et al*., 2021a). Under highly euxinic conditions where free sulphides precipitate in the water column, Hg may be associated with that phase (Shen *et al*., 2019a, 2020). Mercury may be adsorbed on to clay minerals if neither organic carbon or sulphides are present (Kongchum *et al*., 2011; Shen *et al*., 2020). Adsorption on to iron-manganese oxides or hydroxides has also been reported in oxidised settings, particularly for some riverine, lacustrine and estuarine environments (e.g., Quémerais *et al*., 1998; Driscoll *et al*., 2013; Maher *et al*., 2020), although studies of other sites have reported preferential binding on to organic compounds (e.g., Feyte *et al*., 2010; Cossa *et al*., 2021).

Any or all of remobilisation of sedimentary mercury related to water-column and/or sediment redox changes, input from wildfires or enhanced terrigenous runoff, variation in organic-matter type (from marine to terrestrial), and diagenetic removal of sedimentary TOC can alter sedimentary Hg contents and Hg/TOC ratios independently of volcanism (e.g., Hammer *et al*., 2019 Them *et al*., 2019; Charbonnier *et al*., 2020a; Frieling *et al*., 2023). Thus, reconstructing a volcanically triggered perturbation to the global mercury cycle depends on documenting stratigraphically correlative Hg enrichments in multiple sites distributed across the world and considering any potential local inputs of the element. Moreover, submarine volcanic activity may have a very limited dispersal range of mercury due to the rapid scavenging and transformation of mercury species in hydrothermal vents, resulting in an apparent nearfield drawdown of Hg emitted directly into seawater (within 100s km; Bowman *et al*., 2015; see also Scaife *et al*., 2017; Percival *et al*., 2018, 2021b).

Despite the advances in tracking LIP volcanism in stratigraphic records of major climate/environmental change, relatively few studies have combined geochemical proxies of volcanism and surface temperature in the same site (but see Robinson *et al*., 2009; Bottini *et al*., 2015; Schoene *et al*., 2019; Percival *et al*., 2020). Thus, questions remain regarding the extent to which volcanic activity triggered climate warming and consequent environmental degradation during the Cretaceous. These questions particularly pertain to OAE 1a, with magmatic CO_2, thermogenic carbon, and methane clathrate release all suggested as a cause of climate warming during the onset of the event (e.g., Jahren *et al*., 2001; Méhay *et al*., 2009; Naafs *et al*., 2016; Adloff *et al*., 2020; Deegan *et al*., 2022). Moreover, hydrothermal nutrient (e.g., Fe, V, Cu) output from submarine G-OJP volcanism may have directly enhanced primary productivity and triggered widespread marine anoxia during OAE 1a independently of global temperature change (see Erba *et al*., 2015). Here, the record of LIP volcanism during OAE 1a is investigated at two sites that have been previously studied for palaeotemperature trends (Figure 2): DSDP Site 398 (Vigo Seamount, Atlantic Ocean), and Alstätte-1 (Lower Saxony Basin, NW Germany). The documented relationship between volcanism and environmental change during OAE 1a is placed into the wider context of how LIP activity impacted the global climate during that event. This scenario is then discussed in a broader overview of the geochemical records and environmental and biotic impacts of large igneous provinces during the Cretaceous Period.

3. STUDY SITES

The expanded Early Aptian stratigraphic record recovered from DSDP Site 398 consists of repeating dark grey–green turbiditic sedimentary sequences spanning several 10s m thickness. The strata are composed primarily of dark mudstones and claystones with some layers of calcareous sandstones and graded quartz-based sandstones–mudstones, deposited on the southern flank of the Vigo Seamount, just off the Iberian Margin (Ryan *et al*., 1979; Sigal, 1979). Preservation of terrigenous material (including terrestrial organic matter) indicates that the sediments were likely deposited as part of a submarine fan, potentially related to deltaic progradation (Arthur, 1979). However, a generally low BIT (branched and isoprenoid tetraether) index of organic matter studied from the sediments suggests that terrestrial organics do not dominate the setting (Naafs and Pancost, 2016). There is no black-shale layer at this locality comparable to those typically associated with Lower Aptian stratigraphic records (Arthur, 1979). Instead, OAE 1a strata have been identified by trends in the $\delta^{13}C$ composition of organic matter, in combination with calcareous nannofossil biostratigraphy (Bralower *et al.*, 1994; Li *et al.*, 2008). Palaeoenvironmental reconstructions from this site, based on TEX_{86}, have highlighted warm sea-surface temperatures prior to OAE 1a, which rose slightly during the event but significantly declined after it (Naafs and Pancost, 2016).

The Alstätte-1 section represents a boreal record of OAE 1a, and primarily consists of organic-rich laminated mudstones and marlstones that were deposited into the epicontinental Lower Saxony Basin during the Early Aptian (Hoffmann and Mutterlose, 2011). Palaeogeographic reconstructions, geochemical data, palaeontological findings, and the preservation of organic-rich sediments deposited under anoxic conditions all indicate that the basin was likely hydrographically restricted to some degree during Barremian–Aptian times, potentially including the OAE 1a interval (Pauly *et al.*, 2013). However, Aptian fauna recovered from strata below and in the OAE 1a interval are mainly of Boreal endemic composition, and co-occur with cosmopolitan taxa (ammonites, belemnites), with the earliest cosmopolitan species documented a few meters below the OAE 1a level. Highly distinctive Tethyan belemnites are preserved directly above OAE 1a strata, suggesting strong sea-way connectivity and faunal exchange with the NW Tethys immediately following the event (Mutterlose, 1998; Mutterlose and Böckel, 1998). Lower Aptian strata and the OAE 1a interval have been identified from a combination of belemnite, ammonite, and nannofossil biostratigraphy, integrated with $\delta^{13}C$ studies (Bottini *et al.*, 2012). TEX_{86}-derived sea-surface temperature reconstructions highlight a sharp rise from <30 °C prior to OAE 1a to 33 °C during the event, but mild cooling during the middle of the OAE and after it had concluded (Mutterlose *et al.*, 2014). The initial warming is potentially supported by a negative excursion in belemnite $\delta^{18}O$ correlative with the shift in TEX_{86} (Mutterlose *et al.*, 2014).

4. METHODOLOGY

4.1. Osmium-isotope analysis

Osmium abundances and isotopic values were determined by isotope dilution and negative thermal ionization mass spectrometry (N-TIMS) on a Thermo Fisher Scientific TRITON at the Japan Agency for Marine-Earth Science and Technology (JAMSTEC), Japan. Sample preparation followed the protocol described in Ishikawa *et al.* (2014) and Matsumoto *et al.* (2020), and broadly follows the procedures developed by Cohen and Waters (1996) and Birck *et al.* (1997). Briefly, powdered samples were spiked with a ^{185}Re and ^{190}Os-rich solution and sealed in quartz glass tubes with 4 mL of inverse aqua regia. After being heated at 230°C for 48 hours, osmium was separated and purified by CCl_4 extraction, HBr back extraction, and standard micro-distillation techniques. Rhenium was purified from the aqua regia phase through anion chromatography, with Re concentrations determined via quadrupole inductively coupled plasma mass spectrometry (Thermo Fisher Scientific iCapQ) at JAMSTEC. Procedural blanks averaged 0.10 ± 0.08 pg Os and 22 ± 10 pg Re, with a $^{187}Os/^{188}Os$ ratio of 0.166 ± 0.004 (1SD, n = 3). Analytical uncertainty and precision were monitored through repeated measurements of the JMC Os standard, giving $^{187}Os/^{188}Os$ values of 0.1069 ± 0.0008 (1SD, n = 3), consistent with previously reported values ($^{187}Os/^{188}Os$ = 0.106838 ± 0.000015; Nozaki et al., 2012). The past seawater Os-isotope composition at the time of deposition ($^{187}Os/^{188}Os_{(i)}$) is calculated from the modern-day measured $^{187}Os/^{188}Os$ and $^{187}Re/^{188}Os$ compositions of a sedimentary rock sample and its age in order to account for the post-depositional decay of ^{187}Re to ^{187}Os (Cohen *et al.*, 1999). The initial sedimentary Os concentration at the time of deposition [$Os_{(i)}$] is determined by utilizing the determined $^{187}Os/^{188}Os_{(i)}$ ratio together with the measured $^{187}Os/^{188}Os$ composition and Os and ^{192}Os concentrations of a rock sample, assuming $^{192}Os/^{188}Os$ of 3.08271 (Percival *et al.*, 2021b).

4.2. Mercury concentrations

Mercury concentrations were determined on an Advanced Mercury Analyser (AMA) 254.7 at the Vrije Universiteit Brussel (VUB), Belgium, following the procedure outlined in Liu *et al.* (2021). The limit of detection for the AMA based on repeated blank analyses (n = 33 across the two sample sets) was 0.09 ng, calculated as 3 times the standard deviation on the blank measurements, one–two orders of magnitude below the content in a measured sample. 100 ± 2 mg of powdered sample was used per analysis, with repeatability of the results monitored through at least two measurements for each sample. Analytical accuracy was further tested through repeated measurements of the certified reference materials MESS-3 (marine sediment) and JP-1 (peridotite), yielding average concentrations of 89.50±1.93 ng/g (1 SD, n = 24) and 4.86±0.38 ng/g (1SD, n = 6), respectively, across analysis of the two sample sets, consistent with established compiled values (MESS-3 = 91±9 ng/g; JP-1 = 5.3 ng/g).

4.3. Total organic carbon and total sulphur contents

Total organic carbon (TOC) and total sulphur (TS) contents were determined on a Nu Instruments Horizon 2 coupled to a Eurovector isotope ratio mass spectrometer (IRMS) elemental analyzer EuroEA3000 at the VUB. Prior to TOC analyses, the samples were decarbonated with 10% HCl following the procedure outlined in Liu *et al.* (2021), in order to remove inorganic carbon (assumed to be entirely in carbonate form). Carbon content calibration was performed using the certified reference material IAEA-CH-6 (sucrose). Data accuracy and reproducibility was monitored through repeated analyses of international standards IVA33802151 (organic-rich sediment) and IVA33802153 (organic-poor soil), with analytical uncertainty typically better than ±0.1 wt% (1SD). The measured carbon content in decarbonated aliquots of each sample was converted to a bulk rock TOC value by accounting for the percentage sample mass lost following decarbonation. TS contents were measured on bulk-rock powder samples without any chemical pre-treatment. Sulphur content calibration on the IRMS was performed using the certified reference material IAEA-S-1 (silver sulphide), with data accuracy and reproducibility again better than ±0.1 wt% (1SD) based on repeated analyses of international standards: IVA33802151 and MESS-2 (estuarine sediment).

5. RESULTS

Early Aptian strata from DSDP Site 398 record a shift in $^{187}Os/^{188}Os_{(i)}$ ratios from a mean background of ~0.60 to a highly unradiogenic composition of ~0.20 across the OAE 1a level, before a return towards more radiogenic pre-event values above it (Figure 3A). The sample with the most unradiogenic Os-isotope composition is also marked by a large enrichment in $[Os]_{(i)}$ (1323 pg/g, compared to a mean of 173 pg/g for the rest of the record). A transient rise in $^{187}Os/^{188}Os_{(i)}$ up to 0.69 in basal OAE strata is superimposed on to the initial unradiogenic signal. Mercury concentrations show significant variation, ranging from 18–100 ng/g (mean 49 ng/g) below the OAE 1a level and in basal OAE strata, before rising slightly to an average of 63 ng/g with a peak of 129 ng/g in upper part of the OAE level, and further still above it (averaging 86 ng/g with spikes up to 220 ng/g). Whilst TOC and TS contents also vary considerably at DSDP Site 398 (between 0.19–2.09 wt% and 0.10–1.25 wt%, respectively), there is no clear stratigraphic trend. Thus, the Hg enrichments are largely mirrored by peaks in Hg/TOC and Hg/TS ratios. There is a clear Hg/TOC peak in the middle part of the OAE 1a level between 1563 and 1557 mbsf (average Hg/TOC = 197 ng/g/wt%; average Hg/TS = 342 ng/g/wt%), and additional spikes of up to 394 ng/g/wt% and 1054 ng/g/wt%, respectively, above it (Figure 3A). There is no clear linear relationship between Hg and either TOC or TS (R^2 values of 0.09 and 0.07, respectively).

The $^{187}Os/^{188}Os_{(i)}$ trends documented at Alstätte-1 differ markedly from those of DSDP Site 398, rising from a background average of ~0.77 to over 0.9 at the base of the OAE 1a level, but with values remaining high ($^{187}Os/^{188}Os_{(i)}$ >0.7) throughout the OAE strata (Figure 3B). A shift to more unradiogenic Os-isotope compositions of ~0.34 (and slight increase in $[Os]_{(i)}$ concentrations from 95 to 173 pg/g) only takes place above OAE 1a strata. Mercury concentrations at Alstätte-1 are also elevated around the OAE 1a level (mean 49 ng/g) with three spikes to ~100 ng/g or more, compared to background contents of 27 ng/g (Figure 3B). However, TOC and TS contents also rise in OAE strata; thus, there is no systematic increase in Hg/TOC or Hg/TS in basal OAE 1a strata. There is an increase in Hg/TS from ~32 to 100 ng/g/wt% in the upper part of the OAE level, but this rise is not correlative with any increase in Hg concentrations; rather with a fall to very low TS contents. Some small spikes in Hg/TOC (up to 109 ng/g/wt% compared to a background of 29 ng/g/wt%) do correlate with the three peaks in Hg concentrations; however, those samples also have very high sulphur contents. Indeed, there is a strong linear correlation between Hg and TS concentrations at Alstätte-1 ($R^2 = 0.73$; compared to $R^2 = 0.05$ between Hg and TOC), potentially suggesting that local drawdown with sulphide was the main control on Hg deposition under the highly oxygen-depleted conditions in the Lower Saxony Basin. OAE 1a black shales from Alstätte-1 are known to yield abundant pyrite, suggesting that sulphide sorption was the main control on Hg contents in this oxygen-depleted setting.

6. DISCUSSION

6.1. OAE 1a as a case study of how LIPs impacted the Cretaceous global environment

The $^{187}Os/^{188}Os_{(i)}$ and $[Os]_{(i)}$ trends recorded at DSDP Site 398 closely resemble those from previous studies of OAE 1a. Very low $^{187}Os/^{188}Os_{(i)}$ values recorded in middle–upper OAE 1a strata support a major influx of unradiogenic osmium to the global ocean during that event, likely linked to G-OJP activity (Tejada *et al.*, 2009; Bottini *et al.*, 2012; Adloff *et al.*, 2020; Martínez-Rodríguez *et al.*, 2021; Percival *et al.*, 2021b). Recorded Os-isotope trends from several other sites also document a volcanically triggered shift towards a more unradiogenic seawater composition immediately prior to OAE 1a, with this change also potentially documented at DSDP Site 398 by a single data point (1171.33 mbsf). Basal OAE 1a strata only show a clear mercury enrichment at a single site very close to that LIP (Percival *et al.*, 2021b). This non-dispersal of mercury is consistent with the short residence time of volcanic Hg emitted into seawater (see Bowman *et al.*, 2015), and supports submarine volcanism on the G-OJP as the main source of unradiogenic Os to the global ocean during OAE 1a.

The shift to more radiogenic $^{187}Os/^{188}Os_{(i)}$ compositions across OAE 1a strata at Alstätte-1 represents a markedly different trend from that recorded at all other sites. This disparity likely indicates that the Lower Saxony Basin was too hydrographically restricted for significant water-mass exchange with the global ocean, despite having enough connection to permit faunal migration. In this context, the shift to higher $^{187}Os/^{188}Os_{(i)}$ values across the OAE 1a level at Alstätte-1 may highlight a rise in local riverine runoff to the Lower Saxony Basin from enhanced continental weathering in response to elevated atmospheric CO_2 and global temperatures, given that this flux typically represents the main source of radiogenic osmium to seawater. Notably, the radiogenic shift at Alstätte-1 begins at the base of C3 (3.8 m), and age-equivalent C3 strata at DSDP Site 398 (1169.8–1164.54 mbsf) and other locations are also marked by a transient rise in $^{187}Os/^{188}Os_{(i)}$ values between the unradiogenic pulses (Figure 4). This stratigraphic correlation supports previous interpretations that the transient radiogenic Os-isotope shift recorded in C3 strata at DSDP Site 398 and elsewhere likely reflects a weathering pulse superimposed on an overarching signal of submarine LIP activity, rather than a spell of volcanic quiescence between two distinct pulses of volcanism (e.g., Tejada *et al.*, 2009; Bottini *et al.*, 2012; Martínez-Rodríguez *et al.*, 2021). Strontium-, calcium-, and lithium-isotope studies of OAE 1a also support a rise in global weathering rates during the onset of the event (Jones and Jenkyns, 2001; Blättler *et al.*, 2011; Lechler *et al.*, 2015).

When stratigraphic trends in $^{187}Os/^{188}Os_{(i)}$ are compared with temperature proxies from records of OAE 1a, it is clear that the highest temperatures indicated by $\delta^{18}O$ or TEX_{86} data are documented above the radiogenic osmium shift and the C3 excursion, stratigraphically correlative with the most unradiogenic $^{187}Os/^{188}Os_{(i)}$ compositions recorded in OAE 1a strata (upper C3–lower C4; see also Bottini *et al.*, 2015). These trends support an intensification in LIP volcanism and associated carbon emissions as the main driver of this further rise in global temperatures during OAE 1a. A pronounced increase in Hg contents and Hg/TOC enrichments across upper C3–lower C4 strata at DSDP Site 398 and some (though not all) other sites across the globe might reflect a potential intensification in volcanic activity or switch to subaerial eruptions after the start of OAE 1a (see Charbonnier and Föllmi, 2017; Percival *et al.*, 2021b; Vickers *et al.*, 2023). The latter possibility is consistent with a scenario in which the G-OJP was initially emplaced through submarine volcanism (enabling worldwide dispersal of unradiogenic Os but only nearfield Hg enrichment), before becoming emergent above the sea surface and leading to more global distribution of mercury from subaerial eruptions. However, it should be noted that the C3–C4 Hg enrichments could also reflect localised environmental perturbations such as redox changes or enhanced wildfires/runoff of terrestrial organic matter (see Percival *et al.*, 2021b). A not-exclusively-volcanic cause of the C3–C4 mercury enrichments is supported by the enhanced Hg and Hg/TOC values recorded above the OAE 1a level at DSDP Site 398, in strata that postdate the time of LIP volcanism reconstructed from $^{187}Os/^{188}Os_{(i)}$ trends. Unless subaerial eruptions occurred later than and entirely separately from submarine volcanism (which is implausible if both were related to the same LIP), it is highly unlikely that these post-event Hg peaks were volcanically derived. Instead, the post-OAE Hg enrichments may have been caused by variability in the input of terrestrial organic matter from the nearby palaeoshoreline (Hammer *et al.*, 2019), or the return to a more oxygenated water column (Frieling *et al.*, 2023), although there is no direct evidence of major redox change at DSDP Site 398.

There is also a potential correlation between an initial shift towards more unradiogenic Os-isotope values and possible higher sea-surface temperatures below the C3 negative $\delta^{13}C$ excursion at DSDP Site 398. This earlier temperature rise is less pronounced than the later one during the OAE itself, and the fall in $^{187}Os/^{188}Os_{(i)}$ values is based on one data point. Nonetheless, an unradiogenic shift in the marine Os-isotope composition and rise in surface temperatures just prior to the C3 excursion and onset of OAE 1a is supported by data from other stratigraphic archives in the NW Tethys and the Subbetic margin (e.g., Tejada *et al.*, 2009; Keller *et al.*, 2011; Bottini *et al.*, 2012, 2015; Lorenzen *et al.*, 2013; Castro *et al.*, 2021; Martínez-Rodríguez *et al.*, 2021; Figure 4). A crisis in nannoconid fauna is also recorded below the base of OAE 1a strata *sensu stricto* in several sites (see section 6.3). Lead-isotope and trace-element datasets further support an onset of volcanic activity that was coeval with the nannoconid crisis but prior to the C3 (Kuroda *et al*., 2011; Erba *et al*., 2015; Figure 4). Assuming that there was a single prolonged pulse in G-OJP activity recorded by the unradiogenic shifts in $^{187}Os/^{188}Os_{(i)}$, which began before and continued after a transient increase in continental weathering rates, the combined geochemical and palaeontological datasets suggest that magmatic carbon emissions associated with submarine LIP volcanism likely triggered the initial warming and nannoconid crisis immediately prior to the onset of OAE 1a.

These datasets also support a non-volcanic carbon source, likely related to thermogenic emissions or methane clathrate release, as the driver of the C3 $\delta^{13}C$ negative excursion. Osmium-isotope trends in those strata primarily record enhanced continental weathering rather than LIP activity. Furthermore, there is no clear global mercury signal of volcanism at that time. Both methane clathrates and thermogenic carbon are isotopically lighter than magmatic CO_2, with the latter potentially sourced from intrusive magmatism related to the HALIP (see above; also Polteau *et al*., 2016). Thus, either carbon source could potentially have caused the $\delta^{13}C$ negative shift without greatly changing atmospheric CO_2 levels or affecting global temperatures (Méhay *et al*., 2009; Naafs and Pancost, 2016; Adloff *et al*., 2020). This scenario is consistent with the geochemical and palaeontological evidence for volcanism as the main driver of climate warming and biota stress prior to and during OAE 1a, but with a non-volcanic carbon source as the driver of the C3 negative excursion (Méhay *et al*., 2009; Adloff *et al*., 2020). However, it is less clear which carbon source (if either) played the dominant role in initiating the widespread marine anoxia that characterised this event.

6.2. Overview of geochemical evidence for the (variable) links between LIP volcanism and Cretaceous episodes of major environmental change

The entirety of Cretaceous stratigraphic history has been investigated for trends in oceanic strontium-isotope compositions (see reviews by Jones and Jenkyns, 2001; McArthur *et al*., 2020), and large parts also for seawater $^{187}Os/^{188}Os_{(i)}$ reconstructions (see e.g., Peucker-Ehrenbrink and Ravizza, 2020; Matsumoto *et al.*, 2022; and Figure 5). Reconstructed $^{187}Os/^{188}Os_{(i)}$ trends for most Cretaceous episodes of environmental change are similar to OAE 1a, showing pronounced unradiogenic shifts that are assumed to result from one or more of submarine volcanism, weathering of juvenile LIP basalts, or some other form of basalt-seawater interaction (Figure 5A, and references therein). Some more local-scale episodes of environmental perturbation are also marked by unradiogenic shifts of a smaller magnitude (Matsumoto *et al.*, 2021). Thus, osmium-isotope stratigraphy strongly supports the link between LIP emplacement and Cretaceous climate/environmental change. Additionally, a more gradual $^{187}Os/^{188}Os_{(i)}$ trend towards more unradiogenic compositions in the Late Cretaceous following OAE 2, an interval not coeval with environmental change, has been linked with weathering of Caribbean and Madagascan LIP basalts (Matsumoto *et al.*, *in press*). Interestingly, clear shifts towards primitive-mantle compositions of strontium isotopes are only documented for OAE 1a and OAE 2 (Figure 5B), albeit with less sharp stratigraphic trends due to the longer residence time of strontium in seawater (>2 Myr; Palmer and Edmond, 1989). Those intervals are also associated with the highest magnitude unradiogenic Os-isotope shifts in the Cretaceous. Collectively, the strontium and osmium trends may suggest that LIP activity, or at least the flux of mafic elements to seawater, was greater during those intervals than for other Cretaceous events. In addition to strontium and osmium datasets, evidence for some form of magmatic activity during OAEs 1a and 2 has also been inferred on the basis of lead-, neodymium-, chromium-, and zinc-isotope studies, and trace-element enrichments (Larson and Erba, 1999; Snow *et al.*, 2005; Kuroda *et al.*, 2007; Zheng *et al.*, 2013; Erba *et al.*, 2015; Holmden *et al.*, 2016; Sweere *et al.*, 2018).

Stratigraphic mercury records of Cretaceous events also yield information on the style and/or provenance of magmatic activity. Like OAE 1a, where mercury enrichment in basal C3 strata was only documented at a site proximal to the G-OJP, there is limited global evidence for peaks in Hg and Hg/TOC in OAE 2 strata, with small enrichments at some records deposited relatively proximally to LIPs (Scaife *et al.*, 2017, Percival *et al.*, 2018). This pattern of a more localised mercury enrichment proximal to a LIP source is consistent with largely submarine volcanism during both events (Scaife *et al.*, 2017; Percival *et al.*, 2018, 2021b). Mercury records associated with OAE 1b are more limited, but spikes have been reported from the NW Tethys (Sabatino *et al.*, 2018). If these Hg enrichments were indeed volcanically derived, it may indicate that some Kerguelen Plateau volcanism at that time was subaerial. Albian-age mercury enrichments have also been reported from a lacustrine record in North China (Zhao *et al.*, 2022), although stratigraphic uncertainties hinder a clear correlation with the Tethys record or a connection to Kerguelen volcanism.

Interestingly, mercury records of Paraná-Etendeka and Deccan volcanism show considerable variability across different sites, despite both LIPs forming through subaerial eruptions (e.g., Percival *et al.*, 2018; Fendley *et al.*, 2019; Charbonnier *et al.*, 2020b). Hg enrichments have been reported from strata that record the onset of the Weissert Event (Charbonnier *et al.*, 2017, 2020b), but because the duration of Paraná-Etendeka volcanism was at least 2–3 Myr (see section 2.1; also Dodd *et al.*, 2015; Gomes and Vasconcelos, 2021; Bacha *et al.*, 2022), those peaks cannot reflect the entire eruptive history of that LIP. It is possible that the less clear global mercury signals of the Paraná-Etendeka LIP reflect a generally lower volatile output or slower eruption rate than for other subaerial provinces (see Callegaro *et al.*, 2014; Dodd *et al.*, 2015). In this case, the Hg enrichments reported by Charbonnier *et al.*, (2017, 2020b) in basal Weissert Event strata could record a peak in the intensity of Paraná-Etendeka volcanism coeval with the onset of the crisis, consistent with the geochronological models of Gomes and Vasconcelos (2021) and Bacha *et al.* (2022). However, local environmental or sedimentological causes for those Hg peaks cannot be ruled out, particularly if significant Paraná-Etendeka volcanism post-dated the onset of the Weissert event, as suggested by Rocha *et al.* (2020). Similarly, uppermost Maastrichtian Hg peaks have been associated with Deccan eruptions (Keller *et al.*, 2020), most notably just below the KPg boundary (e.g., Font *et al.*, 2016; Keller *et al.*, 2018; Percival *et al.*, 2018; Fendley *et al.*, 2019). This peak stands in contrast to a comparative lack of evidence for a global-scale systematic enrichment in mercury at the onset of Deccan volcanism 300–400 kyr prior to the end of the Maastrichtian (Percival *et al.*, 2018). Thus, it may reflect an intensification of volcanism immediately prior to the extinction, consistent with the U-Pb geochronological model of Deccan eruptions (Schoene *et al.*, 2019). However, given that this Hg enrichment is not recorded globally, a non-volcanic cause cannot be excluded (which would be potentially consistent with the Deccan $^{40}Ar/^{39}Ar$ geochronology of Renne *et al.*, 2015, and Sprain *et al.*, 2019). Hg enrichments have also been reported for more minor episodes of environmental change, such as OAE 1d and the Faraoni Event (Charbonnier *et al.*, 2018; Yao *et al.*, 2021), but the possible existence and nature of any causal relationship between those crises and volcanism remains unclear.

Cyclostratigraphic correlation of KPg records clearly shows that the main phase of Deccan volcanism commenced coevally with the onset of late Maastrichtian climate warming (Schoene *et al.*, 2019; Hull *et al.*, 2020), as appears to have been the case for LIP activity and global temperature increases during OAE 1a. Geochemical evidence for a causal link between volcanism and climate warming during OAE 2 is also well documented at the stratigraphically condensed record of ODP Site 1260 (Forster *et al.*, 2007; Turgeon and Creaser, 2008). More expanded OAE 2 records, with better temporal resolution, show that LIP activity began prior to the onset of the OAE *sensu stricto*, leaving the exact chronology of volcanism *vs* climate warming at that time unclear (e.g., Du Vivier *et al.*, 2014). However, evidence of transient cooling pulses during both OAE 1a and OAE 2, such as the Plenus Cold Event (see section 2.4), is recorded in strata which also record Os-isotope evidence of intense LIP activity (Bottini *et al.*, 2015; Jenkyns, 2018; Percival *et al.*, 2020). The late Maastrichtian climate warming was also alleviated whilst Deccan volcanism was ongoing (e.g., Sprain *et al.*, 2019; Hull *et al.*, 2020). There are two possible explanations for these transient falls in temperature during times of LIP volcanism. The first model is that the LIP eruptions associated with those events featured spells during which volcanic carbon emissions were reduced (e.g., Sprain *et al.*, 2019, Hull *et al.*, 2020; Hernandez Nava *et al.*, 2021). Alternatively, and more plausibly for the OAEs, magmatic CO_2 output may have been offset by one or both of enhanced organic-carbon burial and an increase in global silicate weathering rates (Pogge van Strandmann *et al.*, 2013; Jenkyns *et al.*, 2017; Jenkyns, 2018; Robinson *et al.*, 2019; Percival *et al.*, 2020; Papadomanolaki *et al.*, 2022). Whilst the latter scenario might be expected to increase the input of radiogenic osmium to the ocean, apparently at odds with the low $^{187}Os/^{188}Os$ values documented during the Plenus Cold Event and other transient intervals of cooling during OAEs 1a and 2, it is possible that any continental weathering signal was overprinted by the unradiogenic Os flux from volcanism, or that primitive LIP basalts were the main lithology being eroded.

Climate cooling associated with the Weissert Event may have been caused by carbon sequestration during weathering of newly-erupted Paraná-Etendeka basalts, based on stratigraphic correlations between unradiogenic Os-isotope shifts and evidence of surface temperature decrease in Valanginian strata (Percival *et al.*, 2023). Elevated organic-matter burial in the terrestrial realm may have further drawn down carbon at that time (Westermann *et al.*, 2010). Alternatively, volcanic SO_2 emissions might have caused the cooling by leading to the formation of stratospheric sulphate aerosols, which may also have helped cause transient temperature falls during the latest Maastrichtian (see Self *et al.*, 2006; Schmidt *et al.*, 2016; Callegaro *et al.*, 2023). However, the short atmospheric residence time of those compounds and the slow eruption rate and potentially low sulphur content of Paraná-Etendeka basalts do not support this link (Callegaro *et al.*, 2014; Dodd *et al.*, 2015). Alternatively, the surface-temperature warming reconstructed from some NW Tethyan and proto-Atlantic records of the Weissert Event could suggest significant volcanic emission of CO_2 and other volatiles to the atmosphere, which may be supported by Hg enrichments in sedimentary records of that time (Charbonnier *et al.*, 2017, 2020b). Direct stratigraphic comparisons between global temperature and volcanic activity are currently lacking for other Cretaceous events. Nonetheless, it is clear that at least some Cretaceous LIPs had a pronounced impact on global climate, through volcanic CO_2 emissions and/or weathering of newly formed basalts.

Aside from changes in global climate, the environmental changes associated with the emplacement of Cretaceous LIPs were highly variable. Evidence of ocean acidification has been reported from stratigraphic records of OAEs 1a and 2, as well as the late Maastrichtian, with this fall in seawater pH likely resulting chiefly from the same carbon emissions that triggered climate warming during those time intervals (e.g., Erba *et al.*, 2010; Dameron *et al.*, 2017; Hart *et al.*, 2019; Jones *et al.*, 2023). To date, these postulated episodes of ocean acidification have largely been inferred from sedimentological and palaeontological evidence (see section 6.3), with little geochemical information regarding seawater pH.

Whilst the rises in global temperature during OAEs 1a and 2 were marked by the development of widespread marine anoxia/euxinia in both epicontinental shelf basins and across the global ocean, evidence for similar oceanic redox changes during the Late Maastrichtian warming or Weissert Event is limited. For example, numerous sedimentary records of OAEs 1a and 2 from both epicontinental shelf basins and open-ocean sites are marked by the appearance of organic-rich shales and changes in organic biomarker data, iron speciation, and changes in sedimentary elemental contents (particularly P, V, Mn, Mo, U, and TOC/P and I/Ca ratios) and N-, S-, Fe-, Mo-, Tl-, and U-isotope compositions, all of which are redox-sensitive proxies (e.g., Sinninghe Damsté and Köster, 1998; Kuypers *et al.*, 2004; Pancost *et al.*, 2004; Jenkyns *et al.*, 2007, 2017; Junium and Arthur, 2007; Mort *et al.*, 2007; van Bentum *et al.*, 2009; Lu *et al.*, 2010; Montoya-Pino *et al.*, 2010; Föllmi, 2012; Owens *et al.*, 2012, 2013; Ruvalcaba Baroni *et al.*, 2015; Dickson *et al.*, 2016; Ostrander *et al.*, 2017; Clarkson *et al.*, 2018; Siebert *et al.*, 2021; see also a review by Jenkyns, 2010). In the case of the Weissert Event, the limited expansion of anoxic water masses (and lithological/geochemical evidence thereof) may be attributed to the apparent lack of a clear temperature increase and associated seawater stratification/nutrient runoff and eutrophication in many parts of the world. However, the Late Maastrichtian Warming Event featured a temperature rise of 2 °C (Hull *et al.*, 2020); thus, an increase in seawater deoxygenation and evidence of this phenomenon might be expected. It is possible that the continued break-up of Pangaea through the Cretaceous caused evolution in global palaeogeography, shelf-basin extent, and ocean circulation, potentially decreasing the propensity of marine environments to become oxygen-depleted by the Maastrichtian. This mechanism has been proposed to explain the far greater extent of marine anoxia during OAEs 1a and 2 than the Palaeocene–Eocene Thermal Maximum (56 Ma), despite the latter event being marked by climate warming of a similar or greater magnitude and at a faster rate than for the Cretaceous events (e.g., Jenkyns, 2010; Dickson *et al.*, 2014; Clarkson *et al.*, 2021).

Another hypothesised trigger of marine anoxia during OAEs 1a and 2 is the enhanced output of trace-metal micronutrients from submarine ocean-plateau volcanism directly into seawater, elevating primary productivity and consumption of oxygen from the water-column (Kerr, 1998; Snow *et al.*, 2005; Erba *et al.*, 2015; see Figure 6). As a mechanism that depends on submarine LIP activity instead of continental volcanism, rather than global temperature increase, this model is consistent with the lack of widespread marine anoxia during the Weissert and Late Maastrichtian events, and is supported by enriched abundances of micronutrient metals in sedimentary records of OAEs 1a and 2, particularly those proximal to the G-OJP and Caribbean LIP (Larson and Erba, 1999; Snow *et al.*, 2005; Erba *et al.*, 2015). However, OAE 1b also coincided with submarine volcanism during emplacement of the Kerguelen Plateau, and has also been associated with climate warming, yet anoxic sediments are largely found in Atlantic and NW Tethyan sites (see section 2.3 above). It is possible that this distribution may reflect the relative paucity of OAE 1b sites studied thus far. However, the Os-isotope record of OAE 1b documents a much lower-magnitude unradiogenic shift than those recorded for OAEs 1a and 2 (see Figure 4). Thus, submarine LIP volcanism and associated trace metal output was likely more intense at the time of OAEs 1a and 2 than during OAE 1b (or any other time in the Cretaceous, see above). OAE 2 was also coeval with enhanced seasonality related to a peak in orbital eccentricity, which could have increased the susceptibility of the Earth system to the development of marine anoxia (Batenburg *et al.*, 2016). Furthermore, the relatively protracted nature of environmental change during OAE 1b (~4 Myr; Gale *et al.*, 2020; Ait-Itto *et al.*, 2023), compared to the geologically rapid onset of OAEs 1a and 2, may have mitigated the severity of environmental change during the Aptian–Albian transition.

6.3. The biotic response to Cretaceous LIP formation

Fossil evidence of biotic changes during times of LIP formation during the Cretaceous highlights considerable variation in the response of the marine biosphere to these major volcanic episodes. Furthermore, diversity patterns of the main planktonic and benthic carbonate producers in the Cretaceous, evaluated at the generic level, document disjunct trends for the two groups (Steuber et al., 2023). These differences suggest the importance of distinct environmental parameters in controlling the radiation and decline of marine groups, following different ecological strategies. The terrestrial biosphere was also impacted to some degree by different Cretaceous LIPs, with some indication of at least regional vegetation changes during the Weissert Event (Kujau *et al*., 2013) and OAE 1a (e.g., Cors *et al*., 2015; Galloway *et al*., 2022). A rise in terrestrial organic-matter burial associated with the Weissert Event $\delta^{13}C$ positive excursion may also reflect changes in the continental biosphere (Westermann *et al*., 2010). Furthermore, charcoal preservation in Aptian–Albian and OAE 2 strata suggest increased wildfire activity during parts of the Cretaceous (Brown *et al*., 2012; dos Santos *et al*., 2016; Wang *et al*., 2019; Baker *et al*., 2020; Xu *et al*., 2022), potentially resulting from climate warming and elevated atmospheric oxygen levels following enhanced primary productivity in the case of the latter time interval (Baker *et al*., 2020). However, Heimhofer *et al*. (2004) reported relatively stable terrestrial vegetation during and after OAE 1a. Overall, the comparative paucity of the continental stratigraphic record compared to that of the marine realm means that the ocean biosphere is much more studied and better understood, and is the focus of this section hereafter.

A pronounced impact of environmental change associated with Cretaceous LIPs has been documented for benthic carbonate platform dwellers (dasycladales, larger benthic foraminifera, corals, rudists; see overview by Steuber et al., 2023; Figures 5C–E). Shortly before or during the onset of OAE 1a, carbonate platforms and their benthic biota experienced a substantial decline particularly in the mid latitudes. Dasycladacean algae and large benthic foraminifera are marked by significant diversity declines across OAE 1a and (especially) OAE 2, with aragonitic taxa chiefly affected. Rudist genera disappeared during OAE 1a from higher latitudes but survived in more equatorial settings. This abrupt decline of aragonitic taxa is thought to be related to the major increases in atmospheric CO_2 and very high sea-surface temperatures caused by LIP eruptions, resulting in a shallowing of the carbonate-compensation depth (e.g., Ridgwell, 2005; Foster *et al*., 2017), reduced seawater carbonate saturation, and a subsequent calcification crisis (Bauer *et al*., 2017).

The same mechanism could have caused the retreat of shallow-water carbonate platforms to low latitudes in the aftermath of OAEs 1a and 2. Coral diversity was significantly reduced in the aftermath of OAE 2, and to a lesser extent after OAE 1a (Figure 5E), with high sea-surface temperatures and presumably low seawater pH likely reducing the photosymbiotic activity of zooxanthellid corals and large benthic forams (Kiessling and Kocsis, 2015; Reddin *et al.*, 2021; Steuber *et al.*, 2023). This interpretation is supported by an increase of azooxanthellate coral genera after OAE 1a, potentially reflecting a bleaching effect. Corals living in symbioses with dinoflagellates were thus partly replaced by corals missing these symbionts, supporting a decline of photosymbiosis due to high temperatures (e.g., Kiessling and Kocsis, 2015). Carbonate platform drowning has been documented during several intervals in the Early Cretaceous, particularly in the NW Tethys, and is often linked with increased volcanic activity on one or both of the G-OJP or Kerguelen Plateau (e.g., Föllmi *et al.*, 1994; Weissert *et al.*, 1998; Föllmi, 2012; Charbonnier *et al.*, 2018; Matsumoto *et al.*, 2020, 2021b, 2022). A spread of warm-water scleractinian corals has been documented in uppermost Maastrichtian strata of Belgium and the Netherlands, and is correlative with evidence for rising seawater temperatures (Leloux, 1999; O'Hora *et al.*, 2022). This relationship supports some benthic response to rising global temperatures associated with early Deccan volcanism. However, the extent of biospheric changes during the Late Maastrichtian Warming Event remains debated (see e.g., Witts *et al.*, 2016; Tobin *et al.*, 2017; regarding high-latitude molluscs).

The diversity of planktonic carbonate producers (calcareous nannofossils, calcispheres, planktonic foraminifera) was apparently less impacted by environmental change related to Cretaceous LIP volcanism. A major turnover in planktonic carbonate producers did occur during the KPg mass extinction (e.g., Smit, 1982; Olsson and Liu, 1993; Pospichal, 1996), but no specific declines in diversity have been recorded at the generic level for other intervals associated with Cretaceous LIPs (Steuber *et al.*, 2023). Rather, planktonic taxa diversity increased consistently throughout the Cretaceous, reaching a broad maximum between the Albian and Maastrichtian stages, peaking around the Campanian (Suchéras-Marx *et* al., 2019; Steuber *et al.*, 2023; Figure 5F). In general, this trend towards increased diversity applies to both calcareous nannofossils and planktonic foraminifera (Suchéras-Marx *et* al., 2019; Steuber *et al.*, 2023), despite their disparate trophic levels. However, phytoplanktonic organisms show some change in records of the Late Maastrichtian warming, with warm-water species tending to spread in favour of cold-water taxa, together with blooms in both dinoflagellate and calcareous nannoplankton highlighting stressed ecosystems in response to the rise in global temperatures caused by Deccan volcanism at that time (e.g., Thibault and Gardin, 2007;

Sheldon *et al*., 2010; Vellekoop *et al*., 2019). Planktonic foraminifera show a more locally variable response to Maastrichtian warming, possibly related to local controls such as nutrient levels and/or freshwater runoff as well as temperature changes (e.g., Abramovich and Keller, 2002; Woelders *et al*., 2017).

Slightly elevated rates of turnover (extinction and speciation) in planktonic foraminifers, and to a lesser extent in calcareous nannofossils, have also been documented for OAEs 1a, 1b, and 2 (Leckie *et al*., 2002), and potentially the Late Maastrichtian (e.g., Li and Keller, 1998b; Dameron *et al*., 2017; Hart *et al*., 2019). In particular, pronounced changes in the abundance patterns of calcareous nannofossils are recorded in stratigraphic records of the Cretaceous OAEs, particularly OAE 1a, as well as the Weissert Event and OAE 2 (Erba, 1994, 2004; Mutterlose and Böckel, 1998; Erba *et al*., 2010; Bottini and Mutterlose, 2012; Faucher *et al*., 2017; Erba *et al*., 2019). This change is most prominently shown by a significant decline of the heavily calcified nannoconids just prior to OAE 1a (Erba, 1994; Erba *et al*., 2010; Erba *et al*., 2019) and around the latest Aptian OAE 1b (nannoconid final collapse: Herrle and Mutterlose, 2003; Bottini *et al*., 2015). A nannoconid decline slightly preceeded the Weissert Event, also characterized by a general decrease in micrite production at pelagic and hemipelagic sites associated to an increase in abundance of higher-fertility taxa (Erba *et al*. 2004; Bornemann and Mutterlose, 2008; Gréselle *et al*., 2011; Barbarin *et al*., 2012; Pauly *et al*., 2012; Duchamp-Alphonse *et al*., 2014; Mattioli *et al*., 2014; Möller *et al*., 2015, 2020; Erba *et al*., 2019; Shmeit *et al*., 2022).

Extensive study of the nannoconid crisis associated with OAE 1a has shown it to be synchronous at a global scale, and apparently representing the culmination of a decrease in nannofossil calcite production that commenced in the latest Barremian (Erba, 1994, 2004; Bottini and Mutterlose, 2012; Aguado *et al*., 2014; Erba *et al*., 2015; Bonin *et al*., 2016; Giraud *et al*., 2018; Mahanipour *et al*., 2019). In addition to major changes in nannofossil abundance, species-specific decreases in size have been detected for both OAE 1a and OAE 2. Specifically, *Biscutum constans* shows a marked reduction in coccolith size across OAE 1a at global scale (Erba *et al*., 2010; Lübke *et al*., 2015; Lübke and Mutterlose, 2016; Bottini and Faucher 2020). Coccolith dwarfism of *B. constans* during OAE 2 has also been documented globally, alongside a fall in nannofossil abundance and species richness worldwide (Nederbragt and Fiorentino, 1999; Hardas and Mutterlose, 2007; Linnert *et al*., 2010, 2011; Corbett and Watkins, 2013; Faucher *et al*., 2017). It should be noted that these changes did not result in extinctions, with species recovering following the alleviation of environmental changes, and some nannofossil taxa actually increasing in abundance (Erba and Tremolada, 2004; Erba *et al*., 2019). Nonetheless, the transient net decrease in carbonate producers reduced the availability of nannofossil micrite reflected as a biocalcification crisis, since nannoconids were the main rock-forming nannofossils during the Early Cretaceous (Erba and Tremolada, 2004; Weissert and Erba, 2004). This interpretation has been challenged recently by Slater *et al.* (2022), who argued that the apparent decrease in nannoplankton preservation results from post-depositional removal of carbonate from the rock record and that diversity increased during OAEs. However, whilst both of these phenomena did indeed occur, they do not explain the geologically rapid loss of heavily calcified nannoconids compared to other calcifiers (Erba *et al*., 2010), which is more consistent with a biocalcification crisis. Furthermore, fossil evidence of reduced biocalcification during OAE 2 is supported by sedimentological changes consistent with a shallowing of the seawater carbonate compensation depth in response to ocean acidification at that time (Erba, 2004; Faucher *et al*., 2017; Jones *et al*., 2023).

Whilst ocean acidification caused by volcanic CO_2 emissions from LIP eruptions is considered to be the main driver of reduced biocalcification during OAEs 1a, and OAE 2 (Erba, 2004; Erba *et al*., 2010), alternative processes may also have played a role. Enhanced seawater fertility and subsequent eutrophication has also been proposed as a cause of nannoplankton stress and reduced species richness that favoured smaller taxa (Bersezio *et al*., 2002; Gréselle *et al*., 2011; Aguado *et al*., 2014; Duchamp-Alphonse *et al*. 2014; Mattioli *et al*., 2014; Giraud *et al*., 2018; Shmeit *et al*., 2022). At open oceanic sites, fertilisation was potentially driven by the hydrothermal output of biolimiting trace metals from G-OJP or Caribbean LIP activity (Snow *et al*., 2005; Bottini *et al*., 2015; Erba *et al*., 2015; Faucher *et al*., 2017; Bottini and Erba, 2018; Bottini and Faucher, 2020). Increased runoff of terrestrial material and nutrients caused by volcanically triggered climate warming could have produced the same effect in continental shelf settings, whilst potentially also reducing light availability in the photic zone (Lübke *et al.*, 2015; Lübke and Mutterlose, 2016). Alternatively, output of toxic volcanic elements may have suppressed biocalcification.

A more progressive decline in nannoconid biocalcification also occurred during OAE 1b, but has been linked with cold conditions (McAnena *et al.*, 2013). Alternatively, volcanic CO_2 output during formation of the Kerguelen Plateau may have lowered seawater pH enough to reduce carbonate saturation, even if the carbon emissions were insufficient to cause prolonged global temperature rise. Longer-term cooling in the Late Aptian may have been linked to enhanced absorption of CO_2 in seawater, lowering its pH (Bottini *et al.*, 2015). The reduction in size, decrease in abundance, and species turnover of planktonic foraminifers (Huber and Leckie, 2011) might reflect the response of calcareous zooplankton to volcanically triggered ocean acidification (Bottini et al., 2015; Bottini and Erba, 2018). Analogous changes in abundance, test size and evolutionary rates of calcareous zooplankton were documented for OAE 1a and OAE 2 (Premoli Silva *et al.*, 1989, 1999; Coccioni *et al.*, 1992; Leckie *et al.*, 2002) and are also consistent with ocean acidification (Kump *et al.*, 2009; Hönisch *et al.*, 2012). The cause of a nannoconid decline associated with the Weissert Event is less clear, although it has also been linked with increased fertility and seawater acidification related to volcanic CO_2 emissions (Erba and Tremolada, 2004; Weissert and Erba, 2004). However, there is no independent evidence for decreased seawater pH during that crisis, and as noted above, possible climate warming signals have only been reported NW Tethyan and proto-Atlantic records of the Weissert Event thus far (see compilations by Charbonnier *et al.*, 2020c; Cavalheiro *et al.*, 2021). At present, the limited evidence for global-scale temperature rise at that time (Meissner *et al.*, 2015; Price *et al.*, 2018; Cavalheiro *et al.*, 2021) hinders argument for a clear causal link between nannoconid stress and climate warming or CO_2 release comparable to that of OAEs 1a and 2.

It is clear that whilst rapid climate warming itself apparently impacted some marine groups during the Cretaceous, biospheric stress during intervals of LIP volcanism may not have been dependent on increased temperatures (Erba, 2006). Nonetheless, aside from the KPg mass extinction (for which the influence of Deccan Trap volcanism was complicated by the coeval climatic effects of the Chicxulub impact), OAEs 1a and 2 were the intervals associated with LIP emplacement that featured the most severe perturbations to Earth's biosphere. Both OAEs featured significant climate warming, unlike the

Weissert Event or OAE 1b. Moreover, the environmental change during OAEs 1a and 2 was also less protracted in nature and had a more rapid onset (likely due to the more intense LIP activity coeval with those intervals), which may have helped drive a more severe biotic response.

6.4. Remaining questions and future perspectives for understanding Cretaceous LIPs

Previous overviews of LIPs and mass extinctions/environmental change have largely focussed on continental provinces. It has been hypothesised that the impact of oceanic LIPs was somewhat muted due to the potentially lower degassing efficiency of submarine eruptions occurring under high seawater pressure (e.g., Courtillot and Renne, 2003; Ganino and Arndt, 2009; Green *et al.*, 2022). However, submarine oceanic-plateau volcanism was likely the main driver of both OAEs 1a and 2, which were marked by the most severe climatic, environmental, and biotic changes during the Cretaceous prior to the KPg extinction. Even if the widespread marine anoxia, ocean acidification, and biocalcifcation crises during those events were driven by the output of trace-metal micronutrients and volcanic CO_2 and/or halogens into seawater (e.g., Kerr, 1998; Erba *et al.*, 2004, 2015; Snow *et al.*, 2005), both events also featured significant climate warming that was apparently driven by magmatic carbon emissions (Larson and Erba, 1999; Jenkyns, 2003; Foster *et al.*, 2007; Méhay *et al.*, 2009; Adloff *et al.*, 2020; *this study*; Figure 6). Thus, submarine LIPs were capable of raising global temperatures as well as triggering oceanic anoxia and acidification, three key processes thought to have helped cause major extinctions.

Recent studies have emphasised that the rate of eruptions (and, consequently, the assumed rate of magmatic CO_2 output) plays a key role in determining the environmental and biotic impact of a LIP (Green *et al.*, 2022; Jiang *et al.*, 2022). Constraining this CO_2 flux depends on both precise geochronology and robust estimates of the magmatic carbon content. Currently, reconstructed eruption histories vary greatly in terms of detail and precision for different LIPs, both from the Cretaceous and other time intervals (see reviews by Kasbohm *et al.*, 2021; Jiang *et al.*, 2023).

Additionally, the CO_2 content of tholeiitic basalts remains relatively poorly constrained. Current estimates for LIP magma carbon contents range between 0.1–2 wt%, based on the study of analogous modern basaltic systems (e.g., Self *et al.*, 2006; Saunders, 2016), rare olivine melt inclusions (Black *et al.*, 2014), and volatile/non-volatile elemental ratios, particularly CO_2/Nb and CO_2/Ba (Black and Gibson, 2019; Hernandez Nava *et al.*, 2021; Boscaini *et al.*, 2022). Thus far, these efforts have only focussed on a few continental LIPs, with the Deccan Traps the only Cretaceous province investigated (Hernandez Nava *et al.*, 2021). Future studies refining both the eruptive history of Cretaceous LIPs, and their magmatic carbon content, are needed in order to better constrain the rate of CO_2 emissions from LIP volcanism and its importance in determining their impact on Earth's environment/biosphere. Such data are especially required for oceanic LIPs, which have been investigated by relatively few geochronological or geochemical studies thus far (but see compilations by Coffin *et al.*, 2002; Kasbohm *et al.*, 2021; Davidson *et al.*, 2023; Jiang *et al.*, 2023). Additional studies of trace-metal and micronutrient distribution from oceanic plateaus are also needed in order to better understand the potential impact of this process in triggering marine anoxia during times of submarine LIP volcanism. In particular, it is unclear whether the distribution of volcanic micronutrients directly into seawater could have enhanced primary productivity and water-column deoxygenation on a global scale. If this effect was largely limited to regions close to the LIP source, anoxia at more distal sites may have depended on terrestrial runoff, upwelling of deepwater nutrients, and/or the development of marine stratification (see Jenkyns, 2010; Föllmi, 2012).

Finally, the sheer number of Cretaceous LIPs remains something of a mystery. As outlined at the start of this chapter, there were at least seven highly voluminous large igneous provinces during the Cretaceous Period, which have been associated with intervals of profound environmental and/or biosphere disturbance. This represents a significantly higher total than for any other geological Period in the last 300 million years since the formation of Pangaea, even accounting for the longer duration of the Cretaceous *vs* other periods (Figure 7). Moreover, seven major Cretaceous LIPs represents a conservative estimate. Some authors have proposed that other extensive igneous formations emplaced geologically rapidly during the Cretaceous represent additional LIPs, or that magmatic areas considered here to be part of the Kerguelen or Greater Ontong-Java plateaus were actually distinct provinces (see compilations by Torsvik, 2019; Ernst *et al*., 2021). It may also be noteworthy that the Cretaceous featured the most oceanic LIPs of any known time in the Phanerozoic. This peak may result partly from preservation bias given the absence of most pre-Cretaceous ocean crust, but there was no comparable level of oceanic LIP formation in the Cenozoic, for which the available geological record is also good.

Why the Cretaceous was apparently 'a time of LIPs' is unclear. The middle part of the period was also marked by a long interval without magnetic reversals (the Cretaceous Normal superchron), and it has been hypothesised that both the LIPs and the superchron resulted from atypical mantle dynamics, such as the formation of a superplume or significant changes in subduction rates (e.g., Larson, 1991; Courtillot and Olson, 2007; Yoshimura, 2022). Alternatively, this superplume may have been an inevitable consequence of the formation and subsequent break-up of the Pangaean supercontinent (Vaughan and Storey, 2007). Whilst these models are speculative, the fact that the Cretaceous was marked by an unusually high number of LIPs, extensive and fast-spreading mid-ocean ridges, enhanced kimberlite emplacement, and even formation of komatiites (the only clear Phanerozoic example of this lithology), suggests that Earth's mantle conditions were highly abnormal during that time (e.g., Kerr, 2005; Seton *et al*., 2009; Heaman *et al*., 2019). Given that numerous supercontinent cycles have taken place in Proterozoic and Phanerozoic eras, it is highly unlikely that there has been only one such spell of high LIP formation in Earth's history. This conclusion raises the tantalising possibility that the Cretaceous Period marked the most recent example of a key mantle phenomenon inherent in Earth's long-term tectonic cycling, which subsequently resulted in profound disturbances to Earth's surface climate, environment, and biosphere.

7. SUMMARY

Large igneous province (LIP) volcanism has been hypothesised as the primary trigger of several intervals of environmental perturbation during the Cretaceous Period, both through eruption of continental flood basalts and the submarine emplacement of oceanic plateaus. This study has generated new mercury-concentration and osmium-isotope datasets to reconstruct the temporal relationships between volcanism, climate warming, and environmental change during the Early Aptian oceanic anoxic event (OAE 1a). By incorporating these results into an overview of sedimentary, geochemical, and palaeontological evidence of episodes of environmental and biotic change, and the geological, geochronological, and geochemical records of LIP activity, the following conclusions are drawn:

1) Climate warming associated with OAE 1a was likely initiated by magmatic CO_2 emissions prior to the onset of the OAE *sensu stricto*, although volcanic activity and global temperatures did not reach their maximum until the middle part of OAE 1a. The initial carbon was likely sourced from submarine volcanism during formation of the Greater Ontong-Java Plateau. As well as potentially initiating climate warming, this magmatic CO_2 drove biotic stress amongst benthic fauna (dasycladalean algae, larger benthic foraminifera, corals, rudists) and dwarfism in calcareous nannoflora. An additional non-magmatic source such as methane clathrate or thermogenic emissions associated with the High Arctic LIP likely played a key role in perturbing the global carbon cycle at the onset of the OAE.
2) The Early Aptian and latest Cenomanian OAEs (OAEs 1a and 2, respectively) represented the episodes of most severe climatic, environmental, and biota stress during the Cretaceous apart from the end-Cretaceous mass extinction (for which the role of volcanism remains contested). OAEs 1a and 2 were also coeval with the times of most intense LIP activity and output of mafic trace-metals (potentially including key micronutrients) to the global ocean from oceanic plateaus. Thus, whilst severe environmental change and mass extinctions are more typically linked with continental LIPs, oceanic plateaus also had the capacity to profoundly impact Earth's surface environment and ecosystems during the Cretaceous Period.
3) The more limited biosphere impact of some Cretaceous LIPs, such as the Paraná-Etendeka and Kerguelen Plateau, may have resulted from their more protracted formation and lower eruption rate. Kerguelen volcanism was apparently less intense than that of the Greater

Ontong-Java and Caribbean/High Arctic LIPs associated with OAEs 1a and 2, potentially leading to lower carbon and trace-metal micronutrient output. Paraná-Etendeka magmas may also have been volatile depleted and did not intrude carbon-rich country rocks. Further work is needed to precisely constrain the eruptive histories and carbon outputs of Cretaceous LIPs (especially oceanic plateaus), and the potential dispersal of micronutrients from submarine volcanism.

4) The high number of LIP events in the Cretaceous compared to times before or afterwards resulted in Earth's carbon cycle and surface environment being frequently perturbed to an extent not documented for any other geological Period in at least the last 300 million years. Why there was such a high rate of LIP formation (and magmatism in general) during the Cretaceous remains unclear. Further work is needed to determine the cause, and whether there were earlier intervals in Earth's history featuring enhanced Large Igneous Province emplacement, or if the Cretaceous represented a unique 'Age of LIPs'.

Acknowledgements

We gratefully acknowledge S. Batenburg for handling this manuscript, and two anonymous reviewers for providing constructive feedback that has improved this overview of Cretaceous LIPs. We greatly appreciate laboratory assistance from Y. Ohtsuki and J. Kikuchi at JAMSTEC (Re-Os analysis) and D. Verstraeten at the VUB (TOC and TS measurements), and further thank P. Claeys and Y. Gao for providing instrument access for the geochemical analyses undertaken at the VUB. We thank C. Cucciniello and J. Vellekoop for helpful discussions on the Madagascan LIP and Late Maastrichtian Warming Event, respectively. We also thank the Research Foundation – Flanders (FWO: grant 12P4522N to LMEP) the Norwegian Research Council (Young Research Talent project number 301096 to SC), the Grant-in-aid for a Japan Society for the Promotion of Science Research Fellow (number 22J00271 to HM), the Japan Society for the Promotion of Science (JSPS) KAKENHI (number 22H01327 to KS), and the Vrije Universiteit Brussel Strategic Research Funding for financial support.

References

Abramovich, S. and Keller, G., 2002, High stress late Maastrichtian paleoenvironment: inference from planktonic foraminifera in Tunisia. Palaeogeography, Palaeoclimatology, Palaeoecology, 178, p. 145–164, https://doi.org/10.1016/S0031-0182(01)00394-7.

Adloff, M., Greene, S.E., Parkinson, I.J., Naafs, B.D.A., Preston, W., Ridgwell, A., Lunt, D.J., Castro, J.M. and Monteiro, F.M., 2020, Unravelling the sources of carbon emissions at the onset of Oceanic Anoxic Event (OAE) 1a. Earth and Planetary Science Letters, 530, 115947, https://doi.org/10.1016/j.epsl.2019.115947.

Aguado, R., de Gea, G.A., Castro, J.M., O'Dogherty, L., Quijano, M.L., Naafs, B.D.A. and Pancost, R.D., 2014, Late Barremian–early Aptian dark facies of the Subbetic (Betic Cordillera, southern Spain): Calcareous nannofossil quantitative analyses, chemostratigraphy and palaeoceanographic reconstructions. Palaeogeography, Palaeoclimatology, Palaeoecology, 395, p. 198–221, https://doi.org/10.1016/j.palaeo.2013.12.031.

Ait-Itto, F.Z., Martinez, M., Deconinck, J.F. and Bodin, S., 2023, Astronomical calibration of the OAE1b from the Col de Pré-Guittard section (Aptian–Albian), Vocontian Basin, France. Cretaceous Research, 150, 105618, https://doi.org/10.1016/j.cretres.2023.105618.

Almeida, V.V., Janasi, V.A., Heaman, L.M., Shaulis, B.J., Hollanda, M.H.B. and Renne, P.R., 2018, Contemporaneous alkaline and tholeiitic magmatism in the Ponta Grossa Arch, Paraná-Etendeka Magmatic Province: Constraints from U–Pb zircon/baddeleyite and 40Ar/39Ar phlogopite dating of the José Fernandes Gabbro and mafic dykes. Journal of Volcanology and Geothermal Research, 355, p. 55–65, https://doi.org/10.1016/j.jvolgeores.2017.01.018.

Allègre, C.J., Birck, J.L., Capmas, F. and Courtillot, V., 1999, Age of the Deccan traps using ^{187}Re–^{187}Os systematics. Earth and Planetary Science Letters, 170, p. 197–204, https://doi.org/10.1016/S0012-821X(99)00110-7.

Alvarez, L.W., Alvarez, W., Asaro, F. and Michel, H.V., 1980, Extraterrestrial cause for the Cretaceous-Tertiary extinction. Science, 208, p. 1095–1108, https://doi.org/10.1126/science.208.4448.1095.

Ando, A., Kaiho, K., Kawahata, H. and Kakegawa, T., 2008, Timing and magnitude of early Aptian extreme warming: Unraveling primary $\delta^{18}O$ variation in indurated pelagic carbonates at Deep Sea Drilling Project Site 463, central Pacific Ocean. Palaeogeography, Palaeoclimatology, Palaeoecology, 260, p. 463–476, https://doi.org/10.1016/j.palaeo.2007.12.007.

Arthur, M.A., 1979, North Atlantic Cretaceous black shales: the record at Site 398 and a brief comparison with other occurrences. Initial Reports of the Deep Sea Drilling Project, 47, p. 719–751, https://doi.org/10.2973/dsdp.proc.47-2.136.1979.

Arthur, M.A., Schlanger, S.T. and Jenkyns, H.C., 1987, The Cenomanian-Turonian Oceanic Anoxic Event, II. Palaeoceanographic controls on organic-matter production and preservation. Geological Society, London, Special Publications, 26, p. 401–420, https://doi.org/10.1144/GSL.SP.1987.026.01.25.

Bacha, R.R., Waichel, B.L. and Ernst, R.E., 2022, The mafic volcanic climax of the Paraná-Etendeka Large Igneous Province as the trigger of the Weissert Event. Terra Nova, 34, p. 28–36, https://doi.org/10.1111/ter.12558.

Baker, S.J., Belcher, C.M., Barclay, R.S., Hesselbo, S.P., Laurin, J. and Sageman, B.B., 2020, CO_2-induced climate forcing on the fire record during the initiation of Cretaceous oceanic anoxic event 2. Geological Society of America Bulletin, 132, p. 321–333, https://doi.org/10.1130/B35097.1.

Baksi, A.K., 1995, Petrogenesis and timing of volcanism in the Rajmahal flood basalt province, northeastern India. Chemical Geology, 121, p. 73–90, https://doi.org/10.1016/0009-2541(94)00124-Q.

Barbarin, N., Bonin, A., Mattioli, E., Pucéat, E., Cappetta, H., Gréselle, B., Pittet, B., Vennin, E. and Joachimski, M., 2012, Evidence for a complex Valanginian nannoconid decline in the Vocontian basin (South East France). Marine Micropaleontology, 84, p. 37–53, https://doi.org/10.1016/j.marmicro.2011.11.005.

Barreto, C.J.S., Lafon, J.M., de Lima, E.F. and Sommer, C.A., 2016, Geochemical and Sr–Nd–Pb isotopic insight into the low-Ti basalts from southern Paraná Igneous Province, Brazil: the role of crustal contamination. International Geology Review, 58, p. 1324–1349, https://doi.org/10.1080/00206814.2016.1147988.

Barnet, J.S., Littler, K., Kroon, D., Leng, M.J., Westerhold, T., Röhl, U. and Zachos, J.C., 2018, A new high-resolution chronology for the late Maastrichtian warming event: Establishing robust temporal links with the onset of Deccan volcanism. Geology, 46, p. 147–150, https://doi.org/10.1130/G39771.1.

Batenburg, S.J., De Vleeschouwer, D., Sprovieri, M., Hilgen, F.J., Gale, A.S., Singer, B.S., Koeberl, C., Coccioni, R., Claeys, P. and Montanari, A., 2016, Orbital control on the timing of oceanic anoxia in the Late Cretaceous. Climate of the Past, 12, p. 1995–2009, https://doi.org/10.5194/cp-12-1995-2016.

Bauer, K.W., Zeebe, R.E. and Wortmann, U.G., 2017, Quantifying the volcanic emissions which triggered Oceanic Anoxic Event 1a and their effect on ocean acidification. Sedimentology, 64, p. 204–214, https://doi.org/10.1111/sed.12335.

Bédard, J.H., Saumur, B.M., Tegner, C., Troll, V.R., Deegan, F.M., Evenchick, C.A., Grasby, S.E. and Dewing, K., 2021a, Geochemical systematics of High Arctic Large Igneous Province continental tholeiites from Canada—evidence for progressive crustal contamination in the plumbing system. Journal of Petrology, 62, https://doi.org/10.1093/petrology/egab042.

Bédard, J.H., Troll, V.R., Deegan, F.M., Tegner, C., Saumur, B.M., Evenchick, C.A., Grasby, S.E. and Dewing, K., 2021b, High Arctic Large Igneous Province alkaline rocks in Canada: evidence for multiple mantle components. Journal of Petrology, 62, https://doi.org/10.1093/petrology/egab041.

Bersezio, R., Erba, E., Gorza, M. and Riva, A., 2002, Berriasian–Aptian black shales of the Maiolica formation (Lombardian Basin, Southern Alps, Northern Italy): local to global events. Palaeogeography, Palaeoclimatology, Palaeoecology, 180, p. 253–275, https://doi.org/10.1016/S0031-0182(01)00416-3.

Birck, J.L., Barman, M.R. and Capmas, F., 1997, Re-Os isotopic measurements at the femtomole level in natural samples. Geostandards newsletter, 21, p. 19–27, https://doi.org/10.1111/j.1751-908X.1997.tb00528.x.

Black, B.A. and Gibson, S.A., 2019, Deep carbon and the life cycle of large igneous provinces. Elements, 15, p. 319–324, https://doi.org/10.2138/gselements.15.5.319.

Black, B.A., Hauri, E.H., Elkins-Tanton, L.T. and Brown, S.M., 2014, Sulfur isotopic evidence for sources of volatiles in Siberian Traps magmas. Earth and Planetary Science Letters, 394, p. 58–69, https://doi.org/10.1016/j.epsl.2014.02.057.

Black, B.A., Karlstrom, L. and Mather, T.A., 2021, The life cycle of large igneous provinces. Nature Reviews Earth & Environment, 2, p. 840–857, https://doi.org/10.1038/s43017-021-00221-4.

Blättler, C.L., Jenkyns, H.C., Reynard, L.M. and Henderson, G.M., 2011, Significant increases in global weathering during Oxeanic Anoxic Events 1a and 2 indicated by calcium isotopes. Earth and Planetary Science Letters, p. 77–88, https://doi.org/10.1016/j.epsl.2011.06.029.

Bodin, S., Meissner, P., Janssen, N.M., Steuber, T. and Mutterlose, J., 2015, Large igneous provinces and organic carbon burial: Controls on global temperature and continental weathering during the Early Cretaceous. Global and Planetary Change, 133, p. 238–253, https://doi.org/10.1016/j.gloplacha.2015.09.001.

Bodin, S., Charpentier, M., Ullmann, C.V., Rudra, A. and Sanei, H., 2023, Carbon cycle during the late Aptian–early Albian OAE 1b: A focus on the Kilian–Paquier levels interval. Global and Planetary Change, 222, 104074, https://doi.org/10.1016/j.gloplacha.2023.104074.

Bond, D.P.G. and Wignall, P.B., 2014, Large igneous provinces and mass extinctions: an update. *In* Keller, G. and Kerr A.C. (Eds.), Volcnanism, Impacts, and Mass Extinctions: Causes and Effects, Geological Society of America Special Papers, 505, SPE505-02, https://doi.org/10.1130/2014.2505(02).

Bond, D.P. and Sun, Y., 2021, Global warming and mass extinctions associated with large igneous province volcanism. In Ernst, R.E., Dickson, A.J., Bekker, A. (Eds.): Large Igneous Provinces: A Driver of Global Environmental and Biotic Changes. AGU Geophysical Monograph 255, p. 83–102, https://doi.org/10.1002/9781119507444.ch3.

Bonin, A., Pucéat, E., Vennin, E., Mattioli, E., Aurell, M., Joachimski, M., Barbarin, N. and Laffont, R., 2016, Cool episode and platform demise in the Early Aptian: New insights on the links between climate and carbonate production. Paleoceanography, 31, p. 66–80, https://doi.org/10.1002/2015PA002835.

Bornemann, A. and Mutterlose, J., 2008, Calcareous nannofossil and δ13C records from the Early Cretaceous of the Western Atlantic Ocean: evidence for enhanced fertilization across the Berriasian–Valanginian transition. Palaios, 23, p. 821–832, https://doi.org/10.2110/palo.2007.p07-076r.

Boscaini, A., Callegaro, S., Sun, Y. and Marzoli, A., 2022, Late Permian to late Triassic large igneous provinces: timing, eruptive style and paleoenvironmental perturbations. Frontiers in Earth Science, 10, https://doi.org/10.3389/feart.2022.887632.

Boschman, L.M., van Hinsbergen, D.J., Torsvik, T.H., Spakman, W. and Pindell, J.L., 2014, Kinematic reconstruction of the Caribbean region since the Early Jurassic. Earth-Science Reviews, 138, p. 102–136, https://doi.org/10.1016/j.earscirev.2014.08.007.

Bottini, C. and Erba, E., 2018, Mid-Cretaceous paleoenvironmental changes in the western Tethys. Climate of the Past, 14, p. 1147–1163, https://doi.org/10.5194/cp-14-1147-2018.

Bottini, C. and Faucher, G., 2020, Biscutum constans coccolith size patterns across the mid Cretaceous in the western Tethys: Paleoecological implications. Palaeogeography, Palaeoclimatology, Palaeoecology, 555, 109852, https://doi.org/10.1016/j.palaeo.2020.109852.

Bottini, C. and Mutterlose, J., 2012, Integrated stratigraphy of Early Aptian black shales in the Boreal Realm: calcareous nannofossil and stable isotope evidence for global and regional processes. Newsletters on Stratigraphy, 45, p. 115–137, https://doi.org/10.1127/0078-0421/2012/0017.

Bottini, C., Cohen, A.S., Erba, E., Jenkyns, H.C. and Coe, A.L., 2012, Osmium-isotope evidence for volcanism, weathering, and ocean mixing during the early Aptian OAE 1a. Geology, 40, p. 583–586, https://doi.org/10.1130/G33140.1.

Bottini, C., Erba, E., Tiraboschi, D., Jenkyns, H.C., Schouten, S. and Sinninghe Damsté, J.S., 2015, Climate variability and ocean fertility during the Aptian Stage. Climate of the Past, 11, p. 383–402, https://doi.org/10.5194/cp-11-383-2015.

Bowman, K.L., Hammerschmidt, C.R., Lamborg, C.H. and Swarr, G., 2015, Mercury in the North Atlantic Ocean: The U.S. GEOTRACERS zonal and meridional sections. Deep-Sea Research II, 116, p. 251–261, https://doi.org/10.1016/j.dsr2.2014.07.004.

Bralower, T.J., Arthur, M.A., Leckie, R.M., Sliter, W.V., Allard, D.J. and Schlanger, S.O., 1994, Timing and paleoceanography of oceanic dysoxia/anoxia in the Late Barremian to Early Aptian (Early Cretaceous). Palaios, p. 335–369, https://doi.org/10.2307/3515055.

Bréhéret, J.G., 1988, Episodes de 53odelling53ion riche en matière organique dans les marnes bleues d'âge aptien et albien de la partie pélagique du 53odel vocontien. Bulletin de la Société géologique de France, 4, p. 349–356, https://doi.org/10.2113/gssgfbull.IV.2.349.

Brown, S.A.E., Scott, A.C., Glasspool, I.J. and Collinson, M.E., 2012, Cretaceous wildfires and their impact on the Earth system. Cretaceous research, 36, p. 162–190, https://doi.org/10.1016/j.cretres.2012.02.008.

Bryan, S.E. and Ernst, R.E., 2008, Revised definition of large igneous provinces (LIPs). Earth-Science Reviews, 86, p. 175–202, https://doi.org/10.1016/j.earscirev.2007.08.008.

Bryan, S.E. and Ferrari, L., 2013, Large igneous provinces and silicic large igneous provinces: Progress in our understanding over the last 25 years. Geological Society of America Bulletin, 125, p. 1053–1078, https://doi.org/10.1130/B30820.1.

Buchs, D.M., Kerr, A.C., Brims, J.C., Zapata-Villada, J.P., Correa-Restrepo, T. and Rodríguez, G., 2018, Evidence for subaerial development of the Caribbean oceanic plateau in the Late Cretaceous and palaeo-environmental implications. Earth and Planetary Science Letters, 499, p. 62–73, https://doi.org/10.1016/j.epsl.2018.07.020.

Callegaro, S., Baker, D.R., De Min, A., Marzoli, A., Geraki, K., Bertrand, H., Viti, C. and Nestola, F., 2014, Microanalyses link sulfur from large igneous provinces and Mesozoic mass extinctions. Geology, 42, p. 895–898, https://doi.org/10.1130/G35983.1.

Callegaro, S., Baker, D.R., Renne, P.R., Melluso, L., Geraki, K., Whitehouse, M.J., De Min, A. and Marzoli, A., 2023, Recurring volcanic winters during the latest Cretaceous: Sulfur and fluorine budgets of Deccan Traps lavas. Science Advances, 9, https://doi.org/10.1126/sciadv.adg8284.

Castro, J.M., Ruiz-Ortiz, P.A., de Gea, G.A., Aguado, R., Jarvis, I., Weissert, H., Molina, J.M., Nieto, L.M., Pancost, R.D., Quijano, M.L. and Reolid, M., 2021, High-resolution C-isotope, TOC and biostratigraphic records of OAE 1a (Aptian) from an expanded hemipelagic cored succession, western Tethys: a new stratigraphic reference for global correlation and paleoenvironmental reconstruction. *Paleoceanography and Paleoclimatology*, *36*, https://doi.org/10.1029/2020PA004004.

Cavalheiro, L., Wagner, T., Steinig, S., Bottini, C., Dummann, W., Esegbue, O., Gambacorta, G., Giraldo-Gómez, V., Farnsworth, A., Flögel, S. and Hofmann, P., 2021, Impact of global cooling on Early Cretaceous high pCO2 world during the Weissert Event. Nature communications, 12, https://doi.org/10.1038/s41467-021-25706-0.

Chambers, L.M., Pringle, M.S. and Fitton, J.G., 2002, Age and duration of magmatism on the Ontong Java Plateau: ^{40}Ar-^{39}Ar results from ODP Leg 192. AGU Fall Meeting Abstracts, 2002, V71B-1271.

Chambers, L.M., Pringle, M.S. and Fitton, J.G., 2004, Phreatomagmatic eruptions on the Ontong Java Plateau: an Aptian ^{40}Ar/^{39}Ar age for volcaniclastic rocks at ODP Site 1184. *In* Fitton, J.G., Mahoney, J.J., Wallace, P.J. and Saunders, A.D. (Eds.), Origin and Evolution of the Ontong Java Plateau, Geological Society of London, Special Publications, 229, p. 325–331, https://doi.org/10.1144/GSL.SP.2004.229.01.18.

Charbonnier, G. and Föllmi, K.B., 2017, Mercury enrichments in lower Aptian sediments support the link between Ontong Java large igneous province activity and oceanic anoxic episode 1a. Geology, 45, p. 63–66, https://doi.org/10.1130/G38207.1.

Charbonnier, G., Morales, C., Duchamp-Alphonse, S., Westermann, S., Adatte, T. and Föllmi, K.B., 2017, Mercury enrichment indicates volcanic triggering of Valanginian environmental change. Scientific reports, 7, https://doi.org/10.1038/srep40808.

Charbonnier, G., Godet, A., Bodin, S., Adatte, T. and Föllmi, K.B., 2018, Mercury anomalies, volcanic pulses, and drowning episodes along the northern Tethyan margin during the latest Hauterivian-earliest Aptian. Palaeogeography, Palaeoclimatology, Palaeoecology, 505, p. 337–350, https://doi.org/10.1016/j.palaeo.2018.06.013.

Charbonnier, G., Adatte, T., Föllmi, K.B. and Suan, G., 2020a, Effect of intense weathering and post-depositional degradation of organic matter on Hg/TOC proxy in organic-rich sediments and its implications for deep-time investigations. Geochemistry, Geophysics, Geosystems, 21, https://doi.org/10.1029/2019GC008707.

Charbonnier, G., Adatte, T., Duchamp-Alphonse, S., Spangenberg, J.E. and Föllmi, K.B., 2020b, Global mercury enrichment in Valanginian sediments supports a volcanic trigger for the Weissert episode. In

Adatte, T., Bond, D.P.G., Keller, G. (Eds.): Mass Extinctions, Volcanism, and Impacts: New Developments, Geological Society of America Special Papers, 544, p. 85–103, https://doi.org/10.1130/2019.2544(04).

Charbonnier, G., Duchamp-Alphonse, S., Deconinck, J.F., Adatte, T., Spangenberg, J.E., Colin, C. and Föllmi, K.B., 2020c, A global palaeoclimatic reconstruction for the Valanginian based on clay mineralogical and geochemical data. Earth-Science Reviews, 202, 103092, https://doi.org/10.1016/j.earscirev.2020.103092.

Chenet, A.L., Quidelleur, X., Fluteau, F., Courtillot, V. and Bajpai, S., 2007, ^{40}K–^{40}Ar dating of the Main Deccan large igneous province: Further evidence of KTB age and short duration. Earth and Planetary Science Letters, 263, p. 1–15, https://doi.org/10.1016/j.epsl.2007.07.011.

Chenet, A.L., Courtillot, V., Fluteau, F., Gérard, M., Quidelleur, X., Khadri, S.F.R., Subbarao, K.V. and Thordarson, T., 2009, Determination of rapid Deccan eruptions across the Cretaceous-Tertiary boundary using paleomagnetic secular variation: 2. Constraints from analysis of eight new sections and synthesis for a 3500-m-thick composite section. Journal of Geophysical Research: Solid Earth, 114, B06103, https://doi.org/10.1029/2008JB005644.

Clarkson, M.O., Stirling, C.H., Jenkyns, H.C., Dickson, A.J., Porcelli, D., Moy, C.M., von Strandmann, P.A.P., Cooke, I.R. and Lenton, T.M., 2018, Uranium isotope evidence for two episodes of deoxygenation during Oceanic Anoxic Event 2. Proceedings of the National Academy of Sciences, 115, p. 2918–2923, https://doi.org/10.1073/pnas.1715278115.

Clarkson, M.O., Lenton, T.M., Andersen, M.B., Bagard, M.L., Dickson, A.J. and Vance, D., 2021, Upper limits on the extent of seafloor anoxia during the PETM from uranium isotopes. Nature Communications, 12, https://doi.org/10.1038/s41467-020-20486-5.

Claeys, P., Kiessling, W. and Alvarez, W., 2002, Distribution of Chicxulub ejecta at the Cretaceous-Tertiary boundary. In Koeberl, C. and MacLeod, K.G. (Eds.): Catastrophic Events and Mass Extinctions: Impacts and Beyond, Geological Society of America Special Papers, 356, p. 55–68, https://doi.org/10.1130/0-8137-2356-6.55.

Coccioni, R., Erba, E. and Premoli-Silva, I., 1992, Barremian-Aptian calcareous plankton biostratigraphy from the Gorgo Cerbara section (Marche, central Italy) and implications for plankton evolution. Cretaceous Research, 13, p. 517–537, https://doi.org/10.1016/0195-6671(92)90015-I.

Coccioni, R., Sabatino, N., Frontalini, F., Gardin, S., Sideri, M. and Sprovieri, M., 2014, The neglected history of Oceanic Anoxic Event 1b: insights and new data from the Poggio le Guaine section (Umbria–Marche Basin). Stratigraphy, 11, p. 245-282.

Coffin, M.F. and Eldholm, O., 1994, Large igneous provinces: crustal structure, dimensions, and external consequences. Reviews of Geophysics, 32, p. 1–36, https://doi.org/10.1029/93RG02508.

Coffin, M.F., Pringle, M.S., Duncan, R.A., Gladczenko, T.P., Storey, M., Müller, R.D. and Gahagan, L.A., 2002, Kerguelen hotspot magma output since 130 Ma. Journal of petrology, 43, p. 1121–1137, https://doi.org/10.1093/petrology/43.7.1121.

Cohen, A.S. and Waters, F.G., 1996, Separation of osmium from geological materials by solvent extraction for analysis by thermal ionisation mass spectrometry. Analytica Chimica Acta, 332, p. 269-275, https://doi.org/10.1016/0003-2670(96)00226-7.

Cohen, A.S., Coe, A.L., Bartlett, J.M. and Hawkesworth, C.J., 1999, Precise Re-Os ages of organic-rich mudrocks and the Os isotope composition of Jurassic seawater. Earth and Planetary Science Letters, 167, p. 159–173, https://doi.org/10.1016/S0012-821X(99)00026-6.

Corbett, M.J. and Watkins, D.K., 2013, Calcareous nannofossil paleoecology of the mid-Cretaceous Western Interior Seaway and evidence of oligotrophic surface waters during OAE2. Palaeogeography, Palaeoclimatology, Palaeoecology, 392, p. 510–523, https://doi.org/10.1016/j.palaeo.2013.10.007.

Corfu, F., Polteau, S., Planke, S., Faleide, J.I., Svensen, H., Zayoncheck, A. and Stolbov, N., 2013, U–Pb geochronology of Cretaceous magmatism on Svalbard and Franz Josef Land, Barents Sea large igneous province. Geological Magazine, 150, p. 1127–1135, https://doi.org/10.1017/S0016756813000162.

Cors, J., Heimhofer, U., Adatte, T., Hochuli, P.A., Huck, S. and Bover-Arnal, T., 2015, Climatic evolution across oceanic anoxic event 1a derived from terrestrial palynology and clay minerals (Maestrat Basin, Spain). Geological Magazine, 152, p. 632–647, https://doi.org/10.1017/S0016756814000557.

Cossa, D., Mucci, A., Guedron, S., Coquery, M., Radakovitch, O., Escoube, R., Campillo, S. and Heussner, S., 2021, Mercury accumulation in the sediment of the Western Mediterranean abyssal plain: A reliable archive of the late Holocene. Geochimica et Cosmochimica Acta, 309, p. 1–15, https://doi.org/10.1016/j.gca.2021.06.014.

Courtillot, V. and Olson, P., 2007, Mantle plumes link magnetic superchrons to Phanerozoic mass depletion events. Earth and Planetary Science Letters, 260, p. 495–504, https://doi.org/10.1016/j.epsl.2007.06.003.

Courtillot, V., and Renne, P.R., 2003, On the ages of flood basalt events. Comptes Rendus Geoscience, 335, p. 113–140, https://doi.org/10.1016/S1631-0713(03)00006-3.

Courtillot, V., Besse, J., Vandamme, D., Montigny, R., Jaeger, J.J. and Cappetta, H., 1986, Deccan flood basalts at the Cretaceous/Tertiary boundary?. Earth and Planetary Science Letters, 80, p. 361–374, https://doi.org/10.1016/0012-821X(86)90118-4.

Courtillot, V., Gallet, Y., Rocchia, R., Feraud, G., Robin, E., Hofmann, C., Bhandari, N. and Ghevariya, Z.G., 2000, Cosmic markers, $^{40}Ar/^{39}Ar$ dating and paleomagnetism of the KT sections in the Anjar area of the Deccan large igneous province. Earth and Planetary Science Letters, 182, p. 137–156, https://doi.org/10.1016/S0012-821X(00)00238-7.

Cox, A.A. and Keller, C.B., 2023, A Bayesian inversion for emissions and export productivity across the end-Cretaceous boundary. Science, 381, p. 1446–1451, https://doi.org/10.1126/science.adh3875.

Cucciniello, C., Conrad, J., Grifa, C., Melluso, L., Mercurio, M., Morra, V., Tucker, R.D. and Vincent, M., 2011, Petrology and geochemistry of Cretaceous mafic and silicic dykes and spatially associated lavas in central-eastern coastal Madagascar. In Srivastava, R.K. (Ed.): Dyke Swarms: Keys for Geodynamic Interpretation: Keys for Geodynamic Interpretation, p. 345–375, https://doi.org/10.1007/978-3-642-12496-9_21.

Cucciniello, C., Melluso, L., Jourdan, F., Mahoney, J.J., Meisel, T. and Morra, V., 2013, ^{40}Ar–^{39}Ar ages and isotope geochemistry of Cretaceous basalts in northern Madagascar: refining eruption ages, extent of crustal contamination and parental magmas in a flood basalt province. *Geological Magazine*, *150*, p. 1–17, https://doi.org/10.1017/S0016756812000088.

Cucciniello, C., Morra, V., Melluso, L. and Jourdan, F., 2021, Constraints on duration, age and migration of the feeder systems of the Madagascan flood basalt province from high-precision $^{40}Ar/^{39}Ar$ chronology. Geological Society, London, Special Publications, 518, p. 325–340, https://doi.org/10.1144/SP518-2020-275.

Cucciniello, C., Langone, A., Melluso, L., Morra, V., Mahoney, J.J., Meisel, T. and Tiepolo, M., 2010, U-Pb Ages, Pb-Os isotope ratios, and Platinum-Group Element (PGE) composition of the west-central Madagascar flood basalt province. The Journal of Geology, 118, p. 523–541, https://doi.org/10.1086/655012.

Dameron, S.N., Leckie, R.M., Clark, K., MacLeod, K.G., Thomas, D.J. and Lees, J.A., 2017, Extinction, dissolution, and possible ocean acidification prior to the Cretaceous/Paleogene (K/Pg) boundary in the tropical Pacific. Palaeogeography, Palaeoclimatology, Palaeoecology, 485, pp.433-454, https://doi.org/10.1016/j.palaeo.2017.06.032.

Davidson, P.C., Koppers, A.A., Sano, T. and Hanyu, T., 2023, A younger and protracted emplacement of the Ontong Java Plateau. Science, 380, p. 1185–1188, https://doi.org/10.1126/science.ade8666.

De Min, A., Callegaro, S., Marzoli, A., Nardy, A.J., Chiaradia, M., Marques, L.S. and Gabbarrini, I., 2018, Insights into the petrogenesis of low-and high-Ti basalts: Stratigraphy and geochemistry of four lava sequences from the central Paraná basin. Journal of Volcanology and Geothermal Research, 355, p. 232–252, https://doi.org/10.1016/j.jvolgeores.2017.08.009.

Deegan, F.M., Bédard, J.H., Grasby, S.E., Dewing, K., Geiger, H., Misiti, V., Capriolo, M., Callegaro, S., Svensen, H.H., Yakymchuk, C. and Aradi, L.E., 2022, Magma–Shale Interaction in Large Igneous Provinces: Implications for Climate Warming and Sulfide Genesis. Journal of Petrology, 63, https://doi.org/10.1093/petrology/egac094.

Desmares, D., Crognier, N., Bardin, J., Testé, M., Beaudoin, B. and Grosheny, D., 2016, A new proxy for Cretaceous paleoceanographic and paleoclimatic reconstructions: Coiling direction changes in the planktonic foraminifera Muricohedbergella delrioensis. Palaeogeography, Palaeoclimatology, Palaeoecology, 445, p. 8–17, https://doi.org/10.1016/j.palaeo.2015.12.021.

Dickson, A.J., Rees-Owen, R.L., März, C., Coe, A.L., Cohen, A.S., Pancost, R.D., Taylor, K. and Shcherbinina, E., 2014, The spread of marine anoxia on the northern Tethys margin during the Paleocene-Eocene Thermal Maximum. Paleoceanography, 29, p. 471–488, https://doi.org/10.1002/2014PA002629.

Dickson, A.J., Cohen, A.S., Coe, A.L., Davies, M., Shcherbinina, E.A. and Gavrilov, Y.O., 2015, Evidence for weathering and volcanism during the PETM from Arctic and Peri-Tethys osmium isotope records. Palaeogeography, Palaeoclimatology, Palaeoecology, 438, p. 300–307, https://doi.org/10.1016/j.palaeo.2015.08.019.

Dickson, A.J., Jenkyns, H.C., Porcelli, D., van den Boorn, S. and Idiz, E., 2016, Basin-scale controls on the molybdenum-isotope composition of seawater during Oceanic Anoxic Event 2 (Late Cretaceous). Geochimica et Cosmochimica Acta, 178, p. 291–306, https://doi.org/10.1016/j.gca.2015.12.036.

Dickson, A.J., Cohen, A.S. and Davies, M., 2021, The Osmium Isotope Signature of Phanerozoic Large Igneous Provinces. In Ernst, R.E., Dickson, A.J., Bekker, A. (Eds.): Large Igneous Provinces: A Driver of Global Environmental and Biotic Changes. AGU Geophysical Monograph 255, p. 229–246, https://doi.org/10.1002/9781119507444.ch10.

Dockman, D.M., Pearson, D.G., Heaman, L.M., Gibson, S.A. and Sarkar, C., 2018, Timing and origin of magmatism in the Sverdrup Basin, Northern Canada—Implications for lithospheric evolution in the High Arctic Large Igneous Province (HALIP). Tectonophysics, 742, p. 50–65, https://doi.org/10.1016/j.tecto.2018.05.010.

Dodd, S.C., Mac Niocaill, C. and Muxworthy, A.R., 2015, Long duration (> 4 Ma) and steady-state volcanic activity in the early Cretaceous Paraná–Etendeka Large Igneous Province: new palaeomagnetic data from Namibia. Earth and Planetary Science Letters, 414, p. 16–29, https://doi.org/10.1016/j.epsl.2015.01.009.

dos Santos, Â.C.S., Holanda, E.C., de Souza, V., Guerra-Sommer, M., Manfroi, J., Uhl, D. and Jasper, A., 2016, Evidence of palaeo-wildfire from the upper lower Cretaceous (Serra do Tucano Formation, Aptian–Albian) of Roraima (North Brazil). Cretaceous Research, 57, p. 46–49, https://doi.org/10.1016/j.cretres.2015.08.003.

Driscoll, C.T., Mason, R.P., Chan, H.M., Jacob, D.J. and Pirrone, N., 2013, Mercury as a global pollutant: sources, pathways, and effects. Environmental science & technology, 47, p. 4967–4983, https://doi.org/10.1021/es305071v.

Du Vivier, A.D.C., Selby, D., Sageman, B.B., Jarvis, I., Gröcke, D.R. and Voigt, S., 2014, Marine $^{187}Os/^{188}Os$ isotope stratigraphy reveals the interaction of volcanism and ocean circulation during Oceanic Anoxic Event 2. Earth and Planetary Science Letters, 389, p. 23–33, https://doi.org/10.1016/j.epsl.2013.12.024.

Du Vivier, A.D.C., Selby, D., Takashima, R. and Nishi, H., 2015, Pacific $^{187}Os/^{188}Os$ isotope geochemistry and U–Pb geochronology: Synchroneity of global Os isotope change across OAE 2. Earth and Planetary Science Letters, 428, p. 204–216, https://doi.org/10.1016/j.epsl.2015.07.020.

Duchamp-Alphonse, S., Gardin, S., Fiet, N., Bartolini, A., Blamart, D. and Pagel, M., 2007. Fertilization of the northwestern Tethys (Vocontian basin, SE France) during the Valanginian carbon isotope perturbation: evidence from calcareous nannofossils and trace element data. Palaeogeography, Palaeoclimatology, Palaeoecology, 243, p. 132–151, https://doi.org/10.1016/j.palaeo.2006.07.010.

Duchamp-Alphonse, S., Gardin, S. and Bartolini, A., 2014, Calcareous nannofossil response to the Weissert episode (Early Cretaceous): Implications for palaeoecological and palaeoceanographic reconstructions. Marine Micropaleontology, 113, p. 65–78, https://doi.org/10.1016/j.marmicro.2014.10.002.

Dumitrescu, M., Brassell, S.C., Schouten, S., Hopmans, E.C. and Damsté, J.S.S., 2006, Instability in tropical Pacific sea-surface temperatures during the early Aptian. Geology, 34, p. 833–836, https://doi.org/10.1130/G22882.1.

Duncan, R.A., 1978, Geochronology of basalts from the Ninetyeast Ridge and continental dispersion in the eastern Indian Ocean. Journal of Volcanology and Geothermal Research, 4, p. 283–305, https://doi.org/10.1016/0377-0273(78)90018-5.

Duncan, R.A., 1991, Age distribution of volcanism along aseismic ridges in the eastern Indian Ocean. In: Weissel, J., Peirce, J., Taylor, E. and Alt, J. (Eds.): Proceedings of the Ocean Drilling Program, Scientific Results, 121, p. 507–517.

Duncan, R.A., 2002, A time frame for construction of the Kerguelen Plateau and Broken Ridge. Journal of Petrology, 43, p. 1109–1119, https://doi.org/10.1093/petrology/43.7.1109.

Eddy, M.P., Schoene, B., Samperton, K.M., Keller, G., Adatte, T. and Khadri, S.F., 2020, U-Pb zircon age constraints on the earliest eruptions of the Deccan Large Igneous Province, Malwa Plateau, India. Earth and Planetary Science Letters, 540, 116249, https://doi.org/10.1016/j.epsl.2020.116249.

Eldrett, J.S., Ma, C., Bergman, S.C., Lutz, B., Gregory, F.J., Dodsworth, P., Phipps, M., Hardas, P., Minisini, D., Ozkan, A. and Ramezani, J., 2015, An astronomically calibrated stratigraphy of the Cenomanian, Turonian and earliest Coniacian from the Cretaceous Western Interior Seaway, USA: Implications for global chronostratigraphy. Cretaceous Research, 56, p. 316–344, https://doi.org/10.1016/j.cretres.2015.04.010.

Erba, E., 1994, Nannofossils and superplumes: the early Aptian “nannoconid crisis”. Paleoceanography, 9, p. 483–501, https://doi.org/10.1029/94PA00258.

Erba, E., 2004, Calcareous nannofossils and Mesozoic oceanic anoxic events. Marine micropaleontology, 52, p. 85–106, https://doi.org/10.1016/j.marmicro.2004.04.007.

Erba, E., 2006, The first 150 million years history of calcareous nannoplankton: biosphere–geosphere interactions. Palaeogeography, Palaeoclimatology, Palaeoecology, 232, p. 237–250, https://doi.org/10.1016/j.palaeo.2005.09.013.

Erba, E. and Tremolada, F., 2004, Nannofossil carbonate fluxes during the Early Cretaceous: Phytoplankton response to nutrification episodes, atmospheric CO_2, and anoxia. Paleoceanography, 19, https://doi.org/10.1029/2003PA000884.

Erba, E., Bartolini, A. and Larson, R.L., 2004, Valanginian Weissert oceanic anoxic event. Geology, 32, p. 149–152, https://doi.org/10.1130/G20008.1.

Erba, E., Bottini, C., Weissert, H.J. and Keller, C.E., 2010, Calcareous nannoplankton response to surface-water acidification around Oceanic Anoxic Event 1a. Science, 329, p. 428–432, https://doi.org/10.1126/science.1188886.

Erba, E., Duncan, R.A., Bottini, C., Tiraboschi, D., Weissert, H., Jenkyns, H.C. and Malinverno, A., 2015, Environmental consequences of Ontong Java Plateau and Kerguelen Plateau volcanism. *In* Neal, C.R., Sager, W.W., Sano, T. and Erba, E. (Eds.), The Origin, Evolution, and Environmental Impact of Oceanic Large Igneous Provinces, Geological Society of America Special Papers, 511, p. 271–303, https://doi.org/10.1130/2015.2511(15).

Erba, E., Bottini, C., Faucher, G., Gambacorta, G. and Visentin, S., 2019, The response of calcareous nannoplankton to Oceanic Anoxic Events: The Italian pelagic record. Bollettino della Società Paleontologica Italiana, 58, p. 51–71, https://doi.org/10.4435/BPSI.2019.08.

Erbacher, J., Huber, B.T., Norris, R.D. and Markey, M., 2001, Increased thermohaline stratification as a possible cause for an ocean anoxic event in the Cretaceous period. Nature, 409, p. 325–327, https://doi.org/10.1038/35053041.

Erbacher, J., Friedrich, O., Wilson, P.A., Birch, H. and Mutterlose, J., 2005, Stable organic carbon isotope stratigraphy across Oceanic Anoxic Event 2 of Demerara Rise, western tropical Atlantic. Geochemistry, Geophysics, Geosystems, 6, Q06010, https://doi.org/10.1029/2004GC000850.

Erlank, A.J., Marsh, J.S., Duncan, A.R., Miller, R.M., Hawkesworth, C.J., Betton, P.J. and Rex, D.C., 1984, Geochemistry and petrogenesis of the Etendeka volcanic rocks from SWA/Namibia. Petrogenesis of the volcanic rocks of the Karoo Province, 13, p. 195–245.

Ernesto, M., Raposo, M.I.B., Marques, L.S., Renne, P.R., Diogo, L.A. and De Min, A., 1999, Paleomagnetism, geochemistry and $^{40}Ar/^{39}Ar$ dating of the North-eastern Paraná Magmatic Province: tectonic implications. *Journal of Geodynamics*, *28*, p. 321–340, https://doi.org/10.1016/S0264-3707(99)00013-7.

Ernst, R.E., 2014, Large igneous provinces. Cambridge University Press.

Ernst, R.E., Bond, D.P., Zhang, S.H., Buchan, K.L., Grasby, S.E., Youbi, N., El Bilali, H., Bekker, A. and Doucet, L.S., 2021, Large igneous province record through time and implications for secular environmental changes and geological time-scale boundaries. In Ernst, R.E., Dickson, A.J., Bekker, A. (Eds.): Large Igneous Provinces: A Driver of Global Environmental and Biotic Changes. AGU Geophysical Monograph 255, p. 3–26, https://doi.org/10.1002/9781119507444.ch1.

Esmeray-Senlet, S., Wright, J.D., Olsson, R.K., Miller, K.G., Browning, J.V. and Quan, T.M., 2015, Evidence for reduced export productivity following the Cretaceous/Paleogene mass extinction. Paleoceanography, 30, p. 718–738, https://doi.org/10.1002/2014PA002724.

Faucher, G., Erba, E., Bottini, C. and Gambacorta, G., 2017, Calcareous nannoplankton response to the latest Cenomanian Oceanic Anoxic Event 2 perturbation. Rivista Italiana di Paleontologia e Stratigrafia, 123, p. 159–176.

Fendley, I.M., Mittal, T., Sprain, C.J., Marvin-DiPasquale, M., Tobin, T.S. and Renne, P.R., 2019, Constraints on the volume and rate of Deccan Traps flood basalt eruptions using a combination of high-resolution terrestrial mercury records and geochemical box models. Earth and Planetary Science Letters, 524, 115721, https://doi.org/10.1016/j.epsl.2019.115721.

Feyte, S., Tessier, A., Gobeil, C. and Cossa, D., 2010, In situ adsorption of mercury, methylmercury and other elements by iron oxyhydroxides and organic matter in lake sediments. Applied Geochemistry, 25, p. 984–995, https://doi.org/10.1016/j.apgeochem.2010.04.005.

Fitton, J.G. and Godard, M., 2004, Origin and evolution of magmas on the Ontong Java Plateau. Geological Society, London, Special Publications, 229, p. 151–178, https://doi.org/10.1144/GSL.SP.2004.229.01.10.

Florisbal, L.M., Heaman, L.M., de Assis Janasi, V. and de Fatima Bitencourt, M., 2014, Tectonic significance of the Florianópolis dyke Swarm, Paraná–Etendeka Magmatic Province: a reappraisal based on precise U–Pb dating. Journal of Volcanology and Geothermal Research, 289, p. 140–150, https://doi.org/10.1016/j.jvolgeores.2014.11.007.

Föllmi, K.B., 2012, Early Cretaceous life, climate and anoxia. Cretaceous Research, 35, p. 230–257, https://doi.org/10.1016/j.cretres.2011.12.005.

Föllmi, K.B., Weissert, H., Bisping, M. and Funk, H., 1994, Phosphogenesis, carbon-isotope stratigraphy, and carbonate-platform evolution along the Lower Cretaceous northern Tethyan margin. Geological Society of America Bulletin, 106, p. 729–746, https://doi.org/10.1130/0016-7606(1994)106<0729:PCISAC>2.3.CO;2.

Föllmi, K.B., Godet, A., Bodin, S. and Linder, P., 2006, Interactions between environmental change and shallow water carbonate buildup along the northern Tethyan margin and their impact on the Early Cretaceous carbon isotope record. Paleoceanography, 21, https://doi.org/10.1029/2006PA001313.

Font, E., Adatte, T., Sial, A.N., de Lacerda, L.D., Keller, G. and Punekar, J., 2016, Mercury anomaly, Deccan volcanism, and the end-Cretaceous mass extinction. Geology, 44, p. 171–174, https://doi.org/10.1130/G37451.1.

Forster, A., Schouten, S., Moriya, K. Wilson, P.A. and Sinninghe Damsté, J.S., 2007, Tropical warming and intermittent cooling during the Cenomanian/Turonian oceanic anoxic event 2: Sea surface temperature records from the equatorial Atlantic. Palaeoceanography, 22, PA1219, https://doi.org/10.1029/2006PA001349.

Foster, G.L., Royer, D.L. and Lunt, D.J., 2017, Future climate forcing potentially without precedent in the last 420 million years. Nature Communications, 8, https://doi.org/10.1038/ncomms14845.

Frey, F.A., McNaughton, N.J., Nelson, D.R., deLaeter, J.R. and Duncan, R.A., 1996, Petrogenesis of the Bunbury Basalt, Western Australia: interaction between the Kerguelen plume and Gondwana lithosphere?. Earth and Planetary Science Letters, 144, p. 163–183, https://doi.org/10.1016/0012-821X(96)00150-1.

Frieling, J., Mather, T.A., März, C., Jenkyns, H.C., Hennekam, R., Reichart, G.J., Slomp, C.P. and van Helmond, N.A.G.M., 2023, Effects of redox variability and early diagenesis on marine sedimentary Hg records. Geochimica et Cosmochimica Acta, 351, p. 78–95, https://doi.org/10.1016/j.gca.2023.04.015.

Gale, A.S. and Christensen, W.K., 1996, Occurrence of the belemnite Actinocamax plenus in the Cenomanian of SE France and its significance. Bulletin of the Geological Society of Denmark, p. 68–77.

Gale, A.S., Mutterlose, J., Batenburg, S., Gradstein, F.M., Agterberg, F.P., Ogg, J.G. and Petrizzo, M.R., 2020, The Cretaceous period. In Gradstein, F.M., Ogg, J.G., Schmitz, M.D. and Ogg, G.M. (Eds.): Geologic time scale 2020, p. 1023–1086, Elsevier, https://doi.org/10.1016/B978-0-12-824360-2.00027-9.

Galloway, J.M., Fensome, R.A., Swindles, G.T., Hadlari, T., Fath, J., Schröder-Adams, C., Herrle, J.O. and Pugh, A., 2022, Exploring the role of High Arctic Large Igneous Province volcanism on Early Cretaceous Arctic forests. Cretaceous Research, 129, 105022, https://doi.org/10.1016/j.cretres.2021.105022.

Ganino, C. and Arndt, N.T., 2009, Climate changes caused by degassing of sediments during the emplacement of large igneous provinces. Geology, 37, p. 323–326, https://doi.org/10.1130/G25325A.1.

Gilabert, V., Batenburg, S.J., Arenillas, I. and Arz, J.A., 2022, Contribution of orbital forcing and Deccan volcanism to global climatic and biotic changes across the Cretaceous-Paleogene boundary at Zumaia, Spain. Geology, 50, p. 21–25, https://doi.org/10.1130/G49214.1.

Giraud, F., Pittet, B., Grosheny, D., Baudin, F., Lécuyer, C. and Sakamoto, T., 2018, The palaeoceanographic crisis of the Early Aptian (OAE 1a) in the Vocontian Basin (SE France). Palaeogeography, Palaeoclimatology, Palaeoecology, 511, p. 483–505, https://doi.org/10.1016/j.palaeo.2018.09.014.

Gladczenko, T.P., Coffin, M.F. and Eldholm, O., 1997, Crustal structure of the Ontong Java Plateau: 65odelling of new gravity and existing seismic data. Journal of Geophysical Research: Solid Earth, 102, p. 22711–22729, https://doi.org/10.1029/97JB01636.

Goderis, S., Sato, H., Ferrière, L., Schmitz, B., Burney, D., Kaskes, P., Vellekoop, J., Wittmann, A., Schulz, T., Chernonozhkin, S.M. and Claeys, P., 2021, Globally distributed iridium layer preserved within the Chicxulub impact structure. Science Advances, 7, https://doi.org/10.1126/sciadv.abe3647.

Gomes, A.S. and Vasconcelos, P.M., 2021, Geochronology of the Paraná-Etendeka large igneous province. Earth-Science Reviews, 220, 103716, https://doi.org/10.1016/j.earscirev.2021.103716.

Grasby, S.E., Beauchamp, B., Bond, D.P.G., Wignall, P.B. and Sanei, H., 2016, Mercury anomalies associated with three extinction events (Capitanian crisis, latest Permian extinction and the Smithian/Spathian extinction) in NW Pangea. Geological Magazine, 153, p. 285–297, https://doi.org/10.1017/S0016756815000436.

Grasby, S.E., Them, T.R., Chen, Z., Yin, R. and Ardakani, O.H., 2019, Mercury as a proxy for volcanic emissions in the geologic record. Earth-Science Reviews, 196, 102880 https://doi.org/10.1016/j.earscirev.2019.102880.

Green, T., Renne, P.R. and Keller, C.B., 2022, Continental flood basalts drive Phanerozoic extinctions. Proceedings of the National Academy of Sciences, 119, https://doi.org/10.1073/pnas.2120441119.

Gréselle, B., Pittet, B., Mattioli, E., Joachimski, M., Barbarin, N., Riquier, L., Reboulet, S. and Pucéat, E., 2011, The Valanginian isotope event: a complex suite of palaeoenvironmental perturbations. Palaeogeography, Palaeoclimatology, Palaeoecology, 306, p. 41–57, https://doi.org/10.1016/j.palaeo.2011.03.027.

Gröcke, D.R., Hesselbo, S.P. and Jenkyns, H.C., 1999, Carbon-isotope composition of Lower Cretaceous fossil wood: Ocean-atmosphere chemistry and relation to sea-level change. Geology, 27, p. 155–158, https://doi.org/10.1130/0091-7613(1999)027<0155:CICOLC>2.3.CO;2.

Gröcke, D.R., Price, G.D., Robinson, S.A., Baraboshkin, E.Y., Mutterlose, J. and Ruffell, A.H., 2005, The Upper Valanginian (Early Cretaceous) positive carbon–isotope event recorded in terrestrial plants. Earth and Planetary Science Letters, 240, p. 495–509, https://doi.org/10.1016/j.epsl.2005.09.001.

Hall, R., Álvarez, J. and Rico, H., 1972, Geología de parte de los departamentos de Antioquia y Caldas (sub-zona II-A). Boletín Geológico, 20, p. 1–85, https://doi.org/10.32685/0120-1425/bolgeol20.1.1972.326.

Hammer, Ø., Jones, M.T., Schneebeli-Hermann, E., Hansen, B.B. and Bucher, H., 2019, Are Early Triassic extinction events associated with mercury anomalies? A reassessment of the Smithian/Spathian boundary extinction. Earth-Science Reviews, 195, p. 179–190, https://doi.org/10.1016/j.earscirev.2019.04.016.

Hardas, P. and Mutterlose, J., 2007, Calcareous nannofossil assemblages of Oceanic Anoxic Event 2 in the equatorial Atlantic: Evidence of an eutrophication event. Marine Micropaleontology, 66, p. 52–69, https://doi.org/10.1016/j.marmicro.2007.07.007.

Hart, M.B., Leighton, A.D., Hampton, M. and Smart, C.W., 2019, Global bioevents and the Cretaceous/Paleogene boundary in Texas and Alabama: Stratigraphy, correlation and ocean acidification. Global and Planetary Change, 175, p. 129–143, https://doi.org/10.1016/j.gloplacha.2019.01.020.

Hasegawa, T., 1997, Cenomanian-Turonian carbon isotope events recorded in terrestrial organic matter from northern Japan. Palaeogeography, Palaeoclimatology, Palaeoecology, 130, p. 251–273, https://doi.org/10.1016/S0031-0182(96)00129-0.

Heaman, L.M., Phillips, D. and Pearson, G., 2019, Dating kimberlites: Methods and emplacement patterns through time. Elements, 15, p. 399–404, https://doi.org/10.2138/gselements.15.6.399.

Heimdal, T.H., Svensen, H.H., Ramezani, J., Iyer, K., Pereira, E., Rodrigues, R., Jones, M.T. and Callegaro, S., 2018, Large-scale sill emplacement in Brazil as a trigger for the end-Triassic crisis. Scientific Reports, 8, https://doi.org/10.1038/s41598-017-18629-8.

Heimhofer, U., Hochuli, P.A., Herrle, J.O., Andersen, N. and Weissert, H., 2004, Absence of major vegetation and palaeoatmospheric *p*CO_2 changes associated with oceanic anoxic event 1a (Early Aptian, SE France). Earth and Planetary Science Letters, 223, p. 303–318, https://doi.org/10.1016/j.epsl.2004.04.037.

Hernandez Nava, A., Black, B.A., Gibson, S.A., Bodnar, R.J., Renne, P.R. and Vanderkluysen, L., 2021, Reconciling early Deccan Traps CO_2 outgassing and pre-KPB global climate. Proceedings of the National Academy of Sciences, 118, https://doi.org/10.1073/pnas.2007797118.

Herrle, J.O. and Mutterlose, J., 2003, Calcareous nannofossils from the Aptian–Lower Albian of southeast France: palaeoecological and biostratigraphic implications. Cretaceous Research, 24, p. 1–22, https://doi.org/10.1016/S0195-6671(03)00023-5.

Herrle, J.O., Pross, J., Friedrich, O. and Hemleben, C., 2003, Short-term environmental changes in the Cretaceous Tethyan Ocean: micropalaeontological evidence from the Early Albian Oceanic Anoxic Event 1b. Terra Nova, 15, p. 14–19, https://doi.org/10.1046/j.1365-3121.2003.00448.x.

Herrle, J.O., Kößler, P., Friedrich, O., Erlenkeuser, H. and Hemleben, C., 2004, High-resolution carbon isotope records of the Aptian to Lower Albian from SE France and the Mazagan Plateau (DSDP Site 545): a stratigraphic tool for paleoceanographic and paleobiologic reconstruction. Earth and Planetary Science Letters, 218, p. 149–161, https://doi.org/10.1016/S0012-821X(03)00646-0.

Herrle, J.O., Schröder-Adams, C.J., Davis, W., Pugh, A.T., Galloway, J.M. and Fath, J., 2015, Mid-Cretaceous High Arctic stratigraphy, climate, and oceanic anoxic events. Geology, 43, p. 403–406, https://doi.org/10.1130/G36439.1.

Hoernle, K., Hauff, F., van den Bogaard, P., Werner, R., Mortimer, N., Geldmacher, J., Garbe-Schönberg, D. and Davy, B., 2010, Age and geochemistry of volcanic rocks from the Hikurangi and Manihiki oceanic Plateaus. Geochimica et Cosmochimica Acta, 74, p. 7196–7219, https://doi.org/10.1016/j.gca.2010.09.030.

Hoffmann, R. and Mutterlose, J., 2011, Stratigraphie und Cephalopodenfauna des Unter-Apt von Alstätte (NRW). Geologie und Paläontologie in Westfalen, 80, p. 43–59.

Holmden, C., Jacobson, A.D., Sageman, B.B. and Hurtgen, M.T., 2016, Response of the Cr isotope proxy to Cretaceous Ocean Anoxic Event 2 in a pelagic carbonate succession from the Western Interior Seaway. Geochimica et Cosmochimica Acta, 186, p. 277–295, https://doi.org/10.1016/j.gca.2016.04.039.

Hönisch, B., Ridgwell, A., Schmidt, D.N., Thomas, E., Gibbs, S.J., Sluijs, A., Zeebe, R., Kump, L., Martindale, R.C., Greene, S.E. and Kiessling, W., 2012, The geological record of ocean acidification. Science, 335, p. 1058–1063, https://doi.org/10.1126/science.1208277.

Huber, B.T. and Leckie, R.M., 2011, Planktic foraminiferal species turnover across deep-sea Aptian/Albian boundary sections. The Journal of Foraminiferal Research, 41, p. 53–95, https://doi.org/10.2113/gsjfr.41.1.53.

Huber, B.T., MacLeod, K.G., Gröcke, D.R. and Kucera, M., 2011, Paleotemperature and paleosalinity inferences and chemostratigraphy across the Aptian/Albian boundary in the subtropical North Atlantic. Paleoceanography, 26, https://doi.org/10.1029/2011PA002178.

Hull, P.M., Bornemann, A., Penman, D.E., Henehan, M.J., Norris, R.D., Wilson, P.A., Blum, P., Alegret, L., Batenburg, S.J., Bown, P.R. and Bralower, T.J., 2020, On impact and volcanism across the Cretaceous-Paleogene boundary. Science, 367, p. 266–272, https://doi.org/science.aay5055.

Ingle, S. and Coffin, M.F., 2004, Impact origin for the greater Ontong Java Plateau?. Earth and Planetary Science Letters, 218, p. 123–134, https://doi.org/10.1016/S0012-821X(03)00629-0.

Ingle, S., Mahoney, J.J., Sato, H., Coffin, M.F., Kimura, J.I., Hirano, N. and Nakanishi, M., 2007, Depleted mantle wedge and sediment fingerprint in unusual basalts from the Manihiki Plateau, central Pacific Ocean. Geology, 35, p. 595–598, https://doi.org/10.1130/G23741A.1.

Ishikawa, A., Senda, R., Suzuki, K., Dale, C. W. and Meisel, T., 2014, Re-evaluating digestion methods for highly siderophile element and ^{187}Os isotope analysis: Evidence from geological reference materials. Chemical Geology, 384, p. 27–46, https://doi.org/10.1016/j.chemgeo.2014.06.013.

Jahren, A.H., Arens, N.C., Sarmiento, G., Guerrero, J. and Amundson, R., 2001, Terrestrial record of methane hydrate dissociation in the Early Cretaceous. Geology, 29, p. 159–162, https://doi.org/10.1130/0091-7613(2001)029<0159:TROMHD>2.0.CO;2.

Janasi, V.d.A., de Freitas, V.A. and Heaman, L.H., 2011, The onset of flood basalt volcanism, Northern Paraná Basin, Brazil: a precise U–Pb baddeleyite/zircon age for a Chapecó-type dacite. Earth and Planetary Science Letters, 302, p. 147–153, https://doi.org/10.1016/j.epsl.2010.12.005.

Jarvis, I., Lignum, J.S., Gröcke, D.R., Jenkyns, H.C. and Pearce, M.A., 2011, Black shale deposition, atmospheric CO_2 drawdown, and cooling during the Cenomanian–Turonian Oceanic Anoxic Event. Paleoceanography, 26, PA3201, https://doi.org/10.1029/2010PA002081.

Jelby, M.E., Śliwińska, K.K., Koevoets, M.J., Alsen, P., Vickers, M.L., Olaussen, S. and Stemmerik, L., 2020, Arctic reappraisal of global carbon-cycle dynamics across the Jurassic–Cretaceous boundary and

Valanginian Weissert Event. Palaeogeography, Palaeoclimatology, Palaeoecology, 555, 109847, https://doi.org/10.1016/j.palaeo.2020.109847.

Jenkyns, H.C., 1995, Carbon-isotope stratigraphy and paleoceanographic significance of the Lower Cretaceous shallow-water carbonates of Resolution Guyot, Mid-Pacific Mountains. *In* Winterer, E.L., Sager, W.W., Firth, J.V. and Sinton J.M. (Eds.), Proceedings of the Ocean Drilling Program, Scientific Results, 143, p. 99–104. College Station, Texas, Ocean Drilling Program, https://doi.org/10.2973/odp.proc.sr.143.213.1995.

Jenkyns, H.C., 2003, Evidence for rapid climate change in the Mesozoic–Palaeogene greenhouse world. Philosophical Transactions of the Royal Society of London. Series A: Mathematical, Physical and Engineering Sciences, 361, p. 1885–1916, https://doi.org/10.1098/rsta.2003.1240.

Jenkyns, H.C., 2010, Geochemistry of oceanic anoxic events. Geochemistry, Geophysics, Geosystems, 11, https://doi.org/10.1029/2009GC002788.

Jenkyns, H.C., 2018, Transient cooling episodes during Cretaceous Oceanic Anoxic Events with special reference to OAE 1a (Early Aptian). Philosophical Transactions of the Royal Society A: Mathematical, Physical and Engineering Sciences, 376, 20170073, https://doi.org/10.1098/rsta.2017.0073.

Jenkyns, H.C., Matthews, A., Tsikos, H., Erel, Y., 2007. Nitrate reduction, sulfate reduction, and sedimentary iron isotope evolution during the Cenomanian–Turonian oceanic anoxic event. Paleoceanography 22, PA3208, https://doi.org/10.1029/2006PA001355.

Jenkyns, H.C., Schouten-Huibers, L., Schouten, S. and Sinninghe Damsté, J.S., 2012, Warm Middle Jurassic–Early Cretaceous high-latitude sea-surface temperatures from the Southern Ocean. Climate of the Past, 8, p. 215–226, https://doi.org/10.5194/cp-8-215-2012.

Jenkyns, H.C., Dickson, A.J., Ruhl, M. and Boorn, S.H., 2017, Basalt-seawater interaction, the Plenus Cold Event, enhanced weathering and geochemical change: deconstructing Oceanic Anoxic Event 2 (Cenomanian–Turonian, Late Cretaceous). Sedimentology, 64, p. 16–43, https://doi.org/10.1111/sed.12305.

Jiang, Q., Jourdan, F., Olierook, H.K., Merle, R.E. and Whittaker, J.M., 2021, Longest continuously erupting large igneous province driven by plume-ridge interaction. Geology, 49, p. 206–210, https://doi.org/10.1130/G47850.1.

Jiang, Q., Jourdan, F., Olierook, H.K., Merle, R.E., Bourdet, J., Fougerouse, D., Godel, B. and Walker, A.T., 2022, Volume and rate of volcanic CO_2 emissions governed the severity of past environmental crises. Proceedings of the National Academy of Sciences, 119, https://doi.org/10.1073/pnas.2202039119.

Jiang, Q., Jourdan, F., Olierook, H.K. and Merle, R.E., 2023, An appraisal of the ages of Phanerozoic large igneous provinces. Earth-Science Reviews, 237, 104314, https://doi.org/10.1016/j.earscirev.2023.104314.

Jones, C.E. and Jenkyns, H.C., 2001, Seawater strontium isotopes, oceanic anoxic events, and seafloor hydrothermal activity in the Jurassic and Cretaceous. American Journal of Science, 301, p. 112–149, https://doi.org/10.2475/ajs.301.2.112.

Jones, M.T., Jerram, D.A., Svensen, H.H. and Grove, C., 2016, The effects of large igneous provinces on the global carbon and sulphur cycles. Palaeogeography, Palaeoclimatology, Palaeoecology, 441, p. 4–21, https://doi.org/10.1016/j.palaeo.2015.06.042.

Jones, M.M., Sageman, B.B., Selby, D., Jicha, B.R., Singer, B.S. and Titus, A.L., 2021, Regional chronostratigraphic synthesis of the Cenomanian–Turonian Oceanic Anoxic Event 2 (OAE 2) interval, Western Interior Basin (USA): New Re-Os chemostratigraphy and $^{40}Ar/^{39}Ar$ geochronology. Geological Society of America Bulletin, 133, p. 1090–1104, https://doi.org/10.1130/B35594.1.

Jones, M.M., Sageman, B.B., Selby, D., Jacobson, A.D., Batenburg, S.J., Riquier, L., MacLeod, K.G., Huber, B.T., Bogus, K.A., Tejada, M.L.G. and Kuroda, J., 2023, Abrupt episode of mid-Cretaceous ocean acidification triggered by massive volcanism. Nature Geoscience, p. 169–174, https://doi.org/10.1038/s41561-022-01115-w.

Junium, C.K. and Arthur, M.A., 2007, Nitrogen cycling during the Cretaceous, Cenomanian-Turonian oceanic anoxic event II. Geochemistry, Geophysics, Geosystems, 8, https://doi.org/10.1029/2006GC001328.

Kasbohm, J., Schoene, B. and Burgess, S., 2021, Radiometric Constraints on the Timing, Tempo, and Effects of Large Igneous Province Emplacement. In Ernst, R.E., Dickson, A.J., Bekker, A. (Eds.): Large Igneous

Provinces: A Driver of Global Environmental and Biotic Changes. AGU Geophysical Monograph 255, p. 27–82, https://doi.org/10.1002/9781119507444.ch2.

Keller, C.E., Hochuli, P.A., Weissert, H., Bernasconi, S.M., Giorgioni, M. and Garcia, T.I., 2011, A volcanically induced climate warming and floral change preceded the onset of OAE1a (Early Cretaceous). Palaeogeography, Palaeoclimatology, Palaeoecology, 305, p. 43–49, https://doi.org/10.1016/j.palaeo.2011.02.011.

Keller, G., 2012, The Cretaceous–Tertiary mass extinction, Chicxulub impact, and Deccan volcanism. In Talent, J.A. (Ed.): Earth and Life: Global Biodiversity, Extinction Intervals and Biogeographic Perturbations Through Time, p. 759–793, Springer, Dordrecht, https://doi.org/10.1007/978-90-481-3428-1_25.

Keller, G., Mateo, P., Punekar, J., Khozyem, H., Gertsch, B., Spangenberg, J., Bitchong, A.M. and Adatte, T., 2018, Environmental changes during the Cretaceous-Paleogene mass extinction and Paleocene-Eocene thermal maximum: Implications for the Anthropocene. Gondwana Research, 56, p. 69–89, https://doi.org/10.1016/j.gr.2017.12.002.

Keller, G., Mateo, P., Monkenbusch, J., Thibault, N., Punekar, J., Spangenberg, J.E., Abramovich, S., Ashckenazi-Polivoda, S., Schoene, B., Eddy, M.P. and Samperton, K.M., 2020, Mercury linked to Deccan Traps volcanism, climate change and the end-Cretaceous mass extinction. Global and Planetary Change, 194, 103312, https://doi.org/10.1016/j.gloplacha.2020.103312.

Kent, R.W., Pringle, M.S., Müller, R.D., Saunders, A.D. and Ghose, N.C., 2002, $^{40}Ar/^{39}Ar$ geochronology of the Rajmahal basalts, India, and their relationship to the Kerguelen Plateau. Journal of Petrology, 43, p. 1141–1153, https://doi.org/10.1093/petrology/43.7.1141.

Kerr, A.C., 1998, Oceanic plateau formation: a cause of mass extinction and black shale deposition around the Cenomanian–Turonian boundary?. Journal of the Geological Society of London, 155, p. 619–626, https://doi.org/10.1144/gsjgs.155.4.0619.

Kerr, A.C., 2005, La Isla de Gorgona, Colombia: a petrological enigma? Lithos, 84, p. 77–101, https://doi.org/10.1016/j.lithos.2005.02.006.

Kerr, A.C., 2014, Oceanic Plateaus. In Holland, H.D. and Turekian K.K. (Eds.), Treatise on Geochemistry: Vol: 4: the Crust, Elsevier, Amsterdam, p. 631–667, https://doi.org/10.1016/B978-0-08-095975-7.00320-X.

Kerr, A.C., Tarney, J., Marriner, G.F., Nivia, A. and Saunders, A.D., 1997, The Caribbean-Colombian Cretaceous igneous province: The internal anatomy of an oceanic plateau. In Mahoney, J.J. and Coffin M.F. (Eds.): Large Igneous Provinces, Continental, Oceanic, and Planetary Flood Volcanism. AGU Geophysical Monograph, 100, p. 123–144.

Kerr, A.C., White, R.V., Thompson, P.M.E., Tarney, J. and Saunders, A.D., 2003, No Oceanic Plateau – No Caribbean Plate? The Seminal Role of an oceanic plateau in Caribbean plate evolution. In: Bartolini, C., Buffler, R.T. and Blickwede, J. (Eds.), The Gulf of Mexico and Caribbean Region: Hydrocarbon Habitats, Basin Formation and Plate Tectonics. AAPG Memoir, 79, p. 126–168.

Kerr, A.C., Tarney, J., Kempton, P.D., Pringle, M. and Nivia, A., 2004, Mafic pegmatites intruding oceanic plateau gabbros and ultramafic cumulates from Bolívar, Colombia: Evidence for a 'wet' mantle plume? Journal of Petrology, 45, p. 1877–1906, https://doi.org/10.1093/petrology/egh037.

Kiessling, W. and Kocsis, Á.T., 2015, Biodiversity dynamics and environmental occupancy of fossil azooxanthellate and zooxanthellate scleractinian corals. Paleobiology, 41, p. 402–414, https://doi.org/10.1017/pab.2015.6.

Kim, J.H., Van der Meer, J., Schouten, S., Helmke, P., Willmott, V., Sangiorgi, F., Koç, N., Hopmans, E.C. and Damsté, J.S.S., 2010, New indices and calibrations derived from the distribution of crenarchaeal isoprenoid tetraether lipids: Implications for past sea surface temperature reconstructions. Geochimica et Cosmochimica Acta, 74, p. 4639–4654, https://doi.org/10.1016/j.gca.2010.05.027.

Kingsbury, C.G., Kamo, S.L., Ernst, R.E., Söderlund, U. and Cousens, B.L., 2018, U-Pb geochronology of the plumbing system associated with the Late Cretaceous Strand Fiord Formation, Axel Heiberg Island, Canada: part of the 130-90 Ma High Arctic large igneous province. Journal of Geodynamics, 118, p. 106–117, https://doi.org/10.1016/j.jog.2017.11.001.

Kongchum, M., Hudnall, W.H. and Delaune, R.D., 2011, Relationship between sediment clay minerals and total mercury. Journal of Environmental Science and Health, Part A, 46, p. 534–539, https://doi.org/10.1080/10934529.2011.551745.

Koutsoukos, E.A.M., 1992, Late Aptian to Maastrichtian foraminiferal biogeography and palaeoceanography of the Sergipe Basin, Brazil. Palaeogeography, palaeoclimatology, palaeoecology, 92, p. 295–324, https://doi.org/10.1016/0031-0182(92)90089-N.

Kuhnt, W., Holbourn, A. and Moullade, M., 2011, Transient global cooling at the onset of early Aptian oceanic anoxic event (OAE) 1a. Geology, 39, p. 323–326, https://doi.org/10.1130/G31554.1.

Kujau, A., Heimhofer, U., Hochuli, P.A., Pauly, S., Morales, C., Adatte, T., Föllmi, K., Ploch, I. and Mutterlose, J., 2013, Reconstructing Valanginian (Early Cretaceous) mid-latitude vegetation and climate dynamics based on spore–pollen assemblages. Review of Palaeobotany and Palynology, 197, p. 50–69, https://doi.org/10.1016/j.revpalbo.2013.05.003.

Kumar, A., Pande, K., Venkatesan, T.R. and Rao, Y.B., 2001, The Karnataka Late Cretaceous Dykes as products of the Marion Hot Spot at the Madagascar-India Breakup Event: Evidence from ^{40}Ar-^{39}Ar geochronology and geochemistry. Geophysical Research Letters, 28, p. 2715–2718, https://doi.org/10.1029/2001GL013007.

Kump, L.R., Bralower, T.J. and Ridgwell, A., 2009, Ocean acidification in deep time. Oceanography, 22, p. 94–107.

Kuroda, J., Ogawa, N.O., Tanimizu, M., Coffin, M.F., Tokuyama, H., Kitazato, H. and Ohkouchi, N., 2007, Contemporaneous massive subaerial volcanism and late cretaceous Oceanic Anoxic Event 2. Earth and Planetary Science Letters, 256, p. 211–223, https://doi.org/10.1016/j.epsl.2007.01.027.

Kuroda, J., Tanimizu, M., Hori, R.S., Suzuki, K., Ogawa, N.O., Tejada, M.L.G., Coffin, M.F., Coccioni, R., Erba, E. and Ohkouchi, N., 2011, Lead isotopic record of Barremian–Aptian marine sediments: Implications for large igneous provinces and the Aptian climatic crisis. Earth and Planetary Science Letters, 307, p. 126–134, https://doi.org/10.1016/j.epsl.2011.04.021.

Kuypers, M.M., van Breugel, Y., Schouten, S., Erba, E. and Damsté, J.S.S., 2004, N_2-fixing cyanobacteria supplied nutrient N for Cretaceous oceanic anoxic events. Geology, 32, p. 853–856, https://doi.org/10.1130/G20458.1.

Larson, R.L., 1991, Latest pulse of Earth: Evidence for a mid-Cretaceous superplume. Geology, 19, p. 547–550, https://doi.org/10.1130/0091-7613(1991)019<0547:LPOEEF>2.3.CO;2.

Larson, R.L. and Erba, E., 1999, Onset of the Mid-Cretaceous greenhouse in the Barremian-Aptian: Igneous events and the biological, sedimentary, and geochemical responses. Paleoceanography, 14, https://doi.org/10.1029/1999PA900040.

Leandro, C.G., Savian, J.F., Kochhann, M.V.L., Franco, D.R., Coccioni, R., Frontalini, F., Gardin, S., Jovane, L., Figueiredo, M., Tedeschi, L.R. and Janikian, L., 2022, Astronomical tuning of the Aptian stage and its implications for age recalibrations and paleoclimatic events. Nature Communications, 13, https://doi.org/10.1038/s41467-022-30075-3.

Lechler, M., Pogge von Strandmann, P.A.E., Jenkyns, H.C., Prosser, G. and Parente, M., 2015, Lithium-isotope evidence for enhanced silicate weathering during OAE 1a (Early Aptian Selli event). Earth and Planetary Science Letters, 432, p. 210–222, https://doi.org/10.1016/j.epsl.2015.09.052.

Leckie, R.M., Bralower, T.J. and Cashman, R., 2002, Oceanic anoxic events and plankton evolution: Biotic response to tectonic forcing during the mid-Cretaceous. Paleoceanography, 17, https://doi.org/10.1029/2001PA000623.

Leloux, J., 1999, Numerical distribution of Santonian to Danian corals (Scleractinia, Octocorallia) of southern Limburg, the Netherlands. Geologie en Mijnbouw, 78, p. 191–195, https://doi.org/10.1023/A:1003743301625.

Li, L. and Keller, G., 1998a, Abrupt deep-sea warming at the end of the Cretaceous. Geology, 26, p. 995–998, https://doi.org/10.1130/0091-7613(1998)026<0995:ADSWAT>2.3.CO;2.

Li, L. and Keller, G., 1998, Maastrichtian climate, productivity and faunal turnovers in planktic foraminifera in South Atlantic DSDP sites 525A and 21. Marine Micropaleontology, 33, p. 55–86, https://doi.org/10.1016/S0377-8398(97)00027-3.

Li, Y.X., Bralower, T.J., Montañez, I.P., Osleger, D.A., Arthur, M.A., Bice, D.M., Herbert, T.D., Erba, E. and Silva, I.P., 2008, Toward an orbital chronology for the early Aptian Oceanic Anoxic Event (OAE1a,

~120 Ma). Earth and Planetary Science Letters, 271, p. 88–100, https://doi.org/10.1016/j.epsl.2008.03.055.

Li, X., Wei, Y., Li, Y. and Zhang, C., 2016, Carbon isotope records of the early Albian oceanic anoxic event (OAE) 1b from eastern Tethys (southern Tibet, China). Cretaceous Research, 62, p. 109–121, https://doi.org/10.1016/j.cretres.2015.08.015.

Lini, A., Weissert, H. and Erba, E., 1992, The Valanginian carbon isotope event: a first episode of greenhouse climate conditions during the Cretaceous. Terra Nova, 4, p. 374–384, https://doi.org/10.1111/j.1365-3121.1992.tb00826.x.

Linnert, C., Mutterlose, J. and Erbacher, J., 2010, Calcareous nannofossils of the Cenomanian/Turonian boundary interval from the Boreal Realm (Wunstorf, northwest Germany). Marine Micropaleontology, 74, p. 38–58, https://doi.org/10.1016/j.marmicro.2009.12.002.

Linnert, C., Mutterlose, J. and Mortimore, R., 2011, Calcareous nannofossils from Eastbourne (southeastern England) and the paleoceanography of the Cenomanian–Turonian boundary interval. Palaios, 26, p. 298–313, https://doi.org/10.2110/palo.2010.p10-130r.

Littler, K., Robinson, S.A., Bown, P.R., Nederbragt, A.J. and Pancost, R.D., 2011, High sea-surface temperatures during the Early Cretaceous Epoch. Nature Geoscience, 4, p. 169–172, https://doi.org/10.1038/ngeo1081.

Liu, Z., Percival, L.M.E., Vandeputte, D., Selby, D., Claeys, P., Over, D.J., Gao, Y., 2021, Late Devonian mercury record from North America and its implications for the Frasnian–Famennian mass extinction. Palaeogeography, Palaeoclimatology, Palaeoecology, 576, 110502, https://doi.org/10.1016/j.palaeo.2021.110502.

Lorenzen, J., Kuhnt, W., Holbourn, A., Flögel, S., Moullade, M. and Tronchetti, G., 2013, A new sediment core from the Bedoulian (Lower Aptian) stratotype at Roquefort-La Bédoule, SE France. Cretaceous Research, 39, p. 6–16, https://doi.org/10.1016/j.cretres.2012.03.019.

Lu, Z., Jenkyns, H.C. and Rickaby, R.E., 2010, Iodine to calcium ratios in marine carbonate as a paleo-redox proxy during oceanic anoxic events. Geology, 38, p. 1107–1110, https://doi.org/10.1130/G31145.1.

Lübke, N. and Mutterlose, J., 2016, The impact of OAE 1a on marine biota deciphered by size variations of coccoliths. Cretaceous Research, 61, p. 169–179, https://doi.org/10.1016/j.cretres.2016.01.006.

Lübke, N., Mutterlose, J. and Bottini, C., 2015, Size variations of coccoliths in Cretaceous oceans—A result of preservation, genetics and ecology? Marine Micropaleontology, 117, p. 25–39, https://doi.org/10.1016/j.marmicro.2015.03.002.

Mahanipour, A., Mutterlose, J. and Eftekhari, M., 2019, Calcareous nannofossils of the Barremian–Aptian interval from the southeastern Tethys (Zagros Basin, West Iran) and their paleoceanographic implications: A record of Oceanic Anoxic Event 1a. Marine Micropaleontology, 149, p. 64–74, https://doi.org/10.1016/j.marmicro.2019.04.003.

Maher, H.D., 2001, Manifestations of the Cretaceous High Arctic large igneous province in Svalbard. The Journal of Geology, 109, p. 91–104, https://doi.org/10.1086/317960.

Maher, W., Krikowa, F. and Ellwood, M., 2020, Mercury cycling in Australian estuaries and near shore coastal ecosystems: Triggers for management. Elementa Science of the Anthropocene, 8, https://doi.org/10.1525/elementa.425.

Mahoney, J., Nicollet, C. and Dupuy, C., 1991, Madagascar basalts: tracking oceanic and continental sources. Earth and Planetary Science Letters, 104, p. 350–363, https://doi.org/10.1016/0012-821X(91)90215-4.

Mahoney, J.J., Storey, M., Duncan, R.A., Spencer, K.J. and Pringle, M., 1993. Geochemistry and age of the Ontong Java Plateau. In Pringle, M., Sager, W.W. Sliter, W.V. and Stein, S. (Eds.): The Mesozoic Pacific: Geology, Tectonics, and Volcanism. AGU Geophysical Monograph 77, p. 233–261, https://doi.org/10.1029/GM077p0233.

Mahoney, J.J., Saunders, A.D., Storey, M. and Randriamanantenasoa, A., 2008, Geochemistry of the Volcan de l'Androy basalt–rhyolite complex, Madagascar Cretaceous igneous province. Journal of Petrology, 49, p. 1069–1096, https://doi.org/10.1093/petrology/egn018.

Malinverno, A., Erba, E. and Herbert, T.D., 2010, Orbital tuning as an inverse problem: Chronology of the early Aptian oceanic anoxic event 1a (Selli Level) in the Cismon APTICORE. Paleoceanography and Paleoclimatology, 25, https://doi.org/10.1029/2009PA001769.

Marks, L., Keiding, J., Wenzel, T., Trumbull, R.B., Veksler, I., Wiedenbeck, M. and Markl, G., 2014, F, Cl, and S concentrations in olivine-hosted melt inclusions from mafic dikes in NW Namibia and implications for the environmental impact of the Paraná–Etendeka Large Igneous Province. Earth and Planetary Science Letters, 392, p. 39–49, https://doi.org/10.1016/j.epsl.2014.01.057.

Marsh, J.S., Ewart, A., Milner, S.C., Duncan, A.R. and Miller, R.M., 2001, The Etendeka Igneous Province: magma types and their stratigraphic distribution with implications for the evolution of the Paraná-Etendeka flood basalt province. Bulletin of Volcanology, 62, p. 464–486, https://doi.org/10.1007/s004450000115.

Martinez, M., Deconinck, J.F., Pellenard, P., Riquier, L., Company, M., Reboulet, S. and Moiroud, M., 2015, Astrochronology of the Valanginian–Hauterivian stages (Early Cretaceous): Chronological relationships between the Paraná–Etendeka large igneous province and the Weissert and the Faraoni events. Global and Planetary Change, 131, p. 158–173, https://doi.org/10.1016/j.gloplacha.2015.06.001.

Martinez, M., Aguirre-Urreta, B., Dera, G., Lescano, M., Omarini, J., Tunik, M., O'Dogherty, L., Aguado, R., Company, M. and Bodin, S., 2023, Synchrony of carbon cycle fluctuations, volcanism and orbital forcing during the Early Cretaceous. Earth-Science Reviews, 104356, https://doi.org/10.1016/j.earscirev.2023.104356.

Martínez-Rodríguez, R., Selby, D., Castro, J.M., de Gea, G.A., Nieto, L.M. and Ruiz-Ortiz, P.A., 2021, Tracking magmatism and oceanic change through the early Aptian Anoxic Event (OAE 1a) to the late Aptian: Insights from osmium isotopes from the westernmost Tethys (SE Spain) Cau Core. Global and Planetary Change, 207, 103652, https://doi.org/10.1016/j.gloplacha.2021.103652.

Matsumoto, H., Kuroda, J., Coccioni, R., Frontalini, F., Sakai, S., Ogawa, N.O. and Ohkouchi, N., 2020, Marine Os isotopic evidence for multiple volcanic episodes during Cretaceous Oceanic Anoxic Event 1b. Scientific Reports, 10, https://doi.org/10.1038/s41598-020-69505-x.

Matsumoto, H., Coccioni, R., Frontalini, F., Shirai, K. and Kuroda, J., 2021a, Osmium Isotopic Evidence for Eccentricity-Paced Increases in Continental Weathering During the Latest Hauterivian, Early

Cretaceous. Geochemistry, Geophysics, Geosystems, 22, e2021GC009789, https://doi.org/10.1029/2021GC009789.

Matsumoto, H., Coccioni, R., Frontalini, F., Shirai, K., Jovane, L., Trindade, R., Savian, J., Tejada, M.L.G., Gardin, S. and Kuroda, J., 2021b, Long-term Aptian marine osmium isotopic record of Ontong Java Nui activity. Geology, 49, p. 1148–1152, https://doi.org/10.1130/G48863.1.

Matsumoto, H., Coccioni, R., Frontalini, F., Shirai, K., Jovane, L., Trindade, R., Savian, J.F. and Kuroda, J., 2022, Mid-Cretaceous marine Os isotope evidence for heterogeneous cause of oceanic anoxic events. Nature communications, 13, https://doi.org/10.1038/s41467-021-27817-0.

Matsumoto, H., Shirai, K., Huber, B.T., MacLeod, K.G. and Kuroda, J., 2023, High-resolution marine osmium and carbon isotopic record across the Aptian–Albian boundary at the southern Atlantic Ocean: Implication for the enhanced continental weathering and the acidified oceanic condition across the Aptian–Albian boundary. Palaeogeography, Palaeoclimatology, Palaeoecology, 613, 111414, https://doi.org/10.1016/j.palaeo.2023.111414.

Matsumoto, H., Ishikawa, A., Coccioni, R., Frontalini, F. and Suzuki, K., Fine-grained interplanetary dust input during the Turonian (Late Cretaceous): evidence from osmium isotope and platinum group elements. Scientific Reports, https://doi.org/10.1038/s41598-023-49252-5 (*in press*).

Mattioli, E., Pittet, B., Riquier, L. and Grossi, V., 2014, The mid-Valanginian Weissert Event as recorded by calcareous nannoplankton in the Vocontian Basin. Palaeogeography, Palaeoclimatology, Palaeoecology, 414, p. 472–485, https://doi.org/10.1016/j.palaeo.2014.09.030.

Mauffret, A. and Leroy, S., 1997, Seismic stratigraphy and structure of the Caribbean igneous province. Tectonophysics, 283, p. 61–104, https://doi.org/10.1016/S0040-1951(97)00103-0.

McAnena, A., Flögel, S., Hofmann, P., Herrle, J.O., Griesand, A., Pross, J., Talbot, H.M., Rethemeyer, J., Wallmann, K. and Wagner, T., 2013, Atlantic cooling associated with a marine biotic crisis during the mid-Cretaceous period. Nature Geoscience, 6, p. 558–561, https://doi.org/10.1038/ngeo1850.

McArthur, J.M., Janssen, N.M.M., Reboulet, S., Leng, M.J., Thirlwall, M.F. and Van de Schootbrugge, B., 2007, Palaeotemperatures, polar ice-volume, and isotope stratigraphy (Mg/Ca, $\delta^{18}O$, $\delta^{13}C$, $^{87}Sr/^{86}Sr$):

The Early Cretaceous (Berriasian, Valanginian, Hauterivian). Palaeogeography, Palaeoclimatology, Palaeoecology, 248, p. 391–430, https://doi.org/10.1016/j.palaeo.2006.12.015.

McArthur, J.M., Howarth, R.J., Shields, G.A. and Zhou, Y., 2020, Strontium isotope stratigraphy. In Gradstein, F.M., Ogg, J.G., Schmitz, M.D. and Ogg, G.M. (Eds.): Geologic time scale 2020, p. 211–238, Elsevier, https://doi.org/10.1016/B978-0-12-824360-2.00027-3.

Méhay, S., Keller, C.E., Bernasconi, S.M., Weissert, H., Erba, E., Bottini, C. and Hochuli, P.A., 2009, A volcanic CO_2 pulse triggered the Cretaceous Oceanic Anoxic Event 1a and a biocalcification crisis. Geology, 37, p. 819–822, https://doi.org/10.1130/G30100A.1.

Meissner, P., Mutterlose, J. and Bodin, S., 2015, Latitudinal temperature trends in the northern hemisphere during the Early Cretaceous (Valanginian–Hauterivian). Palaeogeography, Palaeoclimatology, Palaeoecology, 424, p. 17–39, https://doi.org/10.1016/j.palaeo.2015.02.003.

Melluso, L., Morra, V., Brotzu, P. and Mahoney, J.J., 2001, The Cretaceous igneous province of Madagascar: geochemistry and petrogenesis of lavas and dykes from the central–western sector. Journal of Petrology, 42, p. 1249–1278, https://doi.org/10.1093/petrology/42.7.1249.

Melluso, L., Morra, V., Brotzu, P., Tommasini, S., Renna, M.R., Duncan, R.A., Franciosi, L. and D'Amelio, F., 2005, Geochronology and petrogenesis of the Cretaceous Antampombato–Ambatovy complex and associated dyke swarm, Madagascar. Journal of Petrology, 46, p. 1963–1996, https://doi.org/10.1093/petrology/egi044.

Mena, M., Goguitchaichvili, A., Solano, M.C. and Vilas, J.F., 2011, Paleosecular variation and absolute geomagnetic paleointensity records retrieved from the Early Cretaceous Posadas Formation (Misiones, Argentina). Studia Geophysica et Geodaetica, 55, p. 279–309, https://doi.org/10.1007/s11200-011-0016-3.

Menegatti, A.P., Weissert, H., Brown, R.S., Tyson, R.V., Farrimond, P., Strasser, A. and Caron, M., 1998, High-resolution $\delta^{13}C$ stratigraphy through the early Aptian "Livello Selli" of the Alpine Tethys. Paleoceanography, 13, https://doi.org/10.1029/98PA01793.

Meyers, S.R., Siewert, S.E., Singer, B.S., Sageman, B.B., Condon, D.J., Obradovich, J.D., Jicha, B.R. and Sawyer, D.A., 2012, Intercalibration of radioisotopic and astrochronologic time scales for the Cenomanian-Turonian boundary interval, Western Interior Basin, USA. *Geology*, *40*, p. 7–10, https://doi.org/10.1130/G32261.1.

Millán, M.I., Weissert, H.J. and López-Horgue, M.A., 2014, Expression of the late Aptian cold snaps and the OAE1b in a highly subsiding carbonate platform (Aralar, northern Spain). Palaeogeography, Palaeoclimatology, Palaeoecology, 411, p. 167–179, https://doi.org/10.1016/j.palaeo.2014.06.024.

Milner, S.C., Duncan, A.R. and Ewart, A., 1992, Quartz latite rheoignimbrite flows of the Etendeka Formation, north-western Namibia. Bulletin of Volcanology, 54, p. 200–219, https://doi.org/10.1007/BF00278389.

Milner, S.C., Duncan, A.R., Whittingham, A.M. and Ewart, A., 1995, Trans-Atlantic correlation of eruptive sequences and individual silicic volcanic units within the Paraná-Etendeka igneous province. Journal of Volcanology and geothermal Research, 69, p. 137–157, https://doi.org/10.1016/0377-0273(95)00040-2.

Mittal, T., Sprain, C.J., Renne, P.R. and Richards, M.A., 2022, Deccan volcanism at K-Pg time. In Koeberl, C., Claeys, P., and Montanari, A. (Eds.): From the Guajira Desert to the Apennines, and from Mediterranean Microplates to the Mexican Killer Asteroid: Honoring the Career of Walter Alvarez, Geological Society of America Special Papers, 557, p. 471–496, https://doi.org/10.1130/2022.2557(22).

Möller, C., Mutterlose, J. and Alsen, P., 2015, Integrated stratigraphy of Lower Cretaceous sediments (Ryazanian–Hauterivian) from North-East Greenland. Palaeogeography, Palaeoclimatology, Palaeoecology, 437, p. 85–97, https://doi.org/10.1016/j.palaeo.2015.07.014.

Möller, C., Bornemann, A. and Mutterlose, J., 2020, Climate and paleoceanography controlled size variations of calcareous nannofossils during the Valanginian Weissert Event (Early Cretaceous). Marine Micropaleontology, 157, 101875, https://doi.org/10.1016/j.marmicro.2020.101875.

Moreno-Sanchez, M. and Pardo-Trujillo, A., 2003, Stratigraphical and sedimentological constraints on western Colombia: Implications on the evolution of the Caribbean plate. In Bartolini, C., Buffler, R.T. and

Blickwede, J. (Eds.): The Circum-Gulf of Mexico and the Caribbean: Hydrocarbon Habitats, Basin Formation, and Plate Tectonics. AAPG Memoir, 79, p. 891–924.

Mort, H.P., Adatte, T., Föllmi, K.B., Keller, G., Steinmann, P., Matera, V., Berner, Z. and Stüben, D., 2007, Phosphorus and the roles of productivity and nutrient recycling during oceanic anoxic event 2. Geology, 35, p. 483–486, https://doi.org/10.1130/G23475A.1.

Mutterlose, J., 1998, The Barremian–Aptian turnover of biota in northwestern Europe: evidence from belemnites. Palaeogeography, Palaeoclimatology, Palaeoecology, 144, p. 161–173, https://doi.org/10.1016/S0031-0182(98)00081-9.

Mutterlose, J. and Böckel, B., 1998, The Barremian–Aptian interval in NW Germany: a review. Cretaceous Research, 19, p. 539–568, https://doi.org/10.1006/cres.1998.0119.

Mutterlose, J., Bottini, C., Schouten, S. and Sinninghe Damsté, J.S., 2014, High sea-surface temperatures during the early Aptian Oceanic Anoxic Event 1a in the Boreal Realm. Geology, 42, p. 439–442, https://doi.org/10.1130/G35394.1.

Naber, T.V., Grasby, S.E., Cuthbertson, J.P., Rayner, N. and Tegner, C., 2021, New constraints on the age, geochemistry, and environmental impact of High Arctic Large Igneous Province magmatism: Tracing the extension of the Alpha Ridge onto Ellesmere Island, Canada. Geological Society of America Bulletin, 133, p. 1695–1711, https://doi.org/10.1130/B35792.1.

Navarro-Ramirez, J.P., Bodin, S., Heimhofer, U. and Immenhauser, A., 2015, Record of Albian to early Cenomanian environmental perturbation in the eastern sub-equatorial Pacific. Palaeogeography, Palaeoclimatology, Palaeoecology, 423, p. 122–137, https://doi.org/10.1016/j.palaeo.2015.01.025.

Naafs, B.D.A. and Pancost, R.D., 2016, Sea-surface temperature evolution across Aptian Oceanic Anoxic Event 1a. Geology, 44, p. 959–962, https://doi.org/10.1130/G38575.1.

Naafs, B.D.A., Castro, J.M., De Gea, G.A., Quijano, M.L., Schmidt, D.N. and Pancost, R.D., 2016, Gradual and sustained carbon dioxide release during Aptian Oceanic Anoxic Event 1a. Nature Geoscience, 9, p. 135–139, https://doi.org/10.1038/ngeo2627.

Neal, C.R., Mahoney, J.J., Kroenke, L.W., Duncan, R.A. and Petterson, M.G., 1997, The Ontong–Java Plateau. *In* Mahoney, J.J. and Coffin, M.F., (Eds.), Large igneous provinces: continental, oceanic and planetary flood volcanism, American Geophysical Union, Washington, DC, p. 183–216, https://doi.org/10.1029/GM100p0183.

Nederbragt, A.J. and Fiorentino, A., 1999, Stratigraphy and palaeoceanography of the Cenomanian-Turonian boundary event in Oued Mellegue, north-western Tunisia. Cretaceous Research, 20, p. 47–62, https://doi.org/10.1006/cres.1998.0136.

Nerlich, R., Clark, S.R. and Bunge, H.P., 2014, Reconstructing the link between the Galapagos hotspot and the Caribbean Plateau. GeoResJ, 1, p. 1–7, https://doi.org/10.1016/j.grj.2014.02.001.

Nozaki, T., Suzuki, K., Ravizza, G., Kimura, J. I. and Chang, Q., 2012, A method for rapid determination of Re and Os isotope compositions using ID-MC-ICP-MS combined with the sparging method. Geostandards and Geoanalytical Research, 36, p. 131–148, https://doi.org/10.1111/j.1751-908X.2011.00125.x.

O'Connor, L.K., Jenkyns, H.C., Robinson, S.A., Remmelzwaal, S.R., Batenburg, S.J., Parkinson, I.J. and Gale, A.S., 2020, A re-evaluation of the Plenus Cold Event, and the links between CO_2, temperature, and seawater chemistry during OAE 2. Paleoceanography and Paleoclimatology, 35, https://doi.org/10.1029/2019PA003631.

O'Connor, L.K., Crampton-Flood, E.D., Jerrett, R.M., Price, G.D., Naafs, B.D.A., Pancost, R.D., McCormack, P., Lempotesis-Davies, A., van Dongen, B.E. and Lengger, S.K., 2023, Steady decline in mean annual air temperatures in the first 30 ky after the Cretaceous-Paleogene boundary. Geology, 51, p. 486–490, https://doi.org/10.1130/G50588.1.

O'Hora, H.E., Petersen, S.V., Vellekoop, J., Jones, M.M. and Scholz, S.R., 2022, Clumped-isotope-derived climate trends leading up to the end-Cretaceous mass extinction in northwestern Europe. Climate of the Past, 18, p. 1963–1982, https://doi.org/10.5194/cp-18-1963-2022.

Olsson, R.K. and Liu, C., 1993, Controversies on the placement of Cretaceous-Paleogene boundary and the K/P mass extinction of planktonic foraminifera. Palaios, p. 127–139, https://doi.org/10.2307/3515167.

Ostrander, C.M., Owens, J.D. and Nielsen, S.G., 2017, Constraining the rate of oceanic deoxygenation leading up to a Cretaceous Oceanic Anoxic Event (OAE-2: ~94 Ma). Science advances, 3, https://doi.org/10.1126/sciadv.1701020.

Palmer, M.R., Edmund, J.M., 1989, The strontium isotope budget of the modern ocean. Earth and Planetary Science Letters 92, 11–26, https://doi.org/10.1016/0012-821X(89)90017-4.

Pancost, R.D., Crawford, N., Magness, S., Turner, A., Jenkyns, H.C. and Maxwell, J.R., 2004, Further evidence for the development of photic-zone euxinic conditions during Mesozoic oceanic anoxic events. Journal of the Geological Society, 161, p. 353–364, https://doi.org/10.1144/0016764903-059.

Pande, K., Sheth, H.C. and Bhutani, R., 2001, ^{40}Ar–^{39}Ar age of the St. Mary's Islands volcanics, southern India: record of India–Madagascar break-up on the Indian subcontinent. Earth and Planetary Science Letters, 193, p. 39–46, https://doi.org/10.1016/S0012-821X(01)00495-2.

Papadomanolaki, N.M., van Helmond, N.A., Pälike, H., Sluijs, A. and Slomp, C.P., 2022, Quantifying volcanism and organic carbon burial across Oceanic Anoxic Event 2. Geology, 50, p. 511–515, https://doi.org/10.1130/G49649.1.

Paquay, F.S. and Ravizza, G., 2012, Heterogeneous seawater ^{187}Os/^{188}Os during the late Pleistocene glaciations. Earth and Planetary Science Letters, 349, p. 126–138, https://doi.org/10.1016/j.epsl.2012.06.051.

Parisio, L., Jourdan, F., Marzoli, A., Melluso, L., Sethna, S.F. and Bellieni, G., 2016, ^{40}Ar/^{39}Ar ages of alkaline and tholeiitic rocks from the northern Deccan Traps: implications for magmatic processes and the K–Pg boundary. Journal of the Geological Society, 173, p. 679–688, https://doi.org/10.1144/jgs2015-133.

Paul, C.R.C., Lamolda, M.A., Mitchell, S.F., Vaziri, M.R., Gorostidi, A. and Marshall, J.D., 1999, The Cenomanian-Turonian boundary at Eastbourne (Sussex, UK): A proposed European reference section. Palaeogeography, Palaeoclimatology, Palaeoecology, 150, p. 83–121, https://doi.org/10.1016/S0031-0182(99)00009-7.

Pauly, S., Mutterlose, J. and Alsen, P., 2012, Early Cretaceous palaeoceanography of the Greenland–Norwegian Seaway evidenced by calcareous nannofossils. Marine Micropaleontology, 90, p. 72–85, https://doi.org/10.1016/j.marmicro.2012.04.004.

Pauly, S., Mutterlose, J. and Wray, D.S., 2013, Palaeoceanography of Lower Cretaceous (Barremian–Lower Aptian) black shales from northwest Germany evidenced by calcareous nannofossils and geochemistry. Cretaceous Research, 42, p. 28–43, https://doi.org/10.1016/j.cretres.2013.01.001.

Peate, D.W.,1997, The Paraná-Etendeka Province. In: Mahoney, J.J. and Coffin, M.F. (Eds.): Large Igneous Provinces: Continental, Oceanic, and Planetary Volcanism. AGU Geophysical Monograph, 100, p. 217–245.

Percival, L.M.E., Jenkyns, H.C., Mather, T.A., Dickson, A.J., Batenburg, S.J., Ruhl, M., Hesselbo, S.P., Barclay, R., Jarvis, I., Robinson, S.A., Woelders, L., 2018, Does Large Igneous Province volcanism always perturb the mercury cycle? Comparing the records of Oceanic Anoxic Event 2 and the end-Cretaceous to other Mesozoic events. American Journal of Science, 318, p. 799–860, https://doi.org/10.2475/08.2018.01.

Percival, L.M.E., van Helmond, N.A.G.M., Selby, D., Goderis, S. and Claeys, P., 2020, Complex interactions between large igneous province emplacement and global temperature changes during the Cenomanian–Turonian oceanic anoxic event (OAE 2). Paleoceanography and Paleoclimatology, 35, https://doi.org/10.1029/2020PA004016.

Percival, L.M.E., Bergquist, B.A., Mather, T.A. and Sanei, H., 2021a Sedimentary mercury enrichments as a tracer of Large Igneous Province volcanism. In Ernst, R.E., Dickson, A.J., Bekker, A. (Eds.): Large Igneous Provinces: A Driver of Global Environmental and Biotic Changes. AGU Geophysical Monograph 255, p. 247–262, https://doi.org/10.1002/9781119507444.ch11.

Percival, L.M.E., Tedeschi, L.R., Creaser, R.A., Bottini, C., Erba, E., Giraud, F., Svensen, H., Savian, J., Trindade, R., Coccioni, R. and Frontalini, F., 2021b, Determining the style and provenance of magmatic activity during the Early Aptian Oceanic Anoxic Event (OAE 1a). Global and Planetary Change, 200, 103461, https://doi.org/10.1016/j.gloplacha.2021.103461.

Percival, L.M.E., Ownsworth, E.M., Selby, D., Robinson, S.A., Goderis, S. and Claeys, P., 2023, Valanginian climate cooling and environmental change driven by Paraná-Etendeka basalt erosion. Geology, 51, p. 753–757, https://doi.org/10.1130/G51202.1.

Petersen, S.V., Dutton, A. and Lohmann, K.C., 2016, End-Cretaceous extinction in Antarctica linked to both Deccan volcanism and meteorite impact via climate change. Nature communications, 7, https://doi.org/10.1038/ncomms12079.

Peucker-Ehrenbrink, B. and Jahn, B.M., 2001, Rhenium-osmium isotope systematics and platinum group element concentrations: Loess and the upper continental crust. Geochemistry, Geophysics, Geosystems, 2, https://doi.org/10.1029/2001GC000172.

Peucker-Ehrenbrink, B. and Ravizza, G., 2000, The marine osmium isotope record. Terra Nova, 12, p. 205–219, https://doi.org/10.1046/j.1365-3121.2000.00295.x.

Phelps, R.M., Kerans, C., Da-Gama, R.O., Jeremiah, J., Hull, D. and Loucks, R.G., 2015, Response and recovery of the Comanche carbonate platform surrounding multiple Cretaceous oceanic anoxic events, northern Gulf of Mexico. Cretaceous Research, 54, p. 117–144, https://doi.org/10.1016/j.cretres.2014.09.002.

Pinto, V.M., Hartmann, L.A., Santos, J.O.S., McNaughton, N.J. and Wildner, W., 2011, Zircon U–Pb geochronology from the Paraná bimodal volcanic province support a brief eruptive cycle at~ 135Ma. Chemical Geology, 281, p. 93–102, https://doi.org/10.1016/j.chemgeo.2010.11.031.

Pogge von Strandmann, P.A.E., Jenkyns, H.C. and Woodfine, R.G., 2013, Lithium isotope evidence for enhanced weathering during Ocean Anoxic Event 2. Nature Geoscience, 6, p. 668–672, https://doi.org/10.1038/ngeo1875.

Polteau, S., Hendriks, B.W.H., Planke, S., Ganerød, M., Corfu, F., Faleide, J.I., Midtkandal, I., Svensen, H. and Kyklebust, R., 2016, The Early Cretaceous Barents Sea Sill Complex: Distribution, $^{40}Ar/^{39}Ar$ geochronology, and implications for carbon gas formation. Palaeogeography, Palaeoclimatology, Palaeoecology, 441, p. 83–95, https://doi.org/10.1016/j.palaeo.2015.07.007.

Pospichal, J.J., 1996, Calcareous nannoplankton mass extinction at the Cretaceous/Tertiary boundary: an update. In Ryder, G., Fastovsky, D.E. and Gartner, S. (Eds.): The Cretaceous-Tertiary event and other catastrophes in Earth history. Geological Society of America Special Papers, 307, p. 335–360, https://doi.org/10.1130/0-8137-2307-8.335.

Premoli Silva, L., Ripepe, M. and Tornaghi, M.E., 1989, Planktonic foraminiferal distribution record productivity cycles: evidence from the Aptian-Albian Piobbico core (central Italy). *Terra nova*, *1*, p. 443-448, https://doi.org/10.1111/j.1365-3121.1989.tb00407.x.

Premoli Silva, I., Erba, E., Salvini, G., Locatelli, C. and Verga, D., 1999, Biotic changes in Cretaceous oceanic anoxic events of the Tethys. The Journal of Foraminiferal Research, 29, p. 352–370.

Price, G.D. and Mutterlose, J., 2004, Isotopic signals from late Jurassic–early Cretaceous (Volgian–Valanginian) sub-Arctic belemnites, Yatria River, Western Siberia. Journal of the Geological Society, 161, p. 959–968, https://doi.org/10.1144/0016-764903-169.

Price, G.D., Janssen, N.M., Martinez, M., Company, M., Vandevelde, J.H. and Grimes, S.T., 2018, A High-Resolution Belemnite Geochemical Analysis of Early Cretaceous (Valanginian-Hauterivian) Environmental and Climatic Perturbations. Geochemistry, Geophysics, Geosystems, 19, p. 3832–3843, https://doi.org/10.1029/2018GC007676.

Punekar, J., Keller, G., Khozyem, H.M., Adatte, T., Font, E. and Spangenberg, J., 2016, A multi-proxy approach to decode the end-Cretaceous mass extinction. Palaeogeography, Palaeoclimatology, Palaeoecology, 441, p. 116–136, https://doi.org/10.1016/j.palaeo.2015.08.025.

Pyle, D.M., and Mather, T.A., 2003, The importance of volcanic emissions for the global atmospheric mercury cycle. Atmospheric Environment, 37, p. 5115–5124, https://doi.org/10.1016/j.atmosenv.2003.07.011.

Quémerais, B., Cossa, D., Rondeau, B., Pham, T.T. and Fortin, B., 1998, Mercury distribution in relation to iron and manganese in the waters of the St. Lawrence river. Science of The Total Environment, 213, p. 193–201, https://doi.org/10.1016/S0048-9697(98)00092-8.

Raup, D.M. and Sepkoski, J.J., 1982, Mass Extinction in the Marine Fossil Record. Science, 215, p. 1501–1503, https://doi.org/10.1126/science.215.4539.1501.

Ravizza, G. and Peucker-Ehrenbrink, B., 2003, Chemostratigraphic evidence of Deccan volcanism from the marine osmium isotope record. Science, 302, p. 1392–1395, https://doi.org/10.1126/science.1089209.

Ravizza, G. and VonderHaar, D., 2012, A geochemical clock in earliest Paleogene pelagic carbonates based on the impact-induced Os isotope excursion at the Cretaceous-Paleogene boundary. Paleoceanography, 27, https://doi.org/10.1029/2012PA002301.

Reddin, C.J., Kocsis, Á.T., Aberhan, M. and Kiessling, W., 2021, Victims of ancient hyperthermal events herald the fates of marine clades and traits under global warming. Global Change Biology, 27, p. 868–878, https://doi.org/10.1111/gcb.15434.

Renne, P.R., Ernesto, M., Pacca, I.G., Coe, R.S., Glen, J.M., Prévot, M. and Perrin, M., 1992, The age of Paraná flood volcanism, rifting of Gondwanaland, and the Jurassic-Cretaceous boundary. Science, 258, p. 975–979, https://doi.org/10.1126/science.258.5084.975.

Renne, P.R., Glen, J.M., Milner, S.C. and Duncan, A.R., 1996, Age of Etendeka flood volcanism and associated intrusions in southwestern Africa. Geology, 24, p. 659–662, https://doi.org/10.1029/2000PA000541.

Renne, P.R., Sprain, C.J., Richards, M.A., Self, S., Vanderkluysen, L. and Pande, K., 2015, State shift in Deccan volcanism at the Cretaceous-Paleogene boundary, possibly induced by impact. Science, 350, p. 76–78, https://doi.org/10.1126/science.aac7549.

Richards, M.A., Alvarez, W., Self, S., Karlstrom, L., Renne, P.R., Manga, M., Sprain, C.J., Smit, J., Vanderkluysen, L. and Gibson, S.A., 2015, Triggering of the largest Deccan eruptions by the Chicxulub impact. Geological Society of America Bulletin, 127, p. 1507–1520, https://doi.org/10.1130/B31167.1.

Ridgwell, A., 2005, A Mid Mesozoic Revolution in the regulation of ocean chemistry. *Marine Geology*, *217*, p. 339–357, https://doi.org/10.1016/j.margeo.2004.10.036.

Robinson, N., Ravizza, G., Coccioni, R., Peucker-Ehrenbrink, B. and Norris, R., 2009, A high-resolution marine $^{187}Os/^{188}Os$ record for the late Maastrichtian: Distinguishing the chemical fingerprints of Deccan volcanism and the KP impact event. Earth and Planetary Science Letters, 281, p. 159–168, https://doi.org/10.1016/j.epsl.2009.02.019.

Robinson, S.A., Clarke, L.J., Nederbragt, A. and Wood, I.G., 2008, Mid-Cretaceous oceanic anoxic events in the Pacific Ocean revealed by carbon-isotope stratigraphy of the Calera Limestone, California, USA. Geological Society of America Bulletin, 120, p. 1416–1426, https://doi.org/10.1130/B26350.1.

Robinson, S.A., Heimhofer, U., Hesselbo, S.P. and Petrizzo, M.R., 2017, Mesozoic climates and oceans – a tribute to Hugh Jenkyns and Helmut Weissert. Sedimentology, 64, p. 1–15, https://doi.org/10.1111/sed.12349.

Robinson, S.A., Dickson, A.J., Pain, A., Jenkyns, H.C., O'Brien, C.L., Farnsworth, A. and Lunt, D.J., 2019, Southern Hemisphere sea-surface temperatures during the Cenomanian–Turonian: Implications for the termination of Oceanic Anoxic Event 2. Geology, 47, p. 131–134, https://doi.org/10.1130/G45842.1.

Rocha, B.C., Davies, J.H., Janasi, V.A., Schaltegger, U., Nardy, A.J., Greber, N.D., Lucchetti, A.C.F. and Polo, L.A., 2020, Rapid eruption of silicic magmas from the Paraná magmatic province (Brazil) did not trigger the Valanginian event. Geology, 48, p. 1174–1178, https://doi.org/10.1130/G47766.1.

Ruvalcaba Baroni, I., Van Helmond, N.A.G.M., Tsandev, I., Middelburg, J.J. and Slomp, C.P., 2015, The nitrogen isotope composition of sediments from the proto-North Atlantic during Oceanic Anoxic Event 2. Paleoceanography, 30, p. 923–937, https://doi.org/10.1002/2014PA002744.

Ryan W.B.F. et al., 1979, Site 398. Initial Reports of the Deep Sea Drilling Project, 47, p. 25–233, https://doi.org/10.2973/dsdp.proc.47-2.102.1979.

Sabatino, N., Ferraro, S., Coccioni, R., Bonsignore, M., Del Core, M., Tancredi, V. and Sprovieri, M., 2018, Mercury anomalies in upper Aptian-lower Albian sediments from the Tethys realm. Palaeogeography, Palaeoclimatology, Palaeoecology, 495, p. 163–170, https://doi.org/10.1016/j.palaeo.2018.01.008.

Sageman, B.B., Meyers, S.R. and Arthur, M.A., 2006, Orbital time scale and new C-isotope record for Cenomanian-Turonian boundary stratotype. Geology, 34, p. 125–128, https://doi.org/10.1130/G22074.1.

Saunders, A.D., 2016, Two LIPs and two Earth-system crises: the impact of the North Atlantic Igneous Province and the Siberian Traps on the Earth-surface carbon cycle. Geological Magazine, 153, p. 201–222, https://doi.org/10.1017/S0016756815000175.

Saunders, A.D., Tarney, J., Kerr, A.C. and Kent, R.W., 1996, The formation and fate of large oceanic igneous provinces. Lithos, 37, p. 81–95, https://doi.org/10.1016/0024-4937(95)00030-5.

Scaife, J.D., Ruhl, M., Dickson, A.J., Mather, T.A., Jenkyns, H.C., Percival, L.M.E., Hesselbo, S.P., Cartwright, J., Eldrett, J.S., Bergman, S.C. and Minisini, D., 2017, Sedimentary Mercury Enrichments as a Marker for Submarine Large Igneous Province Volcanism? Evidence from the Mid-Cenomanian Event and Oceanic Anoxic Event 2 (Late Cretaceous). Geochemistry, Geophysics, Geosystems, 18, https://doi.org/10.1002/2017GC007153.

Schlanger, S.O. and Jenkyns, H.C., 1976, Cretaceous oceanic anoxic events: causes and consequences. Geologie en Mijnbouw, 55, p. 179–184.

Schlanger, S.O., Jenkyns, H.C. and Premoli-Silva, I., 1981, Volcanism and vertical tectonics in the Pacific Basin related to global Cretaceous transgressions. Earth and Planetary Science Letters, 52, p. 435-449, https://doi.org/10.1016/0012-821X(81)90196-5.

Schmidt, A., Skeffington, R.A., Thordarson, T., Self, S., Forster, P.M., Rap, A., Ridgwell, A., Fowler, D., Wilson, M., Mann, G.W. and Wignall, P.B., 2016, Selective environmental stress from sulphur emitted by continental flood basalt eruptions. Nature Geoscience, 9, p. 77–82, https://doi.org/10.1038/ngeo2588.

Schoene, B., Samperton, K.M., Eddy, M.P., Keller, G., Adatte, T., Bowring, S.A., Khadri, S.F. and Gertsch, B., 2015, U-Pb geochronology of the Deccan Traps and relation to the end-Cretaceous mass extinction. Science, 347, p. 182–184, https://doi.org/10.1126/science.aaa0118.

Schoene, B., Eddy, M.P., Samperton, K.M., Keller, C.B., Keller, G., Adatte, T. and Khadri, S.F.R., 2019. U-Pb constraints on pulsed eruption of the Deccan Traps across the end-Cretaceous mass extinction. Science, 363, p. 862–866, https://doi.org/10.1126/science.aau2422.

Scholle, P.A. and Arthur, M.A., 1980, Carbon isotope fluctuations in Cretaceous pelagic limestones: potential stratigraphic and petroleum exploration tool. AAPG Bulletin, 64, p. 67–87, https://doi.org/10.1306/2F91892D-16CE-11D7-8645000102C1865D.

Schröder-Adams, C.J., Herrle, J.O., Selby, D., Quesnel, A. and Froude, G., 2019, Influence of the High Arctic Igneous Province on the Cenomanian/Turonian boundary interval, Sverdrup Basin, High Canadian Arctic. Earth and Planetary Science Letters, 511, p. 76–88, https://doi.org/10.1016/j.epsl.2019.01.023.

Schroeder, W.H. and Munthe J., 1998, Atmospheric mercury - An overview. Atmospheric Environment, 32, p. 809–822, https://doi.org/10.1016/S1352-2310(97)00293-8.

Schulte, P. et al., 2010, The Chicxulub asteroid impact and mass extinction at the Cretaceous-Paleogene boundary. Science, 327, p. 1214–1218, https://doi.org/10.1126/science.1177265.

Selby, D., Mutterlose, J. and Condon, D.J., 2009, U–Pb and Re–Os geochronology of the Aptian/Albian and Cenomanian/Turonian stage boundaries: implications for timescale calibration, osmium isotope seawater composition and Re–Os systematics in organic-rich sediments. Chemical Geology, 265, p. 394–409, https://doi.org/10.1016/j.chemgeo.2009.05.005.

Self, S., Widdowson, M., Thordarson, T. and Jay, A.E., 2006, Volatile fluxes during flood basalt eruptions and potential effects on the global environment: A Deccan perspective. Earth and Planetary Science Letters, 248, p. 518–532, https://doi.org/10.1016/j.epsl.2006.05.041.

Self, S., Schmidt, A. and **Mather**, **T.A., 2014,** Emplacement characteristics, time scales, and volcanic gas release rates of continental flood basalt eruptions on Earth. Geological Society of America Special Papers, 505, https://doi.org/10.1130/2014.2505(16).

Selin, N.E., 2009, Global Biogeochemical Cycling of Mercury: A Review. Annual Review of Environment and Resources, 34, p. 43–63, https://doi.org/10.1146/annurev.environ.051308.084314.

Senel, C.B., Kaskes, P., Temel, O., Vellekoop, J., Goderis, S., DePalma, R., Prins, M.A., Claeys, P. and Karatekin, Ö., 2023, Chicxulub impact winter sustained by fine silicate dust. Nature Geoscience, 16, p. 1033–1040, https://doi.org/10.1038/s41561-023-01290-4.

Senger, K. and Galland, O., 2022, Stratigraphic and Spatial extent of HALIP Magmatism in central Spitsbergen. Geochemistry, Geophysics, Geosystems, 23, https://doi.org/10.1029/2021GC010300.

Senger, K., Tveranger, J., Ogata, K., Braathen, A. and Planke, S., 2014, Late Mesozoic magmatism in Svalbard: A review. Earth-Science Reviews, 139, p. 123–144, https://doi.org/10.1016/j.earscirev.2014.09.002

Seton, M., Gaina, C., Müller, R.D. and Heine, C., 2009, Mid-Cretaceous seafloor spreading pulse: Fact or fiction?. Geology, 37, p. 687–690, https://doi.org/10.1130/G25624A.1.

Sheldon, E., Ineson, J. and Bown, P., 2010, Late Maastrichtian warming in the Boreal Realm: Calcareous nannofossil evidence from Denmark. Palaeogeography, Palaeoclimatology, Palaeoecology, 295, p. 55–75, https://doi.org/10.1016/j.palaeo.2010.05.016.

Shen, J., Algeo, T.J., Chen, J., Planavsky, N.J., Feng, Q., Yu, J. and Liu, J., 2019a, Mercury in marine Ordovician/Silurian boundary sections of South China is sulfide-hosted and non-volcanic in origin. Earth and Planetary Science Letters, 511, p. 130–140, https://doi.org/10.1016/j.epsl.2019.01.028.

Shen, J., Algeo, T.J., Planavsky, N.J., Yu, J., Feng, Q., Song, H., Song, H., Rowe, H., Zhou, L. and Chen, J., 2019b, Mercury enrichments provide evidence of Early Triassic volcanism following the end-Permian mass extinction. Earth-Science Reviews, 195, p. 191–212, https://doi.org/10.1016/j.earscirev.2019.05.010.

Shen, J., Feng, Q., Algeo, T.J., Liu, J., Zhou, C., Wei, W., Liu, J., Them II, T.R., Gill, B.C. and Chen, J., 2020, Sedimentary host phases of mercury (Hg) and implications for use of Hg as a volcanic proxy. Earth and Planetary Science Letters, 543, 116333, https://doi.org/10.1016/j.epsl.2020.116333.

Shmeit, M., Giraud, F., Jaillard, E., Reboulet, S., Masrour, M., Spangenberg, J.E. and El-Samrani, A., 2022, The Valanginian Weissert Event on the south Tethyan margin: a dynamic paleoceanographic evolution based on the study of calcareous nannofossils. Marine Micropaleontology, 175, 102134, https://doi.org/10.1016/j.marmicro.2022.102134.

Siebert, C., Scholz, F. and Kuhnt, W., 2021, A new view on the evolution of seawater molybdenum inventories before and during the Cretaceous Oceanic Anoxic Event 2. Chemical Geology, 582, https://doi.org/10.1016/j.chemgeo.2021.120399.

Sigal, J., 1979, Chronostratigraphy and Ecostratigraphy of Cretaceous Formations Recovered on DSDP Leg 47B, Site 398. Initial Reports of the Deep Sea Drilling Project, 47, p. 287–326, https://doi.org/10.2973/dsdp.proc.47-2.105.1979.

Sinninghe-Damsté, J.S. and Köster, J., 1998, A euxinic southern North Atlantic Ocean during the Cenomanian/Turonian oceanic anoxic event. Earth and Planetary Science Letters, 158, p. 165-173, https://doi.org/10.1016/S0012-821X(98)00052-1.

Sinninghe-Damsté, J.S., Kuypers, M.M., Pancost, R.D. and Schouten, S., 2008, The carbon isotopic response of algae,(cyano) bacteria, archaea and higher plants to the late Cenomanian perturbation of the global carbon cycle: Insights from biomarkers in black shales from the Cape Verde Basin (DSDP Site 367). Organic Geochemistry, 39, p. 1703–1718, https://doi.org/10.1016/j.orggeochem.2008.01.012.

Sinton, C.W. and Duncan, R.A., 1997, Potential links between ocean plateau volcanism and global ocean anoxia at the Cenomanian-Turonian boundary. Economic Geology, 92, p. 836–842, https://doi.org/10.2113/gsecongeo.92.7-8.836.

Sinton, C.W., Duncan, R., Storey, M., Lewis, J. and Estrada, J.J., 1998, An oceanic flood basalt province within the Caribbean plate. Earth and Planetary Science Letters, 155, p. 221–235, https://doi.org/10.1016/S0012-821X(97)00214-8.

Smit, J., Silver, L.T. and Schultz, P.H., 1982, Extinction and evolution of planktonic foraminifera after a major impact at the Cretaceous/Tertiary boundary. In Silver, L.T. and Schultz, P.H. (Eds.): Geological Implications of Impacts of Large Asteroids and Comets on the Earth, Geological Society of America Special Papers, 190, p. 329–352, https://doi.org/10.1130/SPE190-p329.

Snow, L.J., Duncan, R.A., Bralower, T.J., 2005, Trace element abundances in the Rock Canyon Anticline, Pueblo, Colorado, marine sedimentary section and their relationship to Caribbean plateau construction and oxygen anoxic event 2. Paleoceanography 20, PA3005, https://doi.org/10.1029/2004PA001093.

Sprain, C.J., Renne, P.R., Vanderkluysen, L., Pande, K., Self, S. and Mittal, T., 2019, The eruptive tempo of Deccan volcanism in relation to the Cretaceous-Paleogene boundary. Science, 363, p. 866–870, https://doi.org/10.1126/science.aav1446.

Steuber, T., Löser, H., Mutterlose, J. and Parente, M., 2023, Biogeodynamics of Cretaceous marine carbonate production. Earth-Science Reviews, 104341, https://doi.org/10.1016/j.earscirev.2023.104341.

Storey, M., Mahoney, J.J., Saunders, A.D., Duncan, R.A., Kelley, S.P. and Coffin, M.F., 1995, Timing of hot spot related volcanism and the breakup of Madagascar and India, Science, 267, p. 852–855. https://doi.org/10.1126/science.267.5199.852.

Stüben, D., Kramar, U., Berner, Z.A., Meudt, M., Keller, G., Abramovich, S., Adatte, T., Hambach, U. and Stinnesbeck, W., 2003, Late Maastrichtian paleoclimatic and paleoceanographic changes inferred from

Sr/Ca ratio and stable isotopes. Palaeogeography, Palaeoclimatology, Palaeoecology, 199, p. 107–127, https://doi.org/10.1016/S0031-0182(03)00499-1.

Suchéras-Marx, B., Mattioli, E., Allemand, P., Giraud, F., Pittet, B., Plancq, J. and Escarguel, G., 2019, The colonization of the oceans by calcifying pelagic algae. Biogeosciences, 16, p. 2501–2510, https://doi.org/10.5194/bg-16-2501-2019.

Sullivan, D.L., Brandon, A.D., Eldrett, J., Bergman, S.C., Minisini, D., Wright, S., 2020, High Resolution Osmium Data Record Three Distinct Pulses of Magmatic Activity During Cretaceous Ocean Anoxic Event 2 (OAE 2). Geochimica et Cosmochimica Acta, 285, p. 257–273, https://doi.org/10.1016/j.gca.2020.04.002.

Svensen, H., Planke, S., Malthe-Sørenssen, A., Jamtveit, B., Myklebust, R., Eidem, T.R. and Rey, S.S., 2004, Release of methane from a volcanic basin as a mechanism for initial Eocene global warming. Nature, 429, p. 542–545, https://doi.org/10.1038/nature02566.

Svensen, H., Planke, S., Polozov, A.G., Schmidbauer, N., Corfu, F., Podladchikov, Y.Y. and Jamtveit, B., 2009, Siberian gas venting and the end-Permian environmental crisis. Earth and Planetary Science Letters, 277, p. 490–500, https://doi.org/10.1016/j.epsl.2008.11.015.

Svensen, H.H., Jerram, D.A., Polozov, A.G., Planke, S., Neal, C.R., Augland, L.E. and Emeleus, H.C., 2019, Thinking about LIPs: A brief history of ideas in Large igneous province research. Tectonophysics, 760, p. 229–251, https://doi.org/10.1016/j.tecto.2018.12.008.

Sweere, T.C., Dickson, A.J., Jenkyns, H.C., Porcelli, D., Elrick, M., van den Boorn, S.H. and Henderson, G.M., 2018, Isotopic evidence for changes in the zinc cycle during Oceanic Anoxic Event 2 (Late Cretaceous). Geology, 46, p. 463–466, https://doi.org/10.1130/G40226.1.

Tarduno, J., 1998, The High Arctic Large Igneous Province. Paper presented at the Third International Conference on Arctic Margins, p. 12–16, Federal Institute for Geosciences and Natural Resources.

Taylor, B., 2006, The single largest oceanic plateau: Ontong Java–Manihiki–Hikurangi. Earth and Planetary Science Letters, 241, p. 372–380, https://doi.org/10.1016/j.epsl.2005.11.049.

Tedeschi, L.R., Jenkyns, H.C., Robinson, S.A., Lana, C.C., Menezes Santos, M.R.F. and Tognoli, F.M., 2020, Aptian carbon-isotope record from the Sergipe-Alagoas Basin: New insights into oceanic anoxic event 1a and the timing of seawater entry into the South Atlantic. Newsletters on Stratigraphy, 53, p. 333–364, https://doi.org/10.1127/nos/2019/0529.

Tegner, C., Storey, M., Holm, P.M., Thorarinsson, S.B., Zhao, X., Lo, C.H. and Knudsen, M.F., 2011, Magmatism and Eurekan deformation in the High Arctic Large Igneous Province: ^{40}Ar-^{39}Ar age of Kap Washington Group volcanics. North Greenland. Earth and Planetary Science Letters, 303, p. 203–214, https://doi.org/10.1016/j.epsl.2010.12.047.

Tejada, M.L.G., Mahoney, J.J., Duncan, R.A. and Hawkins, M.P., 1996, Age and geochemistry of basement and alkalic rocks of Malaita and Santa Isabel, Solomon Islands, southern margin of Ontong Java Plateau. Journal of Petrology, 37, p. 361–394, https://doi.org/10.1093/petrology/37.2.361.

Tejada, M.L.G., Mahoney, J.J., Neal, C.R., Duncan, R.A. and Petterson, M.G., 2002, Basement geochemistry and geochronology of Central Malaita, Solomon Islands, with implications for the origin and evolution of the Ontong Java Plateau. Journal of Petrology, 43, p. 449–484, https://doi.org/10.1093/petrology/43.3.449.

Tejada, M. L. G., Suzuki, K., Kuroda, J., Coccioni, R., Mahoney, J. J., Ohkouchi, N., Sakamoto, T. and Tatsumi, Y., 2009, Ontong Java Plateau eruption as a trigger for the early Aptian oceanic anoxic event. Geology, 37, p. 855–858, https://doi.org/10.1130/G25763A.1.

Them, T.R., Jagoe, C.H., Caruthers, A.H., Gill, B.C., Grasby, S.E., Gröcke, D.R., Yin, R. and Owens, J.D., 2019, Terrestrial sources as the primary delivery mechanism of mercury to the oceans across the Toarcian Oceanic Anoxic Event (Early Jurassic). Earth and Planetary Science Letters, 507, p. 62–72, https://doi.org/10.1016/j.epsl.2018.11.029.

Thibault, N. and Gardin, S., 2007, The late Maastrichtian nannofossil record of climate change in the South Atlantic DSDP Hole 525A. Marine Micropaleontology, 65, p. 163–184, https://doi.org/10.1016/j.marmicro.2007.07.004.

Thiede, D.S. and Vasconcelos, P.M., 2010, Paraná flood basalts: rapid extrusion hypothesis confirmed by new ^{40}Ar/^{39}Ar results. Geology, 38, p. 747–750, https://doi.org/10.1130/G30919.1.

Thórarinsson, S.B., Söderlund, U., Døssing, A., Holm, P.M., Ernst, R.E. and Tegner, C., 2015, Rift magmatism on the Eurasia basin margin: U–Pb baddeleyite ages of alkaline dyke swarms in North Greenland. Journal of the Geological Society, 172, p. 721–726, https://doi.org/10.1144/jgs2015-049.

Thordarson, T., 2004, Accretionary-lapilli-bearing pyroclastic rocks at ODP Leg 192 Site 1184: a record of subaerial phreatomagmatic eruptions on the Ontong Java Plateau. *In* Fitton, J.G., Mahoney, J.J., Wallace, P.J. and Saunders, A.D. (Eds.), Origin and Evolution of the Ontong Java Plateau, Geological Society of London, Special Publications, 229, p. 275–306, https://doi.org/10.1144/GSL.SP.2004.229.01.16.

Tierney, J.E. and Tingley, M.P., 2014, A Bayesian, spatially-varying calibration model for the TEX_{86} proxy. Geochimica et Cosmochimica Acta, 127, p. 83–106, https://doi.org/10.1016/j.gca.2013.11.026.

Timm, C., Hoernle, K., Werner, R., Hauff, F., van den Bogaard, P., Michael, P., Coffin, M.F. and Koppers, A., 2011, Age and geochemistry of the oceanic Manihiki Plateau, SW Pacific: New evidence for a plume origin. Earth and Planetary Science Letters, 304, p. 135–146, https://doi.org/10.1016/j.epsl.2011.01.025.

Tobin, T.S., Bitz, C.M. and Archer, D., 2017, Modeling climatic effects of carbon dioxide emissions from Deccan Traps volcanic eruptions around the Cretaceous–Paleogene boundary. Palaeogeography, Palaeoclimatology, Palaeoecology, 478, p. 139–148, https://doi.org/10.1016/j.palaeo.2016.05.028.

Torsvik, T.H., 2019, Earth history: A journey in time and space from base to top. Tectonophysics, 760, p. 297–313, https://doi.org/10.1016/j.tecto.2018.09.009.

Torsvik, T.H., Tucker, R.D., Ashwal, L.D., Eide, E.A., Rakotosolofo, N.A. and De Wit, M.J., 1998, Late Cretaceous magmatism in Madagascar: palaeomagnetic evidence for a stationary Marion hotspot. Earth and Planetary Science Letters, 164, p. 221–232, https://doi.org/10.1016/S0012-821X(98)00206-4.

Torsvik, T.H., Tucker, R.D., Ashwal, L.D., Carter, L.M., Jamtveit, B., Vidyadharan, K.T. and Venkataramana, P., 2000, Late Cretaceous India–Madagascar fit and timing of break-up related magmatism. Terra Nova, 12, p. 220–224, https://doi.org/10.1046/j.1365-3121.2000.00300.x.

Trabucho Alexandre, J., van Gilst, R.I., RODRÍGUEZ-LÓPEZ, J.P. and De Boer, P.L., 2011, The sedimentary expression of oceanic anoxic event 1b in the North Atlantic. Sedimentology, 58, p. 1217–1246, https://doi.org/10.1111/j.1365-3091.2010.01202.x.

Tsikos, H., Jenkyns, H.C., Walsworth-Bell, B., Petrizzo, M.R., Forster, A., Kolonic, S., Erba, E., Premoli-Silva, I.P., Baas, M., Wagner, T., Sinninghe Damsté, J.S., 2004a, Carbon-isotope stratigraphy recorded by the Cenomanian–Turonian Oceanic Anoxic Event: correlation and implications based on three key localities. Journal of the Geological Society of London, 161, p. 711–719, https://doi.org/10.1144/0016-764903-077.

Tsikos, H., Karakitsios, V., van Breugel, Y., Walsworth-Bell, B.E.N., Bombardiere, L.U.C.A., Petrizzo, M.R., Damsté, J.S.S., Schouten, S., Erba, E., Silva, I.P. and Farrimond, P.A.U.L., 2004b, Organic-carbon deposition in the Cretaceous of the Ionian Basin, NW Greece: the Paquier Event (OAE 1b) revisited. Geological Magazine, 141, p. 401–416, https://doi.org/10.1017/S0016756804009409.

Turgeon, S.C. and Creaser, R.A., 2008. Cretaceous oceanic anoxic event 2 triggered by a massive magmatic episode. Nature, 454, p. 323–326, https://doi.org/10.1038/nature07076.

van Bentum, E.C., Hetzel, A., Brumsack, H.J., Forster, A., Reichart, G.J. and Damste, J.S.S., 2009, Reconstruction of water column anoxia in the equatorial Atlantic during the Cenomanian–Turonian oceanic anoxic event using biomarker and trace metal proxies. Palaeogeography, Palaeoclimatology, Palaeoecology, 280, p. 489–498, https://doi.org/10.1016/j.palaeo.2009.07.003.

van Breugel, Y., Schouten, S., Tsikos, H., Erba, E., Price, G.D. and Sinninghe Damsté, J.S., 2007, Synchronous negative carbon isotope shifts in marine and terrestrial biomarkers at the onset of the early Aptian oceanic anoxic event 1a: Evidence for the release of ^{13}C-depleted carbon into the atmosphere. Paleoceanography, 22, https://doi.org/10.1029/2006PA001341.

van Helmond, N.A.G.M., Sluijs, A., Reichart, G.J., Sinninghe Damsté, J.S., Slomp, C.P. and Brinkhuis, H., 2014, A perturbed hydrological cycle during Oceanic Anoxic Event 2. Geology, 42, p. 123–126, https://doi.org/10.1130/G34929.1.

van Helmond, N.A.G.M., Sluijs, A., Sinninghe Damsté, J.S., Reichart, G.J., Voigt, S., Erbacher, J., Pross, J. and Brinkhuis, H., 2015, Freshwater discharge controlled deposition of Cenomanian–Turonian black shales on the NW European epicontinental shelf (Wunstorf, northern Germany). Climate of the Past, 11, p. 495–508, https://doi.org/10.5194/cp-11-495-2015.

van Helmond, N.A.G.M., Sluijs, A., Papadomanolaki, N.M., Plint, A.G., Gröcke, D.R., Pearce, M.A., Eldrett, J.S., Trabucho-Alexandre, J., Walaszczyk, I., van de Schootbrugge, B. and Brinkhuis, H., 2016, Equatorward phytoplankton migration during a cold spell within the Late Cretaceous super-greenhouse. Biogeosciences, 13, p. 2859–2872, https://doi.org/10.5194/bg-13-2859-2016.

Vaughan, A.P. and Storey, B.C., 2007, A new supercontinent self-destruct mechanism: evidence from the Late Triassic–Early Jurassic. Journal of the Geological Society, 164, p. 383–392, https://doi.org/10.1144/0016-76492005-109.

Vellekoop, J., Esmeray-Senlet, S., Miller, K.G., Browning, J.V., Sluijs, A., van de Schootbrugge, B., Damsté, J.S.S. and Brinkhuis, H., 2016, Evidence for Cretaceous-Paleogene boundary bolide "impact winter" conditions from New Jersey, USA. Geology, 44, p. 619–622, https://doi.org/10.1130/G37961.1.

Vellekoop, J., Woelders, L., Sluijs, A., Miller, K.G. and Speijer, R.P., 2019, Phytoplankton community disruption caused by latest Cretaceous global warming. Biogeosciences, 16, p. 4201–4210, https://doi.org/10.5194/bg-16-4201-2019.

Vickers, M.L., Price, G.D., Jerrett, R.M. and Watkinson, M., 2016, Stratigraphic and geochemical expression of Barremian–Aptian global climate change in Arctic Svalbard. Geosphere, 12, p. 1594–1605, https://doi.org/10.1130/GES01344.1.

Vickers, M.L., Jelby, M.E., Śliwińska, K.K., Percival, L.M.E., Wang, F., Sanei, H., Price, G.D., Ullmann, C.V., Grasby, S.E., Reinhardt, L. Mather, T.A., Frieling, J., Korte, C., Jerrett, R.M., Jones, M.T., Midtkandal, I. and Galloway, J.M., 2023, Volcanism and carbon cycle perturbations in the High Arctic during the Late Jurassic – Early Cretaceous. Palaeogeography, Palaeoclimatology, Palaeoecology, 613, 111412, https://doi.org/10.1016/j.palaeo.2023.111412.

Wagreich, M., 2012, "OAE 3"–regional Atlantic organic carbon burial during the Coniacian–Santonian. Climate of the Past, 8, p. 1447–1455, https://doi.org/10.5194/cp-8-1447-2012.

Walker, R.J., Echeverria, L.M., Shirey, S.B. and Horan, M.F., 1991, Re—Os isotopic constraints on the origin of volcanic rocks, Gorgona Island, Colombia: Os isotopic evidence for ancient heterogeneities in the mantle. Contributions to Mineralogy and Petrology, 107, p. 150–162, https://doi.org/10.1007/BF00310704.

Walker, R.J., Storey, M., Kerr, A.C., Tarney, J. and Arndt, N.T., 1999, Implications of ^{187}Os isotopic heterogeneities in a mantle plume: evidence from Gorgona Island and Curaçao. Geochimica et Cosmochimica Acta, 63, p. 713–728, https://doi.org/10.1016/S0016-7037(99)00041-1.

Wallace, P.J., Frey, F.A., Weis, D. and Coffin, M.F., 2002, Origin and evolution of the Kerguelen Plateau, Broken Ridge and Kerguelen archipelago. Journal of Petrology, 43, p. 1105–1108, https://doi.org/10.1093/petrology/43.7.1105.

Wang, S., Shao, L.Y., Yan, Z.M., Shi, M.J. and Zhang, Y.H., 2019, Characteristics of Early Cretaceous wildfires in peat-forming environment, NE China. Journal of Palaeogeography, 8, p. 1–13, https://doi.org/10.1186/s42501-019-0035-5.

Weissert, H., 1989, C-isotope stratigraphy, a monitor of paleoenvironmental change: a case study from the Early Cretaceous. Surveys in Geophysics, 10, p. 1–61, https://doi.org/10.1007/BF01901664.

Weissert, H. and Erba, E., 2004, Volcanism, CO_2 and palaeoclimate: a Late Jurassic–Early Cretaceous carbon and oxygen isotope record. Journal of the Geological Society, 161, p. 695–702, https://doi.org/10.1144/0016-764903-087.

Weissert, H., Lini, A., Föllmi, K.B. and Kuhn, O., 1998, Correlation of Early Cretaceous carbon isotope stratigraphy and platform drowning events: a possible link? Palaeogeography, Palaeoclimatology, Palaeoecology, 137, p. 189–203, https://doi.org/10.1016/S0031-0182(97)00109-0.

Westerhold, T., Röhl, U., Donner, B., McCarren, H.K. and Zachos, J.C., 2011, A complete high-resolution Paleocene benthic stable isotope record for the central Pacific (ODP Site 1209). Paleoceanography, 26, https://doi.org/10.1029/2010PA002092.

Westermann, S., Föllmi, K.B., Adatte, T., Matera, V., Schnyder, J., Fleitmann, D., Fiet, N., Ploch, I. and Duchamp-Alphonse, S., 2010, The Valanginian δ^{13}C excursion may not be an expression of a global oceanic anoxic event. Earth and Planetary Science Letters, 290, p. 118–131, https://doi.org/10.1016/j.epsl.2009.12.011.

Widdowson, M., Walsh, J.N. and Subbarao, K.V., 1997, The geochemistry of Indian bole horizons: palaeoenvironmental implications of Deccan intravolcanic palaeosurfaces. Geological Society, London, Special Publications, 120, p. 269–281, https://doi.org/10.1144/GSL.SP.1997.120.01.17.

Wignall, P.B., 2001, Large igneous provinces and mass extinctions. Earth-science reviews, 53, p. 1–33, https://doi.org/10.1016/S0012-8252(00)00037-4.

Witts, J.D., Whittle, R.J., Wignall, P.B., Crame, J.A., Francis, J.E., Newton, R.J. and Bowman, V.C., 2016, Macrofossil evidence for a rapid and severe Cretaceous–Paleogene mass extinction in Antarctica. Nature communications, 7, https://doi.org/10.1038/ncomms11738.

Woelders, L., Vellekoop, J., Kroon, D., Smit, J., Casadío, S., Pramparo, M.B., Dinarès-Turell, J., Peterse, F., Sluijs, A., Lenaerts, J.T. and Speijer, R.P., 2017. Latest Cretaceous climatic and environmental change in the South Atlantic region. Paleoceanography, 32, p. 466–483, https://doi.org/10.1002/2016PA003007.

Woelders, L., Vellekoop, J., Weltje, G.J., de Nooijer, L., Reichart, G.J., Peterse, F., Claeys, P. and Speijer, R.P., 2018, Robust multi-proxy data integration, using late Cretaceous paleotemperature records as a case study. Earth and Planetary Science Letters, 500, p. 215–224, https://doi.org/10.1016/j.epsl.2018.08.010.

Xu, X., Shao, L., Eriksson, K.A., Zhou, J., Wang, D., Hou, H., Hilton, J., Wang, S., Lu, J. and Jones, T.P., 2022, Widespread wildfires linked to early Albian Ocean Anoxic Event 1b: Evidence from the Fuxin lacustrine basin, NE China. Global and Planetary Change, 215, 103858, https://doi.org/10.1016/j.gloplacha.2022.103858.

Yao, H., Chen, X., Yin, R., Grasby, S.E., Weissert, H., Gu, X. and Wang, C., 2021, Mercury evidence of intense volcanism preceded oceanic anoxic event 1d. Geophysical Research Letters, 48, https://doi.org/10.1029/2020GL091508.

Yoshimura, Y., 2022, The Cretaceous normal superchron: a mini-review of its discovery, short reversal events, paleointensity, paleosecular variations, paleoenvironment, volcanism, and mechanism. Frontiers in Earth Science, 10, https://doi.org/feart.2022.834024.

Zhao, X., Zheng, D., Wang, H., Fang, Y., Xue, N. and Zhang, H., 2022, Carbon cycle perturbation and mercury anomalies in terrestrial Oceanic Anoxic Event 1b from Jiuquan Basin, NW China. Geological Society, London, Special Publications, 521, p. 185–196, https://doi.org/10.1144/SP521-2021-149.

Zheng, X.-Y., Jenkyns, H.C., Gale, A.S., Ward, D.J. and Henderson, G.M., 2013, Changing ocean circulation and hydrothermal inputs during Ocean Anoxic Event 2 (Cenomanian–Turonian): Evidence from Nd-isotopes in the European shelf sea. Earth and Planetary Science Letters, 375, p. 338–348, https://doi.org/10.1016/j.epsl.2013.05.053.

Figure Captions

Figure 1: Occurrence of LIP volcanism (vertical orange bars), and episodes of major environmental change (horizontal grey bars), during the Cretaceous Period. Ages and durations of volcanic activity are based on reviews by Kasbohm *et al.* (2021), Jiang *et al.* (2023), and this study. Ages and durations of major events from Wagreich (2009); Jenkyns (2010); Schulte *et al.* (2010); Eldrett *et al.* (2015); Cavalheiro *et al.* (2021) Matsumoto *et al.* (2022); Martinez *et al.* (2023). Palaeogeographic maps show the reconstructed continental positions during the Weissert Event, OAEs 1a, 1b, and 2, and the KPg transition, with the LIPs that have been associated with each event indicated in red (with the Chicxulub impact crater also indicated by the yellow star for the KPg). Palaeogeographical reconstructions are modified from the following sources: Weissert Event from Möller *et al.* (2020) and Charbonnier *et al.* (2020b); OAE 1a from Percival *et al.* (2021b); OAE 1b from Matsumoto *et al.* (2020); OAE 2 from Du Vivier *et al.* (2015); the KPg from Claeys *et al.* (2002).

Figure 2: Palaeogeographic map of the Barremian–Aptian interval, adapted from Percival *et al.* (2021b). The reconstructed locations of the HALIP and G-OJP are shown in red. Sites investigated in this study for mercury and osmium data shown by white circles: A) DSDP Site 398; B) Alstätte-1. Sites previously investigated using both proxies are shown by black circles (C–E), just for osmium isotopes with black squares (F–G), and just for mercury by black triangles (H–O).

Figure 3: Stratigraphic trends in $\delta^{13}C$, TOC, sea-surface temperature (SST) based on TEX_{86}, $^{187}Os/^{188}Os_{(i)}$, $[Os]_{(i)}$, Hg, Hg/TOC, and Hg/TS for DSDP Site 398 and Alstätte-1. Vertical scales are in metres. The stratigraphic extent of the OAE 1a level (here defined as strata spanning the C3–C6 segments) is marked by the horizontal grey bars. For DSDP Site 398, lithological column is from Jenkyns (2018), biostratigraphic and $\delta^{13}C$ information are from Li *et al.* (2008); SST trends are from Naafs and Pancost *et al.* (2016); all other data from this study. For Alstätte-1, lithological, biostratigraphic, $\delta^{13}C$, TOC, and SST information are from Mutterlose *et al.* (2014); all other data are from this study. SST trends based on both the widely applied TEX_{86}^{H} calibration of Kim *et al.* (2010)

and the deep-time analogue outlined by Tierney and Tingley (2014) are presented, as calculated by Naafs and Pancost (2016).

Figure 4: Stratigraphic correlation of OAE 1a geochemical records from DSDP Site 398, Cismon, and Gorgo a Cerbara. Vertical scales are in metres. The stratigraphic extent of the OAE 1a level (here defined as strata spanning the C3–C6 segments) is marked by the horizontal grey bar. DSDP Site 398 are sourced as for Figure 3. Cismon $\delta^{13}C$ and $\delta^{18}O$ data, and the stratigraphic position of the nannoconid crisis, are from Erba *et al.* (2010); $^{187}Os/^{188}Os_{(i)}$ data are from Bottini *et al.* (2012); trace metal data are from Erba *et al.* (2015). Gorgo a Cerbara $\delta^{13}C$ and $^{187}Os/^{188}Os_{(i)}$ data, and the stratigraphic position of the nannoconid crisis, are from Tejada *et al.* (2009); lead-isotope data are from Kuroda *et al.* (2011).

Figure 5: **A**) compiled $^{187}Os/^{188}Os$ and **B**) $^{87}Sr/^{86}Sr$ trends from Cretaceous stratigraphic records. Strontium-isotope trends redrawn from the compilation in McArthur *et al.* (2020). Osmium-isotope data sourced as shown. Changes in biospheric genera throughout the Cretaceous as compiled by Steuber *et al.* (2023) shown for **C**) larger benthic forams, **D**) rudists, and **E**) corals, **F**) planktonic taxa.

Figure 6: Simplified schematic of the climatic and environmental influence, and output of elements used as proxies of LIP activity, during the Cretaceous for A) Continental Flood Basalts and B) Oceanic Plateaus.

Figure 7: Summary of the number of mafic LIPs (continental flood basalt provinces or oceanic plateaus) emplaced during each geological Period since ~300 Ma, the onset of the Permian. For each Period, the total number of mafic LIPs spanning an area of ~0.5 Mkm^2 or more is shown (based on the recent based on the recent compilation of Ernst *et al.*, 2021), together with the ratio between the number of LIPs and proportional duration of the Period relative to the 79 Myr-long Cretaceous. I.e., the Jurassic (56.3 Myr) is 0.71 times the duration of the Cretaceous, whereas the Neogene (23.03 Myr) is only 0.29 of that timespan. This compilation includes the Triassic Wrangellia LIP, despite its preservation as relatively small areas of accreted igneous material obducted on to the western margin of North America, since it was likely a large oceanic plateau originally. Silicic LIPs (see Bryan and Ferrari, 2013) are not included, as they are thought to form over very long time intervals, and are less clearly linked to mantle plume activity.

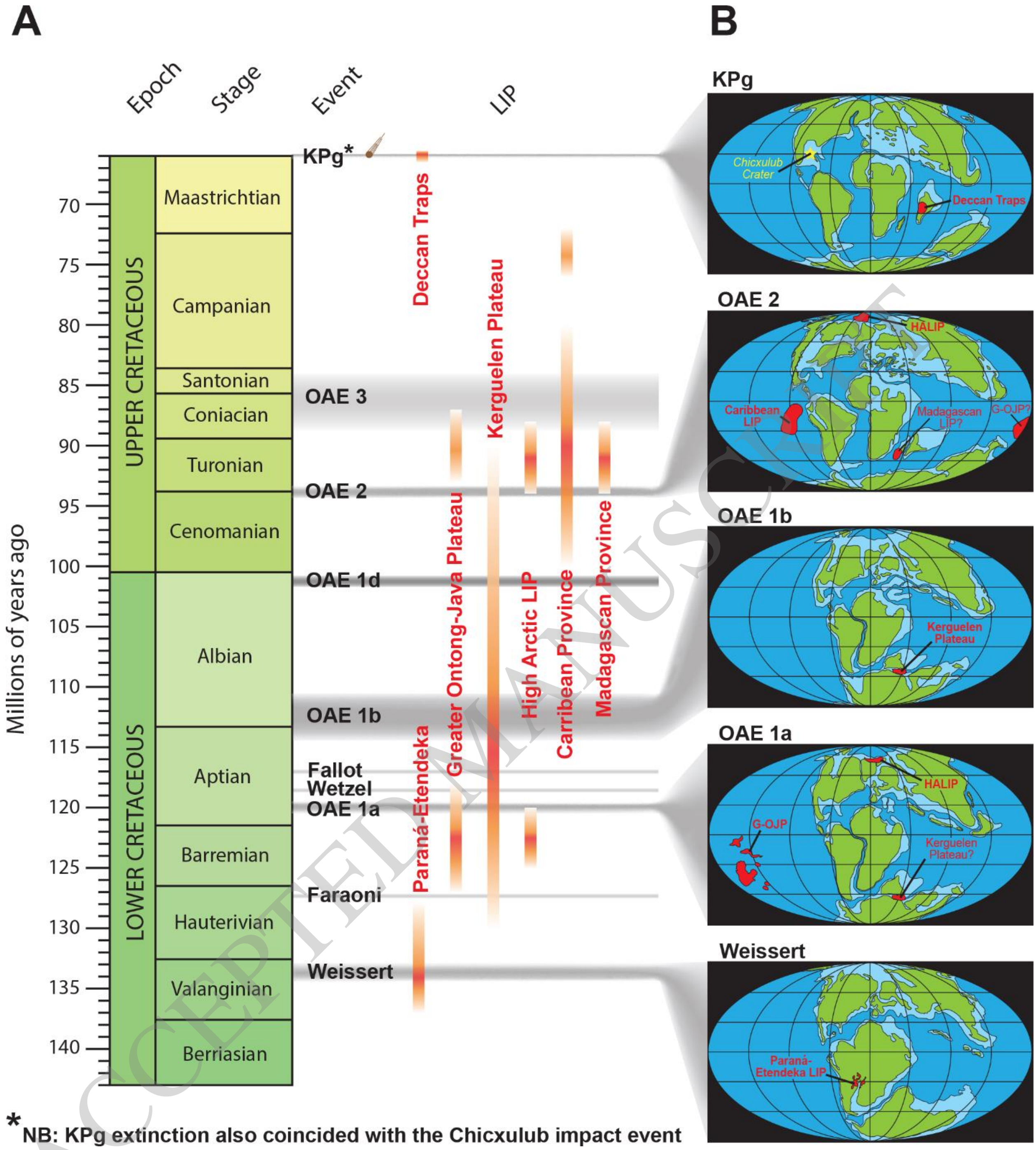

*NB: KPg extinction also coincided with the Chicxulub impact event

Figure 1

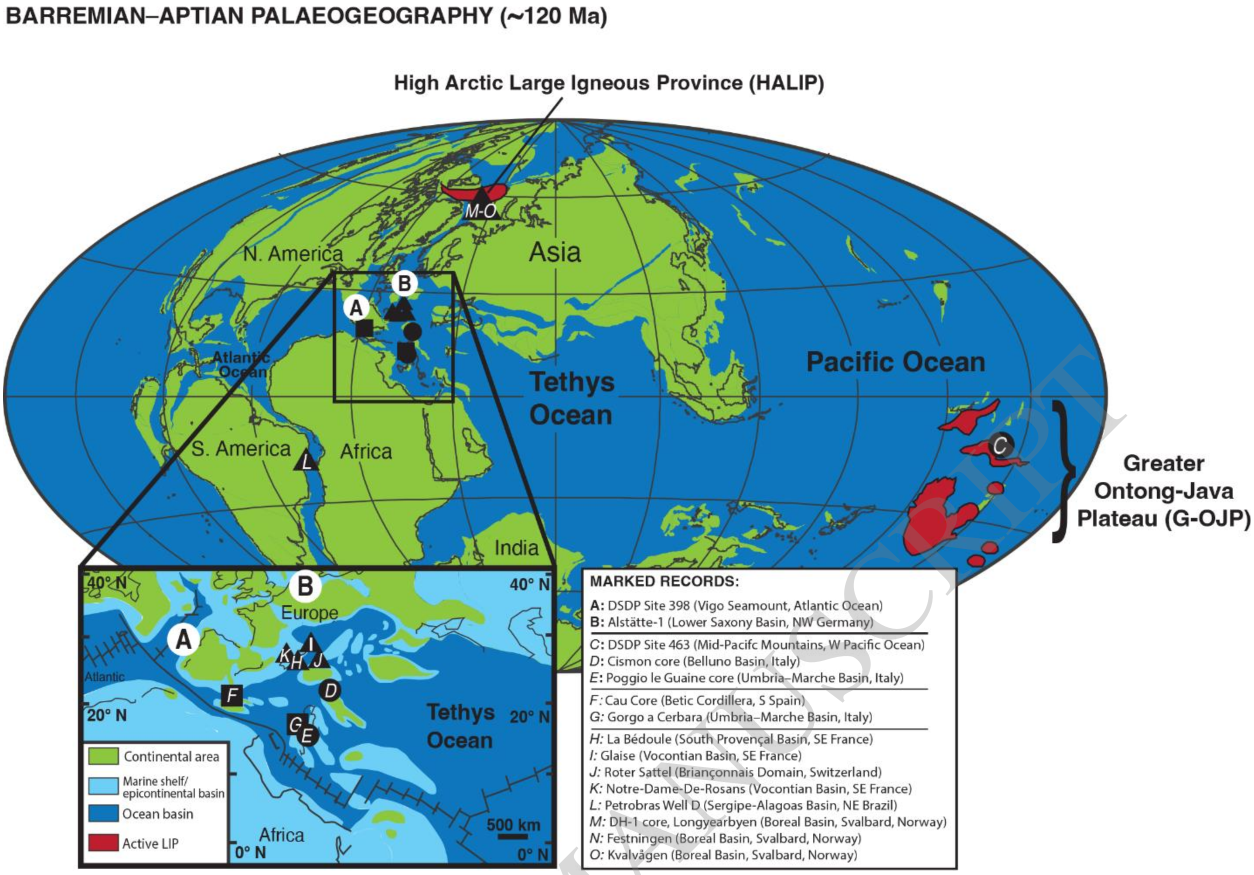
BARREMIAN–APTIAN PALAEOGEOGRAPHY (~120 Ma)
High Arctic Large Igneous Province (HALIP)
M-O
N. America
Asia
A
B
Atlantic Ocean
Tethys Ocean
Pacific Ocean
S. America
L
Africa
C
Greater Ontong-Java Plateau (G-OJP)
India
40° N
Europe
Atlantic
20° N
K H I J
D
F
G E
Tethys Ocean
Continental area
Marine shelf/ epicontinental basin
Ocean basin
Active LIP
Africa
500 km
0° N
MARKED RECORDS:
A: DSDP Site 398 (Vigo Seamount, Atlantic Ocean)
B: Alstätte-1 (Lower Saxony Basin, NW Germany)
C: DSDP Site 463 (Mid-Pacifc Mountains, W Pacific Ocean)
D: Cismon core (Belluno Basin, Italy)
E: Poggio le Guaine core (Umbria–Marche Basin, Italy)
F: Cau Core (Betic Cordillera, S Spain)
G: Gorgo a Cerbara (Umbria–Marche Basin, Italy)
H: La Bédoule (South Provençal Basin, SE France)
I: Glaise (Vocontian Basin, SE France)
J: Roter Sattel (Briançonnais Domain, Switzerland)
K: Notre-Dame-De-Rosans (Vocontian Basin, SE France)
L: Petrobras Well D (Sergipe-Alagoas Basin, NE Brazil)
M: DH-1 core, Longyearbyen (Boreal Basin, Svalbard, Norway)
N: Festningen (Boreal Basin, Svalbard, Norway)
O: Kvalvågen (Boreal Basin, Svalbard, Norway)

Figure 2

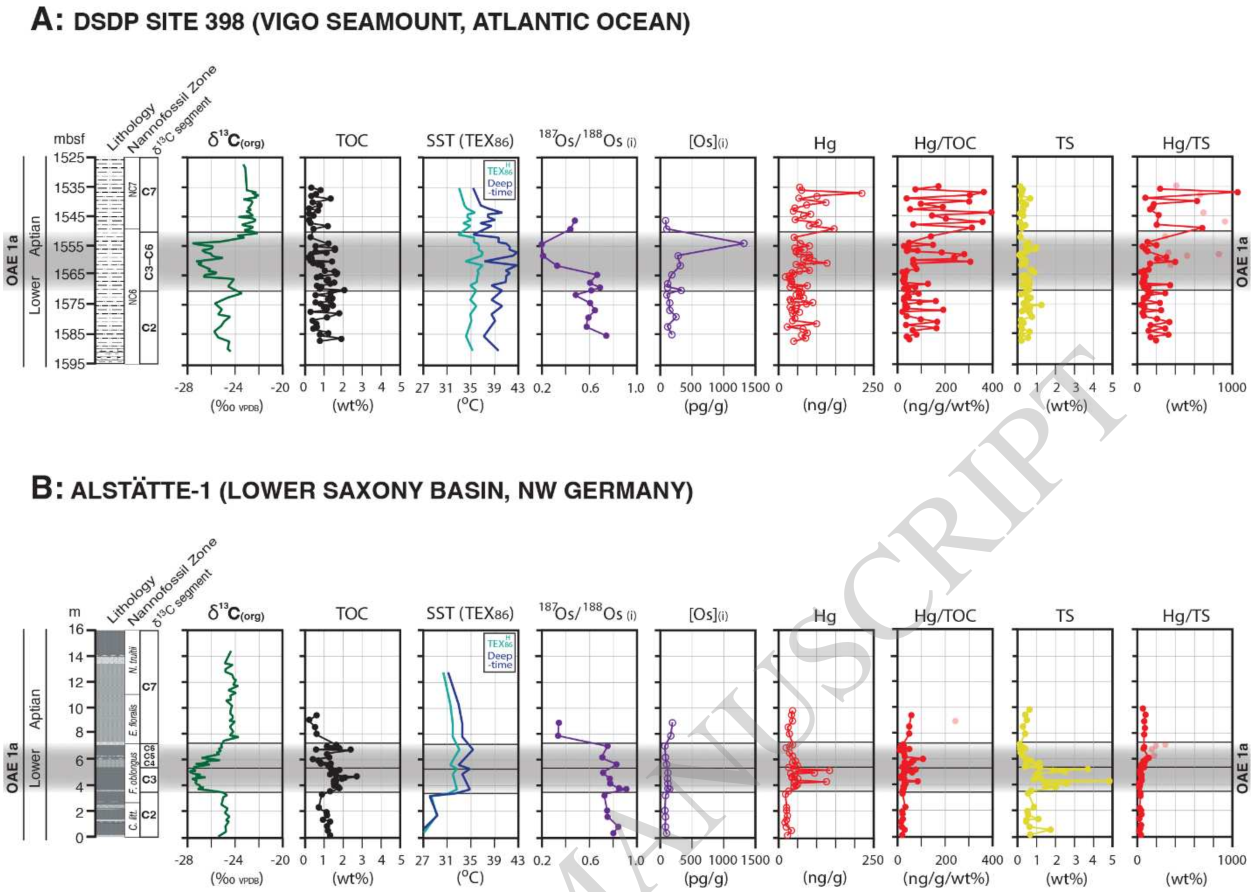
A: DSDP SITE 398 (VIGO SEAMOUNT, ATLANTIC OCEAN)
B: ALSTÄTTE-1 (LOWER SAXONY BASIN, NW GERMANY)
Lithology
Nannofossil Zone
δ13C segment
δ13C(org)
TOC
SST (TEX86)
187Os/188Os (i)
[Os](i)
Hg
Hg/TOC
TS
Hg/TS
OAE 1a
Lower Aptian
mbsf
m
(‰ VPDB)
(wt%)
(°C)
(pg/g)
(ng/g)
(ng/g/wt%)
Deep-time

Figure 3

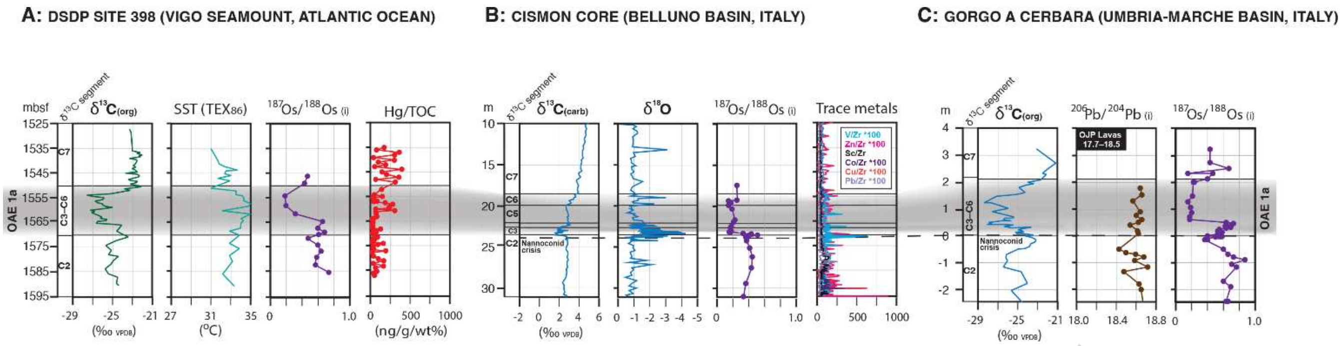
A: DSDP SITE 398 (VIGO SEAMOUNT, ATLANTIC OCEAN)
B: CISMON CORE (BELLUNO BASIN, ITALY)
C: GORGO A CERBARA (UMBRIA-MARCHE BASIN, ITALY)
mbsf
δ13C segment
δ13C(org)
SST (TEX86)
187Os/188Os (i)
Hg/TOC
OAE 1a
C7
C3–C6
C2
(‰ VPDB)
(°C)
(ng/g/wt%)
m
δ13C(carb)
δ18O
Trace metals
V/Zr *100
Zn/Zr *100
Sc/Zr
Co/Zr *100
Cu/Zr *100
Pb/Zr *100
C6
C5
C3
Nannoconid crisis
206Pb/204Pb (i)
OJP Lavas 17.7–18.5

Figure 4

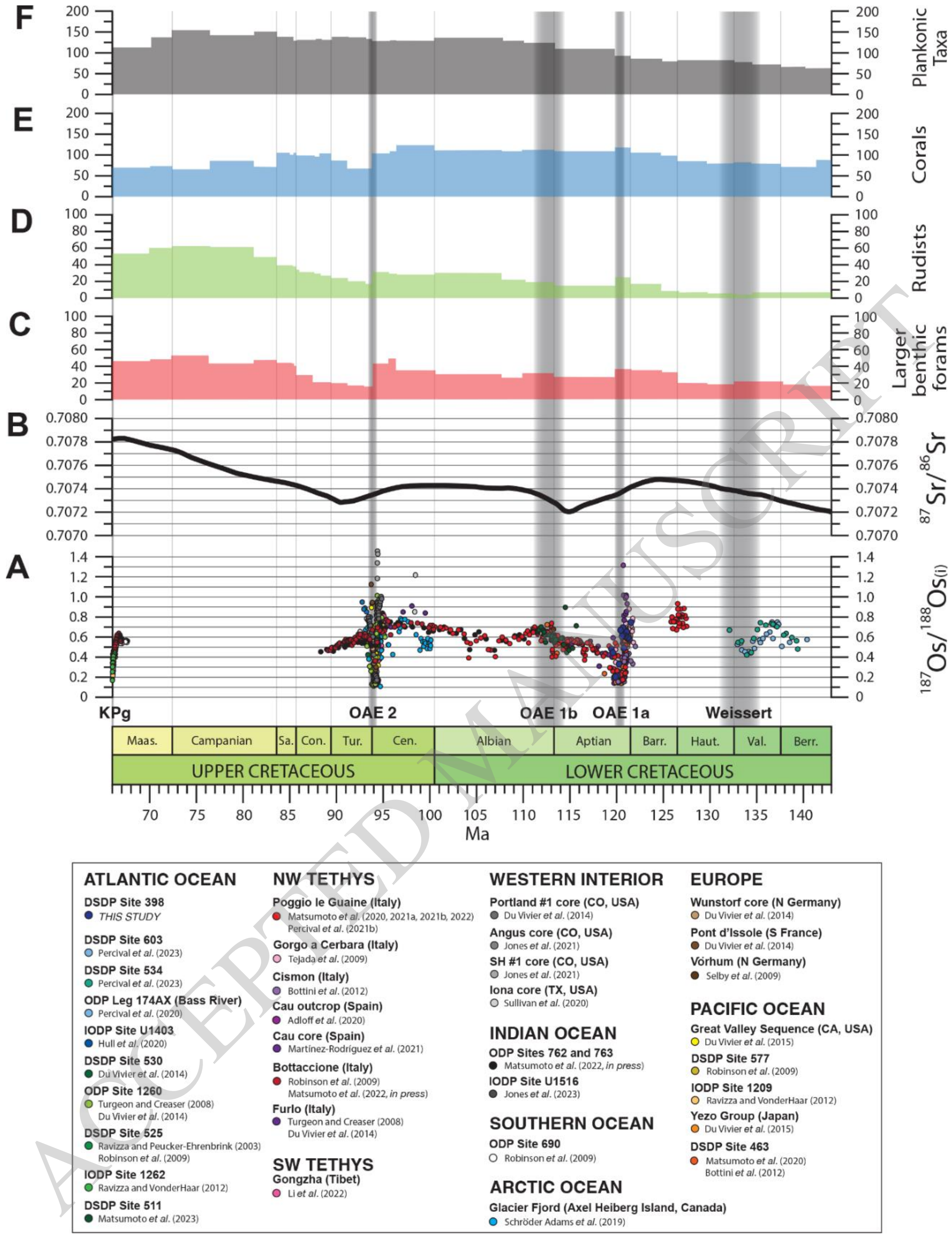
F
E
D
C
B
A
Plankonic Taxa
Corals
Rudists
Larger benthic forams
87Sr/86Sr
187Os/188Os(i)
KPg
OAE 2
OAE 1b
OAE 1a
Weissert
Maas.
Campanian
Sa.
Con.
Tur.
Cen.
Albian
Aptian
Barr.
Haut.
Val.
Berr.
UPPER CRETACEOUS
LOWER CRETACEOUS
Ma
ATLANTIC OCEAN
DSDP Site 398
THIS STUDY
DSDP Site 603
Percival et al. (2023)
DSDP Site 534
Percival et al. (2023)
ODP Leg 174AX (Bass River)
Percival et al. (2020)
IODP Site U1403
Hull et al. (2020)
DSDP Site 530
Du Vivier et al. (2014)
ODP Site 1260
Turgeon and Creaser (2008)
Du Vivier et al. (2014)
DSDP Site 525
Ravizza and Peucker-Ehrenbrink (2003)
Robinson et al. (2009)
IODP Site 1262
Ravizza and VonderHaar (2012)
DSDP Site 511
Matsumoto et al. (2023)
NW TETHYS
Poggio le Guaine (Italy)
Matsumoto et al. (2020, 2021a, 2021b, 2022)
Percival et al. (2021b)
Gorgo a Cerbara (Italy)
Tejada et al. (2009)
Cismon (Italy)
Bottini et al. (2012)
Cau outcrop (Spain)
Adloff et al. (2020)
Cau core (Spain)
Martínez-Rodríguez et al. (2021)
Bottaccione (Italy)
Robinson et al. (2009)
Matsumoto et al. (2022, in press)
Furlo (Italy)
Turgeon and Creaser (2008)
Du Vivier et al. (2014)
SW TETHYS
Gongzha (Tibet)
Li et al. (2022)
WESTERN INTERIOR
Portland #1 core (CO, USA)
Du Vivier et al. (2014)
Angus core (CO, USA)
Jones et al. (2021)
SH #1 core (CO, USA)
Jones et al. (2021)
Iona core (TX, USA)
Sullivan et al. (2020)
INDIAN OCEAN
ODP Sites 762 and 763
Matsumoto et al. (2022, in press)
IODP Site U1516
Jones et al. (2023)
SOUTHERN OCEAN
ODP Site 690
Robinson et al. (2009)
ARCTIC OCEAN
Glacier Fjord (Axel Heiberg Island, Canada)
Schröder Adams et al. (2019)
EUROPE
Wunstorf core (N Germany)
Du Vivier et al. (2014)
Pont d'Issole (S France)
Du Vivier et al. (2014)
Vöhrum (N Germany)
Selby et al. (2009)
PACIFIC OCEAN
Great Valley Sequence (CA, USA)
Du Vivier et al. (2015)
DSDP Site 577
Robinson et al. (2009)
IODP Site 1209
Ravizza and VonderHaar (2012)
Yezo Group (Japan)
Du Vivier et al. (2015)
DSDP Site 463
Matsumoto et al. (2020)
Bottini et al. (2012)

Figure 5

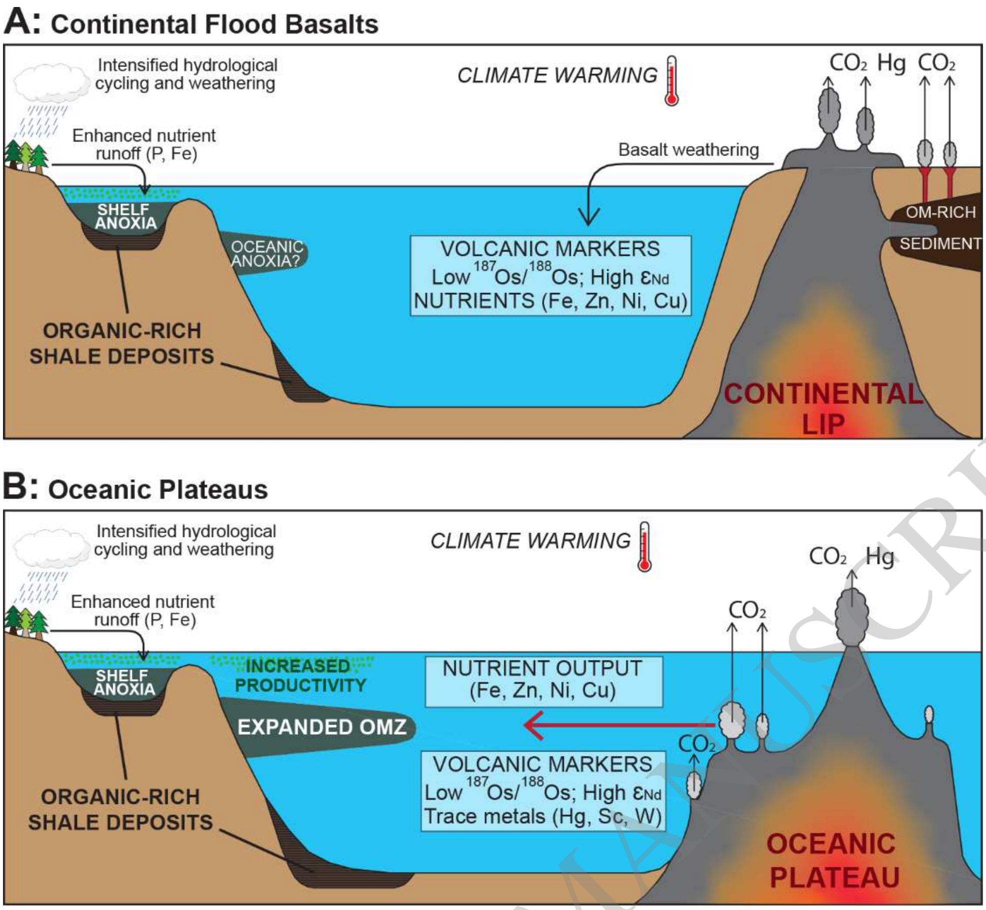

A: Continental Flood Basalts
Intensified hydrological cycling and weathering
CLIMATE WARMING
CO2 Hg CO2
Enhanced nutrient runoff (P, Fe)
Basalt weathering
SHELF ANOXIA
OCEANIC ANOXIA?
OM-RICH
SEDIMENT
VOLCANIC MARKERS
Low 187Os/188Os; High εNd
NUTRIENTS (Fe, Zn, Ni, Cu)
ORGANIC-RICH SHALE DEPOSITS
CONTINENTAL LIP
B: Oceanic Plateaus
Intensified hydrological cycling and weathering
CLIMATE WARMING
CO2 Hg
CO2
Enhanced nutrient runoff (P, Fe)
SHELF ANOXIA
INCREASED PRODUCTIVITY
NUTRIENT OUTPUT (Fe, Zn, Ni, Cu)
EXPANDED OMZ
CO2
VOLCANIC MARKERS
Low 187Os/188Os; High εNd
Trace metals (Hg, Sc, W)
ORGANIC-RICH SHALE DEPOSITS
OCEANIC PLATEAU

Figure 6

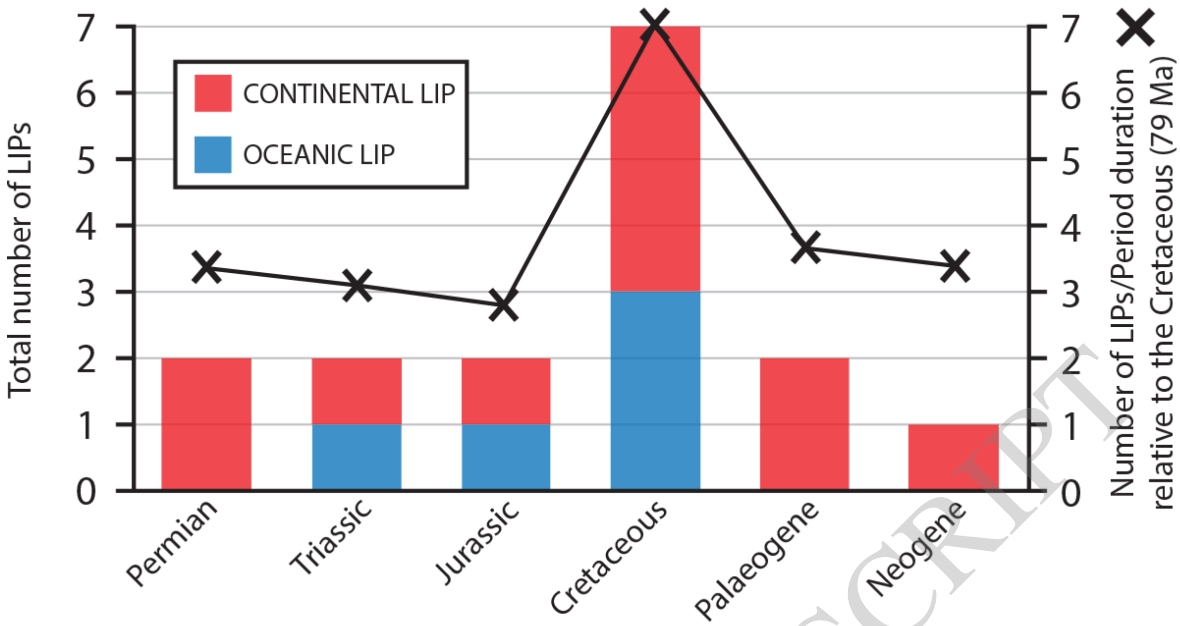
CONTINENTAL LIP
OCEANIC LIP
Total number of LIPs
Number of LIPs/Period duration relative to the Cretaceous (79 Ma)
0
1
2
3
4
5
6
7
Permian
Triassic
Jurassic
Cretaceous
Palaeogene
Neogene

Figure 7